High-impact low-likelihood climate scenarios for the UK

Background report

N.W. Arnell[1], E. Hawkins[2], T.G. Shepherd[1], I.D. Haigh[3], B. Harvey[2], L. Wilcox[2], L. Shaffrey[2] & A.G. Turner[1,2]

1 Department of Meteorology, University of Reading
2 National Centre for Atmospheric Sciences, University of Reading
3 School of Ocean and Earth Science, National Oceanography Centre, University of Southampton

January 2025

Cite this report as:

Arnell, N.W., Hawkins, E., Shepherd, T.G., Haigh, I.D., Harvey, B., Wilcox, L., Shaffrey, L. & Turner, A.G. (2025) *High-impact low-likelihood climate scenarios for the UK: background report*. Department of Meteorology, University of Reading. Produced for the UK Climate Resilience Programme. Project CR20-4. Available from https://www.metoffice.gov.uk/research/approach/collaboration/spf/spf-uk-climate-resilience/

High-impact low-likelihood climate scenarios for the UK

Executive Summary

This report outlines the evidence used to define a series of high-impact low-likelihood climate scenarios for the UK. The scenarios consist of a narrative storyline and an accompanying illustrative quantitative characterisation. The scenarios themselves are described in more detail in the accompanying scenarios report.

The storyline approach provides a framework for the presentation and development of scenarios. The storylines and scenarios are based on theoretical analysis, interpretation of climate model output and observed historical experience. The scenarios are designed to complement the UKCP18 climate projections. The quantitative characterisation of each scenario can be updated as new evidence becomes available. The scenarios describe potential high-impact low-likelihood drivers of impact, rather than high-impact low-likelihood outcomes.

One set of scenarios describe **transient changes** in climate and sea level to 2100, outside the range of changes projected under 'conventional' climate scenarios either because the climate forcings or the climate system response are different. The scenarios are based on six storylines describing (i) accelerated climate change (a world with an increase in global average temperature considerably greater than 4°C above pre-industrial levels), (ii) a substantial reduction in planet-cooling aerosols, (iii) a series of major volcanic eruptions, (iv) enhanced amplification of changes in the Arctic leading to substantial circulation changes, (v) abrupt ocean circulation change, and (vi) enhanced sea level rise due to rapid melting of the Greenland and Antarctic Ice Sheets. Each narrative scenario storyline is accompanied by an indicative quantitative characterisation. The physical mechanisms behind each storyline are presented in this report, along with an assessment of the confidence of their implications for UK weather, climate and sea level. The transient scenarios provide a high-level picture of how future UK climate could be different to that implied by conventional UKCP18 climate projections.

The second set of scenarios describe plausible **extreme monthly and seasonal anomalies**, specifically extreme temperature, rainfall and windspeed. Each scenario is associated with a 'backstory' describing the driving climatic conditions. The scenarios also describe compound extreme months and seasons and sequences of extremes. Each scenario is expressed in quantitative terms as an anomaly from a long-term average and can be implemented at a range of spatial scales. The

scenarios are developed using a combination of theoretical understanding of the drivers of extreme months and seasons in the UK, model simulations and empirical analysis based on observed climate data and a wide range of indicators of climatic variability. This set of scenarios allows an assessment of risks from plausible extreme events. The assumptions underpinning the scenarios are examined and justified in the report.

Contents

Figures

Tables

1. Introduction

The objective of this project is to construct a series of high-impact low-likelihood (HILL) climate scenarios for use in climate change risk assessment and adaptation planning in the United Kingdom. The scenarios are intended to complement the UKCP18 climate projections and are developed around a series of narrative storylines (Shepherd et al., 2018; Shepherd, 2019).

The scenarios are described in a separate Scenarios Report. This report presents the conceptual framework underpinning the scenarios, describes the two types of scenarios developed – transient scenarios and extreme scenarios – and outlines the sources of evidence used to construct the scenarios. First it summarises the context in the UK for the development and use of high-impact low-likelihood scenarios.

The comments of members of the Stakeholder and Technical Advisory Groups are gratefully acknowledged.

2. Context

2.1 Development and use of high-impact low-likelihood climate scenarios in the UK

Although there are no consistent national guidelines for the use of climate scenarios across the UK, there have been several recommendations and sets of guidance for specific sectors (Arnell, 2024). In its independent advice to government for the 3rd Climate Change Risk Assessment (CCRA3), the Climate Change Committee (CCC, 2021) introduced ten principles for good adaptation. One of these recommended 'adapt to 2ºC and assess the risks for 4ºC', and another recommended preparing for 'unpredictable extremes'. The House of Lords Select Committee on Risk Assessment and Risk Planning (House of Lords, 2021) reviewed risk assessment processes in general, and concluded that there was 'a bias against low likelihood-high impact risks'. In response, the government CCRA3 report (HM Government, 2022a: Annex 2) highlights an increasing emphasis on high-impact low-likelihood scenarios, implicitly in both the assessment and management of climate change risks.

The Supplementary Green Book Guidance on accounting for climate change in public investments (Defra, 2024) specifies that assessment should use at least two scenarios – consistent with increases of 2ºC and 4ºC by 2100 – but also states that 'planning for *more extreme change* (emphasis added)…is likely to be appropriate in situations where there are high vulnerabilities, low risk tolerance and long planning

or investment cycles' (p10). Guidance for the planning of Nationally Significant Infrastructure Projects in England (HM Government, 2022b; MHCLG, 2021a), for energy infrastructure with 'safety critical elements' (DESNZ, 2023) and for nuclear sites and infrastructure (ONR, Environment Agency, 2017; Department for Business, Energy and Industrial Strategy, 2019) should all use a 'credible maximum scenario'. Ferranti et al. (2021) recommended to the Office of Rail and Road (ORR) that the resilience plans for the rail network should include 'high-end low-probability' scenarios. See Arnell (2024) for a more detailed review of the use and interpretation of 'extreme' and 'worst case' climate scenarios in the UK.

'Credible maximum scenarios' in the UK have been interpreted as being defined by the H++ scenarios for change in sea level (Lowe et al., 2009) and extreme weather events (Met Office et al., 2015). The H++ sea level rise scenario describes a maximum increase in sea level around the UK coastline of 1.9m above the 1980-1999 mean by 2095. The H++ extreme event scenarios developed for the Second Climate Change Risk Assessment (CCRA2), however, describe plausible extreme temperature, rainfall and windstorm events (Table 2.1) not tied to a specific time period, climate scenario or level of warming (with the exception of cold snaps).

In practice, climate change assessments in the UK typically use the UKCP18 climate and sea-level projections. These are based on four emissions pathways (RCP2.6, RCP4.5, RCP6.0 and RCP8.5) representing low, medium, high and very high emissions, although the most widely used sets of projections from the local and regional strands are available only for RCP8.5. Projections based on RCP8.5 have been variously described by users as 'business-as-usual', a 4^{o}C scenario, a 'worst case', 'adverse' or 'highly precautionary' and even 'low probability-high impact' (Arnell, 2024). RCP8.5 is currently the subject of much debate (e.g. Hausfather & Peters, 2020; Schwalm et al., 2020), as it is often claimed to be based on unrealistically high projections of future emissions and therefore represents a 'worst case'. This is discussed in more detail below. The Evidence Report for CCRA3 (CCC, 2021) interpreted published studies in terms of worlds which reached 2^{o}C and 4^{o}C by 2100 – which are not quite the same as the scenarios implied by the emissions pathways used in UKCP18.

The evidence and technical reports for both CCRA2 and CCRA3 described a set of high-impact low-likelihood scenarios (Table 2.2: Humphrey & Murphy, 2016; Slingo, 2021; Hanlon et al., 2021) intended to inform the qualitative interpretation of climate risks in the UK.

The introductory context chapter of the Working Group I Sixth Assessment Report of the Intergovernmental Panel on Climate Change (IPCC: Chen et al., 2021) described both low-likelihood high-impact scenarios and tipping points, but in practice only

three low-likelihood high-impact scenarios – volcanic cooling, high sea level rise and collapse of the Atlantic Meridional Overturning Circulation - were explicitly discussed as such in the main body of the Working Group 1 report.

Table 2.1: H++ scenarios (Met Office et al., 2015)

Scenario	Description
Heat wave	• Annual average summer maximum temperatures exceeding 30°C over most of the UK and 34°C over much of central and southern England. • Hottest days would exceed 40°C in some locations, with 48°C being reached in extreme cases.
Low rainfall	• 6 month duration summer drought with rainfall deficits of up to 60% below the long term average (1900-1999). • Longer dry periods spanning several years with rainfall deficits of up to 20% below the long term average (1900-1999) across all of England and Wales, similar to the most severe and extensive long droughts in the historical record
Low river flows	• 40-70 % reduction in 'low flows' (Q95) in England and Wales in a single summer. • For multi-season droughts, including 2 summers, a 20 to 60 % reduction in low flows in England and Wales.
High rainfall	• A 70%-100% increase in winter rainfall (Dec to Feb) in a single winter (from a 1961-1990 baseline). An up to five-fold increase in frequency and 60% to 80% increase in heavy daily and sub-daily rainfall depths, for both summer and winter events (all year round).
High river flows	• A 60% to 120% increase in peak flows at the 'lower end' of the H++ scenarios for some regions in England and Wales. The upper limit for any region is a 290% increase in peak flows (1961-1990 baseline).
Wind storms	• A 50-80% increase in the number of days per year with strong winds over the UK (1975-2005 baseline). *A strong wind day is defined as one where the daily mean wind speed at 850 hPa, averaged over the UK (8W-2E, 50N-60N), is greater than the 99th percentile of the historical simulations.*
Cold snaps	• In the 2020s, UK average winter temperatures (December, January and February) of 0.3°C and for the 2080s, UK average winter temperatures would be around -4°C. • In the 2020s, UK average temperatures on the coldest day would be -7°C in some locations. UK average temperature of the coldest day would be around -11°C.

Table 2.2: High-impact low-likelihood earth system changes relevant to the UK as defined in Climate Change Risk Assessments

CCRA2 (Humphrey & Murphy, 2016)	CCRA3 (Slingo, 2021)
Weakening of the Atlantic Meridional Overturning Circulation (AMOC)	Weakening of the Atlantic Meridional Overturning Circulation (AMOC)
Ice sheet collapse	Accelerated loss of ice sheets
Permafrost carbon release	Permafrost thawing
Release of methane from ocean sediments	
Tropical forest dieback	Reduced uptake of carbon by the biosphere
Total loss of Arctic sea ice	
	Change in behaviour of the North Atlantic Jet Stream

Many terms have been used to describe ‘high-impact, low-likelihood’ (sometimes low-likelihood high-impact) scenarios, including ‘high-end’ scenarios, ‘credible maximum scenarios’, ‘physically plausible high impact scenarios’, ‘high-impact low-probability’ and ‘reasonable worst-case scenarios’. ‘Low’ and ‘high’ are rarely explicitly defined, and indeed ‘low likelihood’ is conceptually challenging to define in the presence of the deep uncertainty which characterises the types of extreme scenarios that are of interest. It is better to conceive of high-impact low-likelihood scenarios as being physically plausible.

A key distinction is between scenarios described in terms of the low-likelihood *drivers or causes* which might generate high impacts, and high impact *outcomes* which have a low likelihood. Resilience planning in practice is often based on scenarios of outcomes rather than causes, but much of the focus in the climate science literature is on drivers and causes. The Intergovernmental Panel on Climate Change (IPCC) glossary for example defines a low-likelihood high impact outcome or event as one ‘whose probability of occurrence is low or not well known but whose potential impacts on society and ecosystems could be high’ (IPCC, 2021) – an implicit focus on outcome rather than drivers – but the discussion in Working Group 1 focuses on drivers rather than outcomes. Similarly, whilst the CCRA3 Technical Report described high-impact low-likelihood scenarios in terms of cause and this interpretation was used in the natural environment and infrastructure chapters (Berry & Brown, 2021; Jaroszweski et al., 2021), the health chapter (Kovats & Brisley, 2021) interpreted high-impact low-likelihood scenarios in terms of outcomes. The high-impact low-likelihood scenarios here are presented in terms of the drivers of impact.

A second important but often overlooked distinction is between high-impact low-likelihood scenarios that describe events or shocks – the ‘reasonable worst-case scenarios’ typically used in emergency and resilience planning (for example the H++ temperature, rain and wind scenarios) – and high-impact low-likelihood scenarios that describe persistent and developing conditions outside the range of current expectations (for example the H++ sea level rise scenarios). This is a difference between acute and chronic changes. Here, this distinction is characterised by the construction of ‘**extreme anomaly**’ scenarios, representing extreme or anomalous conditions, and ‘**transient**’ scenarios representing plausible high-impact low-likelihood change as it evolves over the course of the 21st century. Specific definitions for these two types of high-impact low-likelihood scenario are presented in Section 4.1. The transient scenarios are designed to provide a high-level overview of potential large changes to the UK climate outside the range conventionally considered, and the extreme anomaly scenarios are designed to support more specific risk assessment.

There have been few published quantifications of high-impact low-likelihood climate scenarios and their implications for the UK. Most studies have focused on the H++ sea level rise scenario (Weeks et al., 2023; Palmer et al., 2024) and its applications particularly in the assessment of flood risk in the Thames (Ranger et al., 2013). One study has looked specifically at the impacts of the collapse of the Atlantic Meridional Overturning Circulation (AMOC) in the UK (Ritchie et al., 2020), and a couple have sought to quantify effects on climate in Europe in general (Vellinga & Wood, 2008; Jackson et al., 2015). Sgubin et al. (2019) in a very specific study assessed the effects of collapse of the sub-Polar Gyre on European viticulture. An early study by Arnell (2006) estimated the impacts of accelerated climate change, AMOC collapse and climate regime shift for different global regions.

There has been more published work on identifying potential very extreme (or unprecedented) events in the UK, including through the interpretation of historical evidence (e.g. Endfield, 2016; Matthews et al., 2016) and the use of model simulations (e.g. Thompson et al., 2017; Kent et al., 2022; Leach et al., 2022).

2.2 The storyline approach to creating climate scenarios

Conventional climate change impact and risk assessments use scenarios developed from climate models under specific scenarios for the future emissions of the greenhouse gases and atmospheric aerosols that influence future climate. Given the uncertainty in the projected regional and local consequences of a specific emissions scenario, assessments are typically based on an ensemble of projections. This may be either an ensemble of projections from individual climate models which are usually assumed to be equally plausible (as in the UKCP18 global, regional and local strands which use between 12 and 28 models), or a much larger ensemble of projections which can be used to construct probability distributions of measures of interest (as in the UKCP18 probabilistic strand). However, these projections are all based on climate models (and statistical emulators of models) which reflect current understanding of how the climate system works and do not necessarily fully describe the possible range of future climates. This is particularly significant when interest is focused on potential extreme changes in climate. Some of the mechanisms potentially triggering extreme change may not be represented in current climate models, and their spatial resolution and parameterisation may mean that they do not simulate extreme shorter-duration events very realistically.

An alternative approach is to define a small number of narrative storylines (Shepherd et al., 2018; Shepherd, 2019) and characterise these quantitatively. A storyline is a

physically self-consistent unfolding of past events, or of plausible future events or pathways (Shepherd et al., 2018). Storylines are not assigned probabilities or likelihoods and emphasise the underlying driving factors and the plausibility of those factors. Storylines can be constructed from theoretical reasoning, from historical experience, through the interpretation of climate model results, through conducting bespoke simulations, or through any combination of the above. Physical plausibility is central to a storyline. Narrative storylines and their quantitative characterisations are similar in principle to the stress tests that are increasingly used in the banking and financial sector (e.g. Bank of England, 2015).

In an early application of the storyline approach, Zappa & Shepherd (2017) defined a series of plausible changes in atmospheric circulation across the North Atlantic based on changes in three key drivers and estimated from climate models the windiness across Europe (and rainfall around the Mediterranean). Subsequent applications in Europe have described storylines for heatwaves (van Garderen et al., 2021; Sanchez-Benitez et al., 2022; Fischer et al., 2023; Garrido-Perez et al., 2024), drought (Gessner et al., 2022) and extreme rainfall (Gessner et al., 2023). In the UK, Chan et al. (2023; 2024) and Harvey et al. (2023) developed storylines for potential extreme hydrological droughts and the effects of changes in the jet stream respectively.

2.3 The use of UKCP18 land climate projections

The UKCP18 land climate projections have been used in many ways and for many types of application. One broad distinction is between *qualitative* and *quantitative* uses.

A *qualitative* use is where summary results from the UKCP18 climate projections are used directly to provide contextual information on climate change in the UK, either in a report or as a contribution to a high-level assessment of climate change risks. This may involve using graphs showing change over time, or tables, plots or maps showing changes over a particular time period (e.g. the 2050s). Such uses typically focus on mean monthly temperature and rainfall.

A *quantitative* use is where the UKCP18 projections have been used to calculate some indicator or metric. This may be calculated directly from the projections – for example the number of days with temperatures exceeding a threshold – or may be calculated by using the climate projections as input to a model (such as a hydrological model). Some quantitative applications use long time series to simulate change over time (for example between 1980 and 2100), whilst others concentrate on particular time slices (for example comparing 2041-2070, representing the 2050s, with a 1981-2010 baseline). In either case, some applications use the UKCP18

climate projections directly, usually at the daily scale (or finer) and usually (but not always) after some sort of bias adjustment, whilst other applications adopt the delta method. The delta method calculates changes in climate from the climate projections and uses these to perturb an historical observed climate data set: this approach typically calculates changes at the monthly scale and then applies them to observed daily data. Not all of the UKCP18 land strands provide information to allow all of these different approaches. The local projections on a 5km grid, for example, cannot be used to create long time series, and the probabilistic projections do not provide data at less than the monthly scale.

These different ways of using UKCP18 climate projections mean that high-impact low-likelihood scenarios need to be presented in several ways in order to meet the needs of different users.

3. Conceptual framework

Two types of high-impact low-likelihood scenarios are constructed here and described in the Scenario Report. One type of scenario describes **transient change to 2100**, and the other characterises **extreme monthly and seasonal anomalies**. The first type can be interpreted as defining chronic risks, whilst the second type define acute risks. Both types of scenario are defined in terms of the climate *driver* of impact rather than the impact *outcome*. Each scenario has a narrative **qualitative description** and an indictive **quantitative characterisation**.

The **transient scenarios** are based on a set of six plausible and distinctive narrative storylines describing qualitatively different potential drivers of high-impact, low-likelihood changes in UK climate and sea level to 2100. The scenarios are designed to describe changes outside the extreme range conventionally assumed – taken here to be *either* a world reaching an increase in global mean surface temperature of more than 4°C above pre-industrial levels by 2100, *or* outside the range of projections for a given emissions scenario as represented by the majority of current climate models. Such changes could occur because the ***forcings*** of climate change are outside the conventional range, or because the large-scale ***climate system response*** is outside the range projected by most current climate models. Each transient scenario is presented as a single quantification of the storyline to be applied either as a standalone scenario or as a perturbation to be applied to UKCP18 projections with any emissions pathway. The transient scenarios are described in detail in Section 4. These scenarios are primarily designed to provide a high-level overview of potential changes to the UK climate outside the range conventionally considered.

The **extreme anomaly scenarios** represent plausible extreme monthly and seasonal temperature, rainfall and windspeed anomalies, both individually and together as compound scenarios. Each is associated with a narrative 'backstory' describing plausible circulation patterns (such as jet stream position) that generate the extremes. These scenarios are designed to be applied to a long-term mean to represent an individual month or season, or sequence of months. The extreme anomaly scenarios are not intended to describe short-duration events (such as heatwaves, intense rainstorms or windstorms), because the user requirements for such scenarios vary considerably between users. They are not therefore direct replacements for the H++ temperature, rainfall and wind extreme scenarios or indeed Reasonable Worst Case Scenarios used in emergency planning. The monthly and seasonal extreme scenarios are described in detail in Section 5. They represent an application of the 'Tales of Future Weather' approach to the development of narratives of high impact weather in a future climate (Hazeleger et al., 2015). These scenarios are primarily designed to support assessments of the

extreme events to which the UK might become exposed and more specific risk assessments.

The quantifications for both the transient and extreme anomaly scenarios are developed through a combination of theory, historical experience, expert judgment and the interpretation of climate model output, including UKCP18 products. The quantitative scenarios are not to be interpreted too literally. They can be updated or supplemented within the framework presented here as new information becomes available. Extra scenarios can be added within the same framework.

The scenarios are not assigned quantitative likelihoods, but their plausibility is characterised in terms of understanding of (i) the drivers of the scenario (forcing or large-scale response) and (ii) the consequences of the scenario for the UK if it were to occur.

There is considerable uncertainty in projected change in UK climate in the UKCP18 climate projections, and the high-impact low-likelihood scenarios should be interpreted in relation to this uncertainty.

The scenarios only describe high-impact low-likelihood changes directly impacting upon the UK. The UK may also be impacted by high-impact low-likelihood scenarios occurring elsewhere: these are not covered here.

4. Transient scenarios

4.1 Introduction

The transient scenarios describe change in climate (temperature, rainfall, windspeed and sea level) over the 21st century under six storylines representing plausible drivers of high-impact low-likelihood change. These scenarios are outside or at the top of the range of 'conventional' UKCP18 climate projections. One scenario is based on a subset of UKCP18 RCP8.5 projections and another is defined as standalone scenarios for low and very high emissions, but the other four are specified as perturbations which can be applied to any of the UKCP18 projection strands and emissions assumptions.

A number of papers and reports have described potential high-impact low-likelihood scenarios (for example Sutton, 2018; 2019; Slingo, 2021; Hanlon et al., 2021; Armstrong McKay et al., 2022; Wood et al., 2023; Chen et al., 2021). Terminology varies and the definitions of scenarios vary across these reports. Some focus on 'tipping points' (Armstrong McKay et al., 2022; Hanlon et al., 2021) – a critical threshold beyond which a qualitative change occurs in a system – but not all high-impact low-likelihood scenarios involve tipping points or abrupt change (Sutton, 2018; 2019).

Following an extensive survey of the literature, six storylines describing high-impact low-likelihood scenarios were defined. These represent six qualitatively different high-impact low-likelihood scenarios.

HILL-1 Enhanced global warming

The increase in global average temperature is considerably greater than 4°C above pre-industrial levels by 2100. This may be because emissions are greater than conventionally assumed (stronger forcing), because the climate system might respond more strongly to a forcing than conventionally assumed (climate sensitivity is high), or because accelerated feedbacks in the carbon cycle mean that greenhouse gases are released from storage in positive feedbacks. These three potential causes are independent but would have the same overall effect on climate. The accelerated feedbacks are tipping points. This storyline is characterised by a subset of the UKCP18 RCP8.5 projections.

HILL-2 Rapid reductions in aerosol emissions

A rapid reduction in the emission of aerosols and their precursors to the atmosphere – to improve air quality – lead to more rapid warming than conventionally assumed over the next few decades (Persad et al., 2022). This storyline describes an

enhanced forcing of the climate system but is not the same as HILL-1 (i) because aerosols are assumed to decrease more rapidly, (ii) the regional climate response is different and (iii) it can apply with any assumption about future greenhouse gas emissions. It is characterised by change factors which can be applied to any UKCP18 climate projection strand or emissions assumption.

HILL-3 Volcanic cooling

A major volcanic eruption emits aerosols into the stratosphere, which reflect incoming solar radiation and lead to cooling at the surface and changes to the hydrological cycle. This storyline describes an additional forcing on the climate system. It is characterised by change factors which can be applied to any UKCP18 climate projection strand or emissions assumption.

HILL-4 Stronger Arctic Amplification

Rapid increases in temperature in high latitudes and a loss of Arctic Ocean sea ice lead to greater changes in atmospheric circulation than represented in the current generation of climate models, resulting in changes to the jet stream affecting the UK climate and an increased frequency of cold weather outbreaks in winter. This storyline describes an enhanced response of the climate system to forcing. It is characterised by change factors which can be applied to any UKCP18 climate projection strand or emissions assumption.

HILL-5 Abrupt changes to ocean circulation

An abrupt change in ocean circulation in the North Atlantic Ocean leads to cooling across western Europe and the UK. There are two variants to this storyline. One (HILL-5a) assumes a collapse in the Atlantic Meridional Overturning Circulation (AMOC), and the other (HILL-5b) assumes a collapse of the sub-Polar Gyre (SPG). This storyline describes an enhanced response of the climate system to forcing. Both variants are characterised by change factors which can be applied to any UKCP18 climate projection strand or emissions assumption.

HILL-6 Enhanced sea-level rise

Accelerated loss of ice from Greenland and Antarctica leads to increased sea level. This storyline describes an enhanced response of the climate system to forcing and is presented as standalone scenarios corresponding to low and very high emissions to complement UKCP18 sea level rise projections.

The set of storylines does not explicitly include a storyline defining a change in the North Atlantic jet stream (in contrast to Slingo (2021) and Hanlon et al. (2021)), but changes in the jet stream are a core feature of HILL-4. The difference is essentially due to the definition of the starting point for the storyline. The extreme anomaly scenarios (Section 5) specifically include storylines describing jet stream behaviour.

Other potential storylines for high-impact low-likelihood scenarios were considered but rejected because their effects directly on UK weather, climate and sea level were assessed to be small or within the range of the storylines already defined. These include abrupt changes to the South Asian Monsoon or El Nino-Southern Oscillation (ENSO).

Each of the six storylines was developed and quantified using a combination of theoretical reasoning, evidence from published studies, evidence from climate model simulations and historical experience. The quantifications are deliberately highly generalised. A causal loop diagram summarising the drivers and responses was produced for each storyline. No attempt was made to quantify the likelihood of each storyline, but each is considered physically plausible. Expert judgment was used to assess the confidence in the estimated magnitude of the projected changes in temperature, rainfall, windspeed and sea level for the UK, based on (i) the extent of the evidence available and (ii) the agreement amongst the various lines of evidence.

The following sections describe the six storylines in more detail. Figure 4.1 illustrates the effect of HILL-1 to HILL-5 on seasonal temperature, rainfall and windspeed for an example location in southern England, compared with projected changes in a 4^{o}C world. All are based on the 15 member UKCP18 HadGEM PPE-15 RCP8.5 ensemble. The 4^{o}C world projections were produced by scaling the RCP8.5 projections to be consistent with an increase in global mean temperature of 4^{o}C above pre-industrial levels by 2100. The HILL-2 to HILL-5 scenarios were applied as adjustments to the 4^{o}C projections, and HILL-1 was defined as the most extreme of the RCP8.5 projections. Figure 4.2 illustrates the HILL-1, HILL-5a and HILL-6 transient sea level rise scenarios.

The transient scenarios define just changes in temperature, rainfall and windspeed (and for some sea level). Consistent changes in other climatic variables – for example humidity – can be derived if necessary from the narrative storylines.

The quantitative characterisations of the storylines are designed to be able to be implemented however UKCP18 climate and marine projections are used.

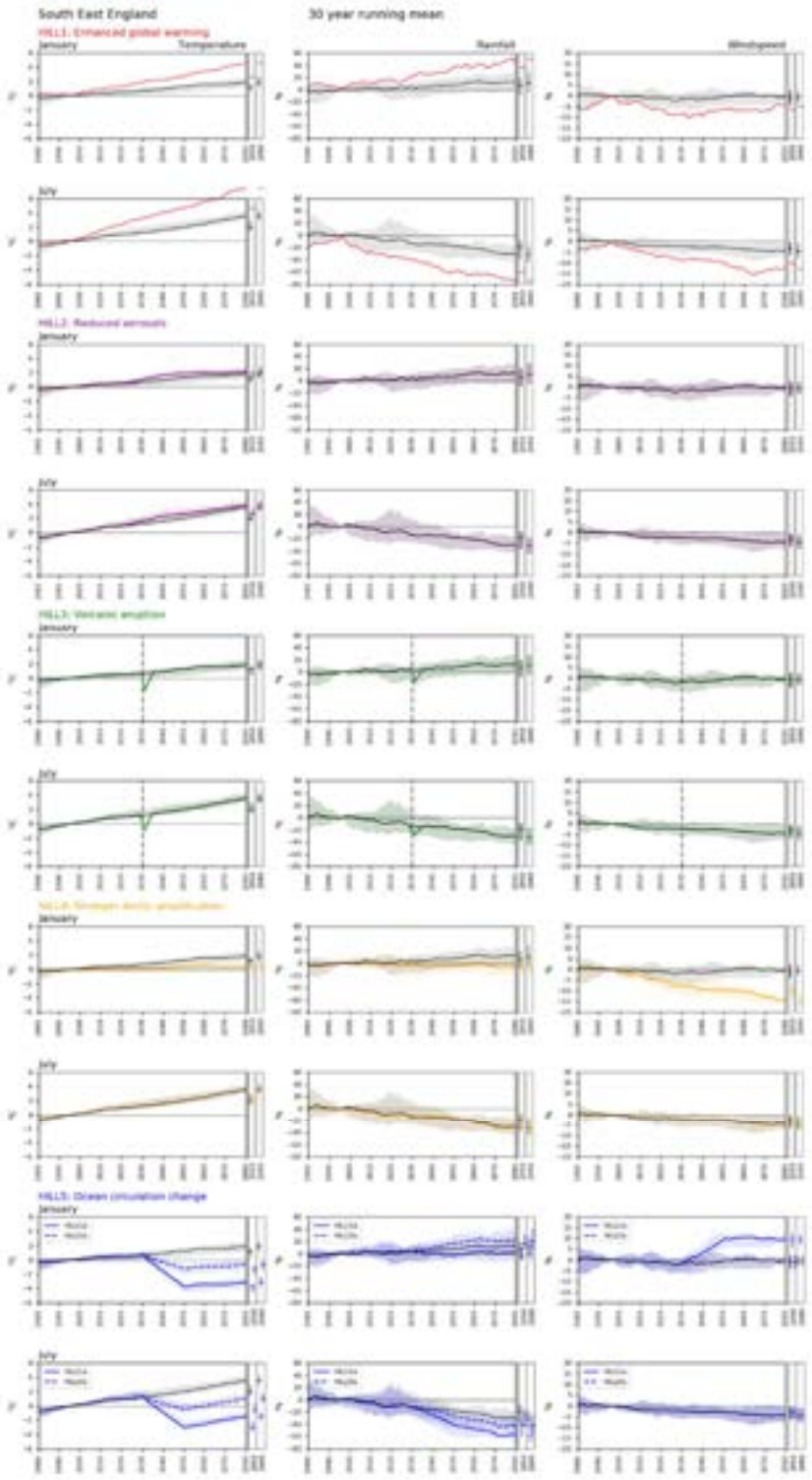

Figure 4.1: The effect of transient scenarios HILL-1 to HILL-5 on January and July temperature, rainfall and windspeed projections for an example location in southern England. The plot also shows the changes in a world which reaches 4ºC above pre-industrial levels by 2100. The changes are relative to the 1981-2010 average. The panels to the right of each plot show changes in 2050 and 2080. Note that not all scenarios describe changes in all variables. HILL-2 to HILL-5 are applied here as perturbations to the UKCP18 HadGEM PPE-15 ensemble, and HILL-1 is defined as the most extreme UKCP18 HadGEM PPE-15 RCP8.5 member

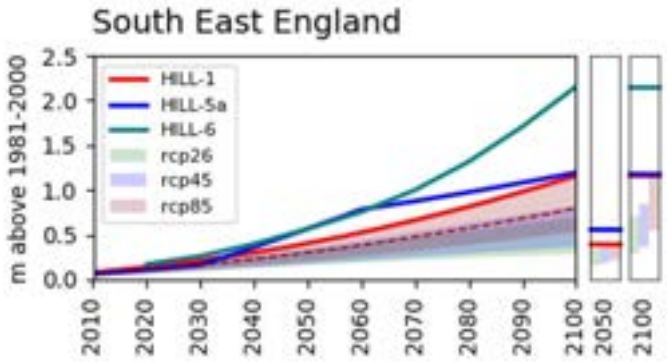

Figure 4.2: The effect of the transient scenarios HILL-1, HILL-5a and HILL-6 on mean sea level rise, for an example location in south east England. The plot also shows rise in sea level (5th to 95th percentile range) with the three UKCP18 sea level rise scenarios. The HILL-5a scenario is applied to the median UKCP18 RCP8.5 projection, shown by the dotted line.

4.2 HILL-1: Enhanced global warming

Climate change by the end of the 21st century depends on future use of fossil fuels, which depends on how economics and energy use change over time – which is strongly influenced by national and international climate policy. Many countries and organisations have already implemented measures to reduce emissions. If there is no further action beyond these current policies, then the Intergovernmental Panel on Climate Change (IPCC) estimated that global average temperature would increase by 2100 by between 2.2ºC and 3.5ºC above pre-industrial levels (IPCC, 2023a;b): this is consistent with the estimates made by the Climate Action Tracker (2023) and in Hausfather's (2025) review.

The Climate Change Committee (2021) recommends that organisations seeking to adapt should 'adapt to 2ºC and assess the risks for 4ºC'. Implicitly, an increase in global mean temperature of 4ºC is seen as a realistic upper limit for global warming by 2100 *if there is no further action on climate change and no significant backtracking*. However, it is possible for climate change to lead to a larger increase in global average temperature. The HILL-1 scenario describes a world with an increase in global mean surface temperature considerably more than 4ºC above pre-industrial levels by 2100.

There are three potential reasons why global average warming might be greater than assumed under current policy scenarios or a 4ºC world (Figure 4.3):

- emissions might be higher than assumed in current policy scenarios;

- the climate system might respond more strongly to a forcing than conventionally assumed (high climate sensitivity);
- accelerated feedbacks mean that more greenhouse gases are released from the earth surface to enhance the greenhouse effect.

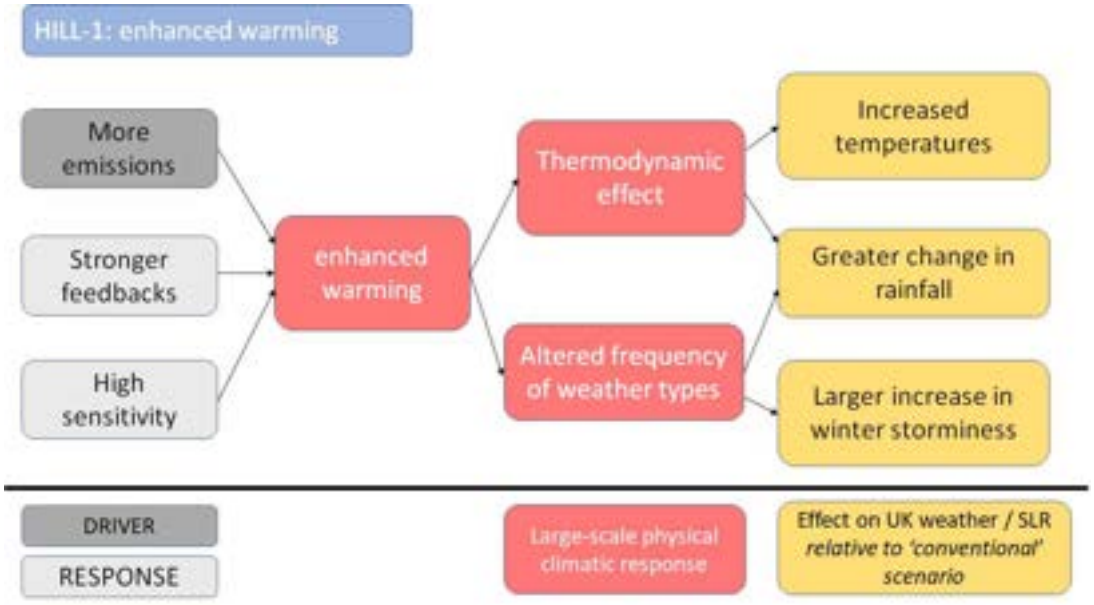

Figure 4.3: Causal loop diagram for the enhanced warming scenario HILL-1. The red boxes describe the large-scale climate processes affected by the storyline, and the yellow boxes describe the consequences for the UK.

The first is a *forcing* of change outside the conventional range, whilst the other two are system *responses* outside the conventional range.

Anthropogenic emissions of greenhouse gases could potentially be larger than assumed in current policy scenarios for several reasons. Rates of economic development could be considerably different to that assumed, or the relative economic costs of different energy sources may change in ways that are not anticipated (renewable sources are generally becoming cheaper relative to fossil fuel sources, but this trend could be reversed). Some policies or technologies assumed in current policy scenarios may not be as effective as anticipated. Climate mitigation policies could potentially be reversed ('backtracking').

The response of the climate system to an external forcing is characterised by the Equilibrium Climate Sensitivity (ECS): this is the increase in global average temperature following a doubling of atmospheric CO_2 concentrations, once all processes have reached equilibrium. The IPCC AR6 concluded, from multiple sources of evidence, that the best estimate of ECS was 3°C, with a likely range of 2.5-4°C and a very likely range of 2-5°C (Forster et al., 2021). The higher the ECS, the greater the increase in global average temperature for a given increase in

greenhouse gas concentrations. The latest (CMIP6) generation of climate models typically have a higher ECS than previous generation models (primarily due to changes in the representation of cloud processes), although the IPCC noted (Forster et al., 2021) that 'some of the high-sensitivity CMIP6 models are less consistent with observed recent changes in global warming' but that they 'provide insights into low-likelihood high-impact outcomes, which cannot be excluded based on currently available evidence'.

Considerable amounts of carbon are stored in soil and vegetation, and as the climate warms some of this carbon could potentially be released (as CO_2 or methane) and further increase warming. Such accelerated feedbacks are currently not explicitly incorporated into climate models used to project future climate change and could potentially lead to greater warming. Four potential feedbacks have received significant attention (Canadell et al., 2021). As permafrost thaws, carbon stored in frozen soil is released to the atmosphere. This is highly likely to occur, but the amount of carbon released and effect on climate is low: it could potentially increase global temperatures by up to 0.4°C (Armstrong McKay et al., 2022). Tropical forest dieback would also potentially release carbon into the atmosphere as vegetation dies due to high temperatures or drought. There is considered to be a low chance that this would happen (Canadell et al., 2021), and the maximum effect on global average temperature is up to 0.2°C (Armstrong McKay et al., 2022). Global warming leads to loss of boreal forest at its southern margin and the potential release of carbon, but this is offset by encroachment of temperate forest and boreal forest gain in the north. The maximum estimated net effect on global average temperature is a reduction of 0.04°C (Armstrong McKay et al., 2022). The fourth potential feedback is the release of methane from frozen ocean sediments, but this is considered unlikely to markedly affect concentrations in the atmosphere over the 21st century (Canadell et al., 2021).

These three drivers are independent and could act separately or in combination. The likelihood of accelerated feedbacks occurring is higher if either of the other two drivers apply. A high ECS with low emissions would lead to greater changes in climate than would otherwise have been anticipated, but in practice these are likely to be similar to or less than the changes projected with higher emissions, so a 'high ECS/low emissions' scenario is not developed here.

The HILL-1 enhanced warming scenario is developed from the UKCP18 RCP8.5 projections. This is because (i) the RCP8.5 forcing scenario assumes emissions that are considerably higher than current policy scenarios (Figure 4.4), and (ii) the HadGEM3-GC3.05 climate model used to construct the UKCP18 climate projections has a high ECS (Andrews et al., 2019): it is implicitly above 5°C. RCP8.5 was never intended to be interpreted as a 'business-as-usual' scenario – it was designed

explicitly as an extreme scenario to explore climate sensitivity to forcing – but (Hausfather & Peters, 2020) has frequently been erroneously interpreted as such.

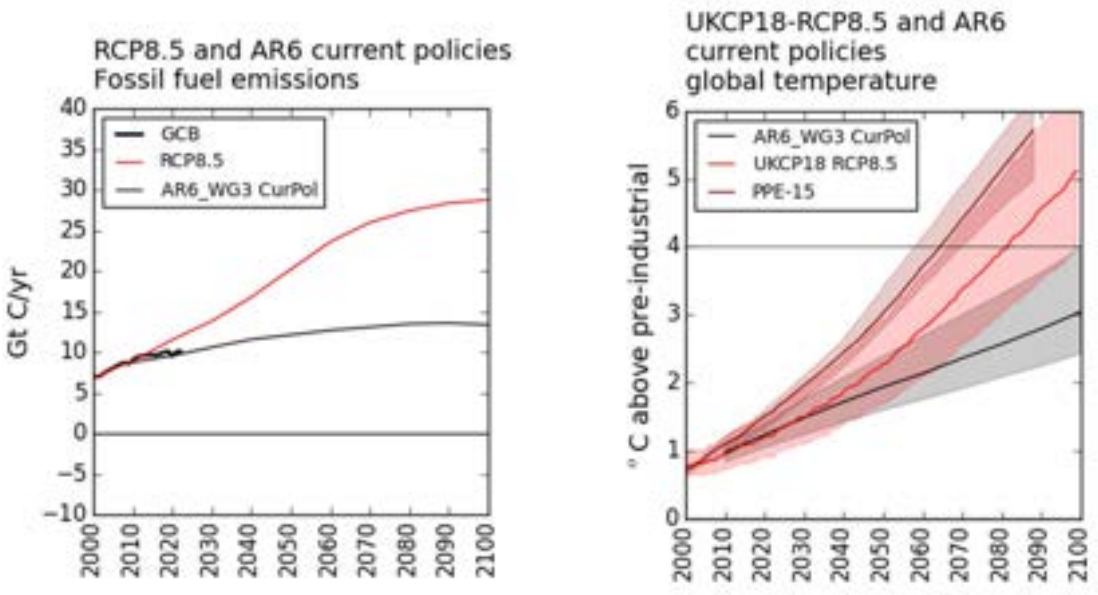

Figure 4.4: Global fossil fuel emissions and global average temperature under RCP8.5 and IPCC AR6 WG3 'current policies' scenarios. The left panel shows global fossil fuel emissions with RCP8.5 and the IPCC AR6 WG3 current policies marker scenario, together with observed emissions from the Global Carbon Budget (Friedlingstein et al., 2023). The right panel shows global average temperature change from the IPCC AR6 WG3 current policies marker scenario (10th to 90th percentile range, plus median), the range from the UKCP18 RCP8 probabilistic strand (10th to 90th percentile range, plus median), and the range from the UKCP18 PPE-15 global strand (lowest to highest, plus median, averaged over 20 years)

RCP8.5 tracked current total CO_2 emissions closely to around 2015, but this is largely because low estimates of land use emissions are offset by high estimates of fossil fuel emissions, so past performance does not necessarily mean RCP8.5 is a good guide to the future. Working Group III of the IPCC AR6 concluded that 'high-end emissions scenarios, such as RCP8.5…, are becoming less likely with climate policy and technology change…but high-end concentration and warming levels may still be reached with the inclusion of strong carbon or climate feedbacks' (Riahi et al., 2022; see also Pederson et al., 2020; Hausfather & Peters, 2020). It also concluded that RCP8.5 is useful as a high-end, high-risk scenario. The IPCC AR6 Synthesis Report concluded that 'very high emissions scenarios have become less likely but cannot be ruled out' (IPCC, 2023b). The technical report for CCRA3 also states that RCP8.5 scenarios that exceed 4°C before the 2080s can be used as proxies for

climate scenarios with high carbon cycle feedbacks or high climate sensitivities (Watkiss & Betts, 2021).

The UKCP18 RCP8.5 probabilistic strand has a median increase in global mean temperature of 5.1°C above pre-industrial levels by 2100 (a 10th to 90th percentile range of 4.0-6.5°C: Figure 4.4). The PPE-15 global, regional and local strand, based on HadGEM3-GC3.05, has a median increase of 5.7°C over the period 2080-2099 (lowest to highest range of 5.0 to 6.3°C). Both are considerably warmer than the IPCC AR6 WGIII 'current policies' estimate. The median PPE-15 increase is greater than the median probabilistic strand increase because HadGEM3-GC3.05 has a higher climate sensitivity than the other models used to construct the probabilistic strand.

Some users use the UKCP18 probabilistic strand and others the global, regional and local strands. The HILL-1 scenario is therefore specifically defined here as *either* the 95th percentile of the UKCP18-RCP8.5 probabilistic strand (or the 5th percentile where climate change leads to a reduction in the climate indicator), *or* the most extreme change (increase or decrease as relevant) from the PPE-15 global, regional or local strand. The changes from the probabilistic strand are larger than the changes from the PPE-15 strands. It is not possible to specify any one member of the PPE-15 ensemble to represent HILL-1 because different members are the most extreme for different climate variables in different times of the year in different places.

The HILL-1 sea level rise scenario is defined as the 95th percentile of the UKCP18 marine strand projections (Palmer et al., 2018a).

The larger the increase in global average temperature, the greater the chance that the climate system crosses a 'tipping point' leading to step changes in global or regional climate response (Armstrong McKay et al., 2022). HILL-1 assumes no tipping points are crossed (except insofar as accelerated feedback is categorised as a tipping point). Scenarios HILL-4 (increased effect of Arctic Amplification), HILL-5 (ocean circulation change) and HILL-6 (accelerated sea-level rise) involve tipping points, and their likelihood is increased under scenario HILL-1.

The difference between the HILL-1 enhanced scenario and a 4°C or current policies scenario increases over time. Until the 2040s there is little difference in either global average or UK temperature, but by the 2050s RCP8.5 produces global average temperatures approximately 0.4°C above a current policies scenario (median global average temperature increase of 2.4°C compared with 2°C: Figure 4.3). There is, however, little difference in change in UK rainfall between low and high greenhouse gas emissions to the 2050s. Before the 2040s, much of the difference in climate

change between emissions scenarios reflects differences in short-lived climate forcings, specifically aerosols. Scenario HILL-2 describes the additional climate effect of a major reduction in aerosols.

4.3 HILL-2 Rapid aerosol reductions

Atmospheric aerosols are small particles suspended in the atmosphere. Some are emitted directly to the atmosphere, whilst others – secondary aerosols - are produced in the atmosphere through chemical reactions with precursor gases (Myhre et al., 2013). Human activities including combustion of fossil fuels and biomass burning release black carbon (soot), organic carbon particles and sulphur dioxide. The sulphur dioxide oxidises to create sulphate aerosols. Aerosols influence climate by directly reflecting incoming solar radiation back to space and by modifying the properties of clouds to make them more reflective. Aerosols cool the planet and therefore offset to a certain extent the effect of increasing greenhouse gas concentrations: historically they have reduced global warming by around a third. High aerosol concentrations also lead to poor air quality, so many countries have enacted and are enhancing measures to reduce emissions of aerosols and their precursors in order to improve air quality. The emissions scenarios used to run climate models include assumptions about how future emissions of aerosols and their precursors may change (Rao et al., 2017), but it is plausible that aerosol emissions might reduce much more rapidly than is assumed in conventional scenarios and lead to larger increases in temperature (Persad et al., 2022). Asia is presently the largest source of aerosol emissions, and the largest future reductions also occur there (Lund et al., 2019; Wilcox et al., 2020). Changes in aerosol emissions have an almost immediate impact on air quality and climate because of the short atmospheric lifetime of aerosols. This is in contrast to CO_2 and other greenhouse gases. Reductions in aerosol emissions therefore have the potential to cause rapid climate changes.

Rapid aerosol reductions would result in increased incident shortwave radiation at the Earth's surface, particularly over Asia, warming the globe (Figure 4.5). This warming is largest in the Northern Hemisphere, where most anthropogenic aerosol sources are located. The asymmetry in the radiative and temperature effects of aerosol between the Northern and Southern Hemispheres drives associated shifts in the position of the Inter-Tropical Convergence Zone (ITCZ: Allen at el., 2015), which moves northward as aerosol emissions are reduced (Allen, 2015). Aerosol reductions also lead to increases in the strength of the monsoons, particularly the Asian summer monsoon, adding to the effects of increases in greenhouse gases (Wilcox et al., 2020). The spatially heterogeneous nature of aerosol emissions means they are likely to influence the atmospheric and oceanic circulation (Douville et al., 2021). Future reductions in predominantly Asian aerosol emissions could

potentially influence UK climate by altering the stationary wave pattern and therefore the location of blocking anticyclones (Wilcox et al., 2019), but these effects are small compared to interannual variability in UK climate, and dependent on the model used in the simulation. Similarly, estimated changes in UK precipitation and storminess are also small and model-dependent. Past aerosol increases have been tied to a strengthening of the Atlantic Meridional Overturning Circulation (see HILL-5). However, this effect is a result of both the hemispheric asymmetry of the aerosol forcing (Menary et al., 2020) and local aerosol forcing around the North Atlantic basin (Hassan et al., 2021; Robson et al., 2022), so may be weaker in future when there will not be large changes in North American and European emissions (Lund et al., 2019).

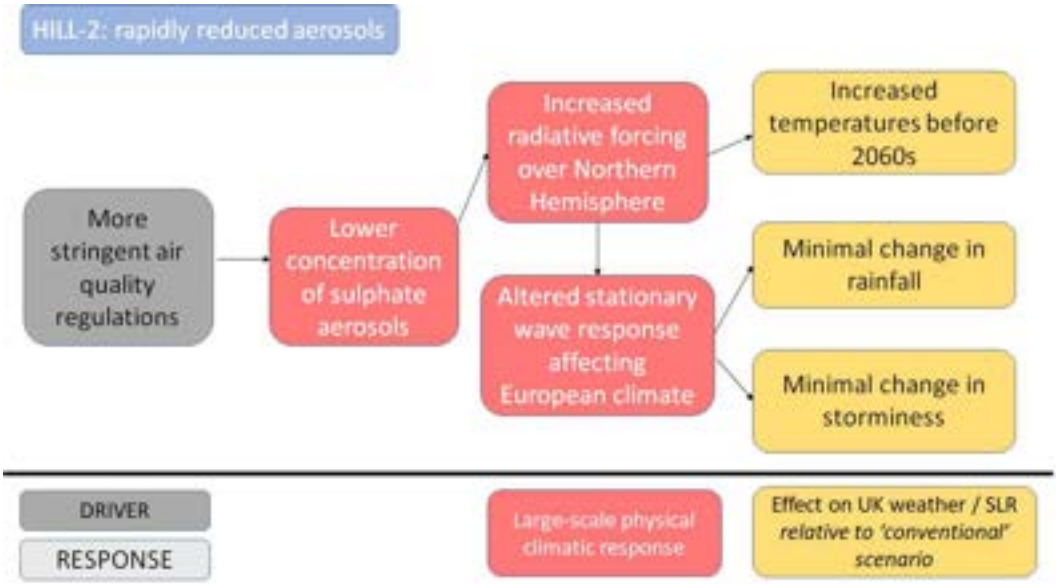

Figure 4.5: Causal loop diagram for the reduced aerosol scenario HILL-2. The red boxes describe the large-scale climate processes affected by the storyline, and the yellow boxes describe the consequences for the UK.

Aerosols cool the Earth by at least 0.5°C, offsetting part of the global warming due to increased atmospheric concentrations of greenhouse gases (GHGs) (Samset et al., 2018; Szopa et al., 2021). However, the magnitude of global and regional aerosol forcing, and its associated effects differs markedly between models. Anthropogenic aerosol forcing represents the largest uncertainty in the anthropogenic forcing of climate (Szopa et al., 2021).

Despite the uncertainty in the representation of aerosol-climate interactions, aerosols have been shown to have driven the magnitude and even sign of observed trends in global temperature, variations in the location of the tropical precipitation belt, monsoon rainfall changes, and wet and dry extreme events over substantial portions of the historical period (Allen et al., 2015; Marvel et al., 2020; Polson et a., 2014; Wilcox et al., 2013). Differences in regional aerosol emission pathways have been

linked to significant differences in how climate will evolve up to 2050, including the Asian summer and winter monsoon, temperature extremes over Europe and China (Luo et al., 2020), East and West African rainfall (Scannell et al., 2019), and Arctic climate (Schmale et al., 2021). However, in contrast to monotonically increasing GHG forcing, the influences of short-lived aerosols are more difficult to separate from decadal climate variability.

The scenario here is based on climate model simulations using three climate models and two aerosol emission scenarios (Luo et al., 2020): one where current legislation determines aerosol emissions to 2050 (Current Legislation - CLE), and one where aerosol emission reductions are made as rapidly as possible using all currently available technology (Maximum Technically Feasible Reductions – MTFR; https://previous.iiasa.ac.at/web/home/research/researchPrograms/air/ECLIPSEv5a.html). In both cases, emissions of all other greenhouse gases follow RCP4.5. The rate of emission reduction included in MTFR is similar to recent reductions seen in China, which has reduced its emissions of sulphur dioxide (an important aerosol precursor) by 70% since 2010 (Li et al., 2017). The comparison between CLE and MTFR represents the largest difference in aerosol pathways currently available in plausible, transient, publicly available emission datasets. Hence, the effect shown here is likely to be close to an upper bound. The difference in emissions by the 2040s between CLE and MTFR is around 1.3 times the difference between RCP8.5 and MTFR (Figure 4.6). This implies that – if the climate response to aerosol forcing is linear – the effect on climate of reducing aerosol emissions to MTFR levels from the levels assumed in RCP8.5 would be around 75% of the effect of moving from CLE to MTFR. The difference between RCP8.5 and MTFR reduces after the 2050s, and the effect of more rapid reductions in aerosols is therefore assumed to be negligible by 2100 because most aerosol emissions have been eliminated by then.

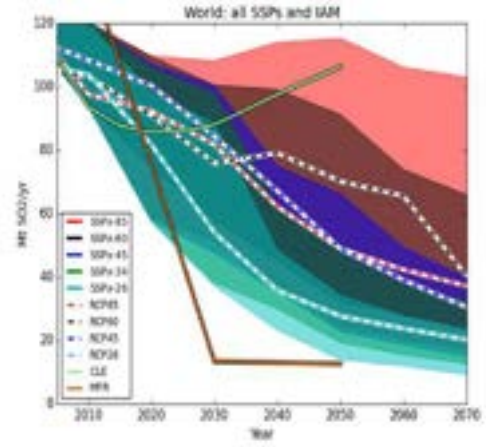

Figure 4.6: Emissions of sulphur dioxide in the Current Legislation (CLE), Maximum Technically Feasible Reductions (MTFR), RCP4.5 and RCP8.5 emissions scenarios (Scannell et al., 2019). Other aerosol and precursor emissions follow similar pathways.

The scenario assumes no difference to conventional projections to 2020, then a linear increase in additional temperature increase to a peak of 0.75°C in 2040, followed by a linear decline to no difference in 2100. The scenario can be applied to any greenhouse gas emissions scenario.

The simulated difference in global mean temperature between the CLE and MTFR scenarios varies between the three climate models (Figure 4.7), reflecting differences in the magnitude of their simulated aerosol forcing. The HadGEM3-GC2 model shows the greatest difference: this model generally shows the greatest sensitivity to future aerosol emissions. The HILL-2 scenario (Figure 4.8) is based on the upper estimates from HadGEM3-GC2.

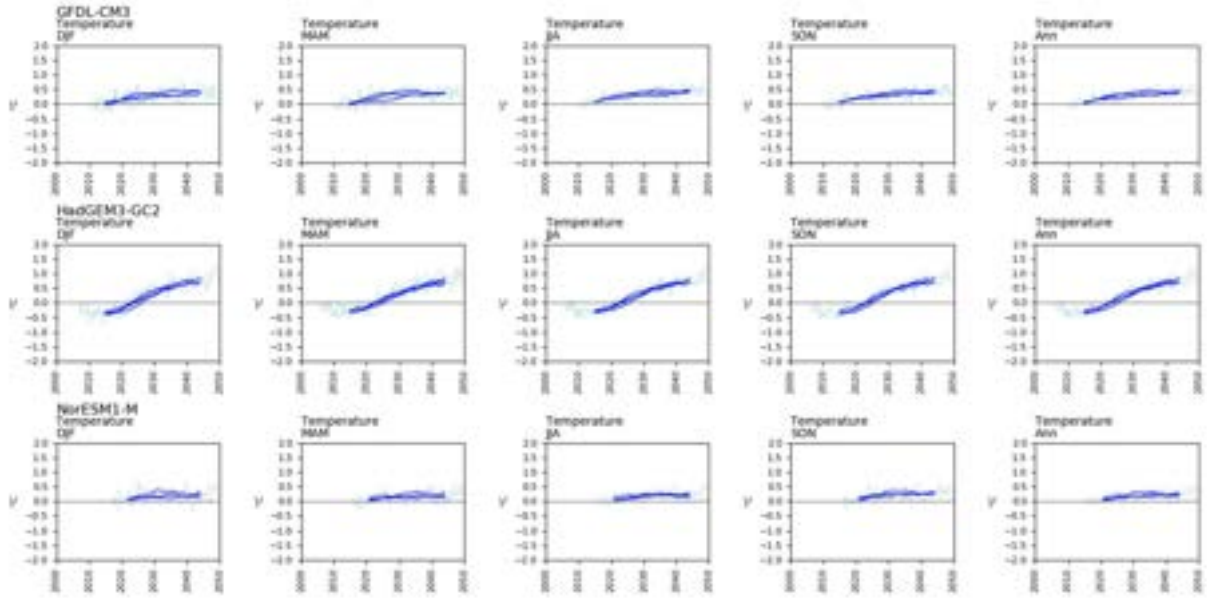

Figure 4.7: The difference in global average temperature between the CLE and MTFR scenarios, by season and for three climate models. Each plot shows the annual difference (pale blue lines) and the difference in the 10-year running mean temperature (dark blue lines) for each ensemble member.

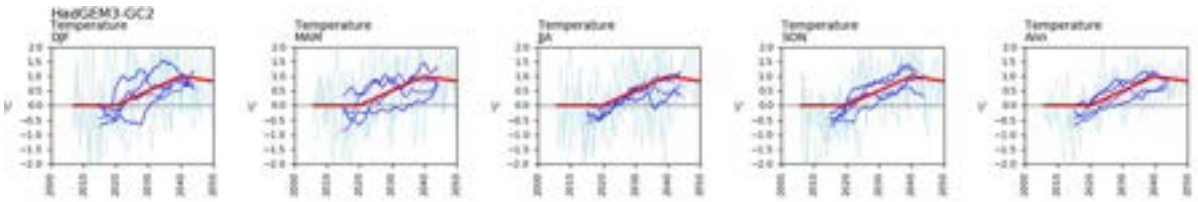

Figure 4.8: The difference in average temperature across the UK between the CLE and MTFR scenarios, by season and for three climate models. Each plot shows the annual difference (pale blue lines) and the difference in the 10-year running mean temperature (dark blue lines) for each ensemble member. The red line shows the stylised summary scenario (see text).

4.4 HILL-3 Volcanic cooling

Volcanism has been a significant driver of past climatic variability (Robock, 2000), and eruptions will continue to affect global and regional climate. The past 150 years have had relatively few major eruptions which have affected climate away from the volcano itself, with the most notable in recent decades being the eruption in June 1991 of Mount Pinatubo in the Philippines. This led to a reduction in global average temperatures of around 0.2ºC in 1992, or a larger reduction of 0.4-0.5ºC correcting for the warming effect of the 1992 ENSO event (McCormick et al., 1999). The eruption of Tambora in August 1815 led to reductions in global average (land) temperature of around 1ºC for around a decade (Kandlbauer et al., 2013), with reductions across northern Europe in the summer of 1816 (the “year without a summer”) of up to 2ºC (Raible et al., 2016).

Volcanic eruptions emit sulphur dioxide (SO_2), which converts over time into sulphate aerosols. Sulphate in the troposphere is quickly washed out by rain, but large explosive eruptions can inject SO_2 high into the stratosphere where sulphate remains for much longer. Observational and proxy evidence (e.g. Stoffel et al., 2016; Tejedor et al., 2021) illustrate the impact of some recent and historical eruptions – for example of Mount Pinatubo – but the climatic effects of past and potential future eruptions can most effectively be assessed using theory and climate models (e.g. Bittner et al., 2016; Bethke et al., 2017; Coupe & Robock, 2021; Lee et al., 2021; Zhou et al., 2021). Different studies using different climate models have simulated different qualitative responses to volcanic forcing, with a large part of the differences due to differences in the assumed volcanic forcing and relationships between aerosol loading and their effects on the radiation balance. However, simulation experiments conducted under VolMIP using consistent forcings produce more similar simulations of the climatic response (Zanchettin et al., 2022).

An increased concentration of sulphate aerosols in the stratosphere leads to an increase in albedo, so a greater proportion of the incoming solar radiation is reflected back to space. This directly leads to surface cooling – a radiative impact – and a weaker hydrological cycle. The coldest decades of the past 2000 years followed volcanic eruptions (Lee et al., 2021). Cooling is greatest over land, and changes in the land-sea contrast lead to a weakening of monsoon systems and reduced rainfall. The sulphate aerosols are also heated by absorption of upwelling longwave radiation leading to increases in temperature in the lower stratosphere. These two effects together alter temperature gradients between the equator and the poles which potentially generates changes to atmospheric circulation patterns – a dynamic impact (Figure 4.9). Theoretical studies suggest a poleward shifted jet stream in response to such a temperature perturbation. Most significantly for the UK, changes in temperature gradients increase the strength of the stratospheric polar vortex in the

first winter after the eruption, which leads to a poleward shift in mid-latitude westerlies and potentially an *increase* in temperature in the first winter. The background state of the climate – and particularly the tropical ocean – affects the response of the climate system to the eruption. Aerosols from tropical eruptions spread globally, due to a general poleward transport of air within the stratosphere, but aerosols from high latitude eruptions remain at high latitudes and get washed out more quickly. Aerosol heating is less at high latitudes, so high latitude eruptions tend to have a limited effect on circulation (Oman et al., 2005). The effects of a sequence of eruptions appear to be additive (Newhall et al., 2017).

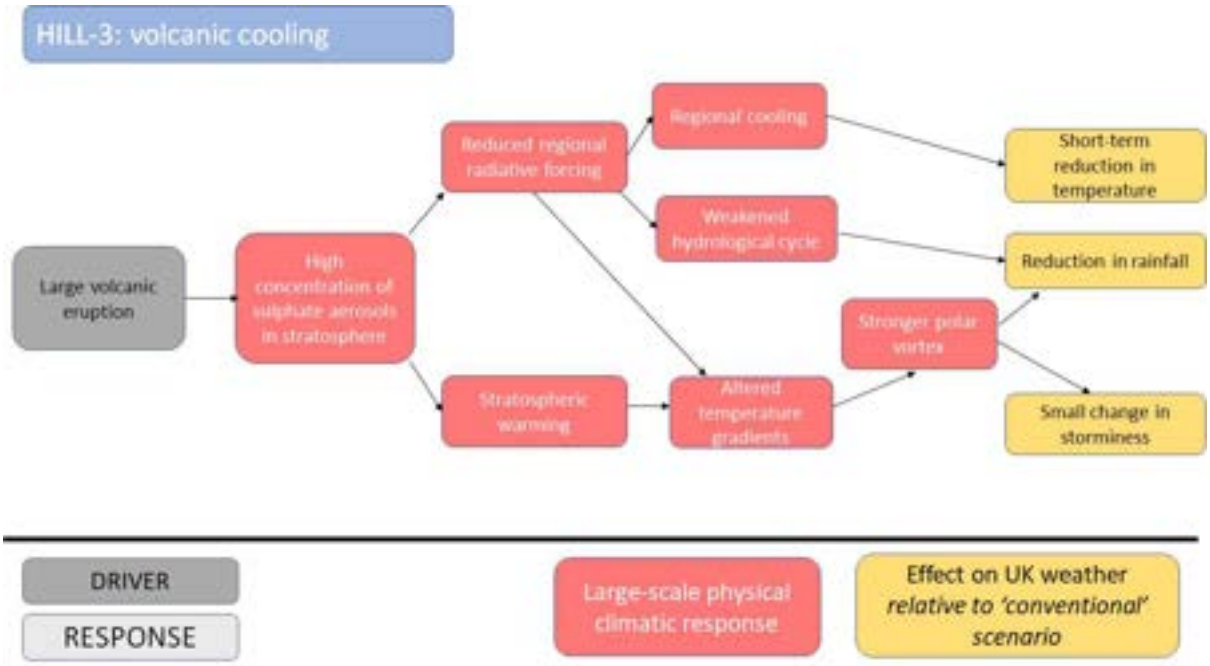

Figure 4.9: Causal loop diagram for the volcanic cooling scenario HILL-3. The red boxes describe the large-scale climate processes affected by the storyline, and the yellow boxes describe the consequences for the UK.

Whilst there is good evidence for very substantial changes in tropical and monsoon precipitation following an eruption, there is much more uncertainty in how precipitation may change across Europe. This is partly due to the large effect of natural variability making it difficult to identify a signal, and potentially partly due to the representation of processes in climate models. The summer of 1816 following Tambora was wet as well as cool (Raible et al., 2016), and information from proxy records suggests that tropical eruptions are followed by wetter conditions in Europe (Tejedor et al., 2021). However, climate model projections show varied responses: some show little change, some suggest a reduction (e.g. Pausata et al., 2015) due to lower sea surface temperatures, and others imply an increase – at least in the first winter – due to stronger westerlies.

The effect of a volcanic eruption on global and regional climate therefore depends on the size and characteristics of eruption (amount of material ejected which reaches the stratosphere, and its size distribution), the location of the eruption and, to a lesser extent, the timing of the eruption. The specific effect over the UK depends further on the nature of the regional response, which as noted above remains uncertain.

Volcanic eruptions are classified using the Volcanic Explosivity Index (VEI), which is based on the total amount of material ejected. Eruptions with a VEI of 7 occur between one and two times per thousand years (Newhall et al., 2017): the most recent was Tambora in 1815, and the previous was Samalas (again in present-day Indonesia) in 1257. The scenario here assumes a VEI-7 eruption broadly equivalent in terms of sulphate aerosols to Tambora. The scenario is based on an analysis by Bethke et al. (2017), which compared an ensemble of simulations assuming averaged volcanic forcing with a set of scenarios assuming different series of stochastically-generated volcanic events. Specifically, the scenario is constructed by comparing the time series with the largest synthetic event (series 45 out of the 60 stochastic series) with the ensemble mean climate with averaged volcanic forcing (Figure 4.10) but is compared with responses from other observational and modelling studies.

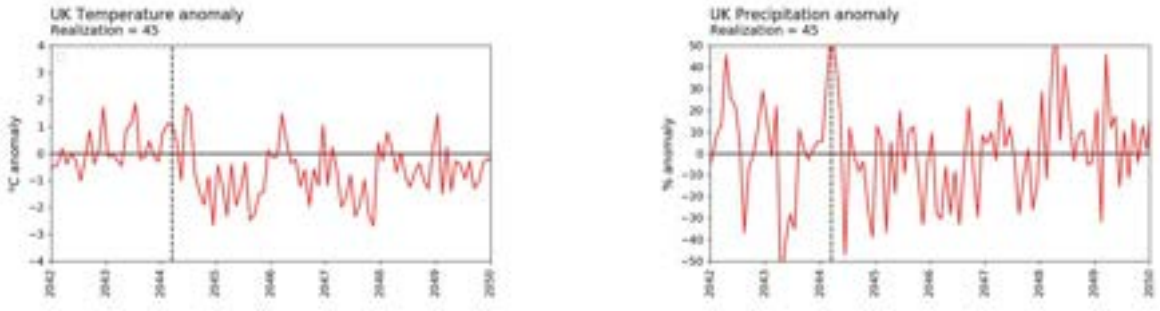

Figure 4.10: Variability in temperature and precipitation across the UK following an eruption, relative to the average over the preceding five years. Realization 45 from Bethke et al. (2017), with an assumed eruption in 2044.

The scenario assumes a reduction in temperature of 2.5°C and reduction in rainfall of 20% nine months after the assumed date of the eruption, returning to the original trend after 60 months. The effects of a series of eruptions can be estimated by repeating this scenario. This extreme reduction in monthly temperature and rainfall is *smaller* than assumed for the Set 1 extreme monthly scenarios (Section 5.6.2), but the cold and dry anomaly is assumed to persist for up to 60 months. It can be applied to any emissions scenario.

4.5 HILL-4 Stronger Arctic Amplification

It is well established both from observations and model simulations that average temperatures increase more at northern high latitudes than at low latitudes: this is known as Arctic Amplification (e.g. Barnes & Screen, 2015; Previdi et al., 2021; Shu et al., 2022). This is partly due to positive feedbacks with the land surface (less snow and Arctic sea ice cover means less of the incoming solar radiation is reflected back to the atmosphere and therefore more is absorbed at the surface) and partly due to positive feedbacks within the atmosphere (Goosse et al., 2018). The precise mechanisms for this well-documented effect, however, are complicated (Overland et al., 2016) and there is no simple clear causal pathway. Accelerated loss of Arctic sea ice is both a driver and a consequence of Arctic Amplification. The IPCC AR6 (Fox-Kemper et al., 2021) concluded that it was very likely that the Arctic Ocean would be ice-free in summer under intermediate and high emissions, and very likely that it would remain ice-covered in winter. However, it also noted the high uncertainty in how Arctic sea ice cover responds to increased global warming (Notz & SIMIP Community, 2020), and that different methods yield different estimates of the rate of decline. A number of more recent studies (e.g. Docquier & Koenigk, 2022; Zhao et al., 2022; Kim et al., 2023) based on weighting climate model projections according to their skill in simulating the observed decline have suggested that sea ice cover is more sensitive to warming than most climate models imply.

Arctic Amplification reduces surface temperature gradients between the equator and the pole and increases geopotential heights in high latitudes (Figure 4.11). Both temperature and pressure gradients are therefore reduced, and this would lead to both a reduction in the strength and a southwards shift of the jet stream and therefore weaker storm tracks and an increased chance of persistent stable weather conditions across the UK and northern Europe. However, stronger warming in the upper troposphere in the tropics than at high latitudes acts in the opposite direction and leads to an *increase* in gradients and a *poleward* shift in the jet stream: the effect of Arctic Amplification therefore depends on this ‘tug-of-war’ between opposing drivers. Increased geopotential heights could potentially generate upward wave propagation into the stratosphere leading to a weakened stratospheric polar vortex and more frequent sudden stratospheric warmings leading to cold events. Arctic Amplification is strongest in winter so its potential effects are likely to be greater then, although weaker storm tracks in summer could plausibly lead to warmer and drier conditions and a greater risk of heatwaves (Coumou et al., 2018; Rousi et al., 2022).

The potential effects of Arctic Amplification on mid-latitude weather were first raised in the early 2010s following a series of cold winters in North America and northern Europe which appeared to follow seasons with large reductions in Arctic sea ice

(Francis & Vavrus, 2012; 2015), and observational evidence has subsequently showed that there is no detectable reduction in cold events in mid-latitudes despite recent Arctic Amplification and global warming (Cohen et al., 2023). The issue has remained controversial, however, partly because subsequent years with low ice cover have not led to cold extremes (Blackford & Screen, 2020) and partly because considerable year-to-year variability in both Arctic conditions and circulation patterns makes identifying causal relations challenging. Mainly, however, it is controversial because climate models typically underestimate Arctic Amplification (Rantenen et al., 2022) and differ widely in their simulation of the effects of Arctic Amplification (Cohen et al., 2020; Overland et al., 2021; Lo et al., 2023). Climate models typically simulate a strengthening of the winter jet stream over the North Atlantic and an extension eastwards into Europe (e.g. Harvey et al., 2020; 2023) as an outcome of competing effects, but do not necessarily simulate very well subsequent weaking of the polar vortex. The HadGEM3.05 PPE15 ensemble used to construct UKCP18 climate projections simulates a poleward shift in the jet stream in winter. The most recent comprehensive assessment of the effects of Arctic Amplification in the Polar Amplification Model Intercomparison Project (Smith et al., 2019; 2022) concluded that Arctic Amplification (specifically due to sea ice loss) led to a slight weakening of mid-latitude westerlies, but that the modelled response was possibly underestimated.

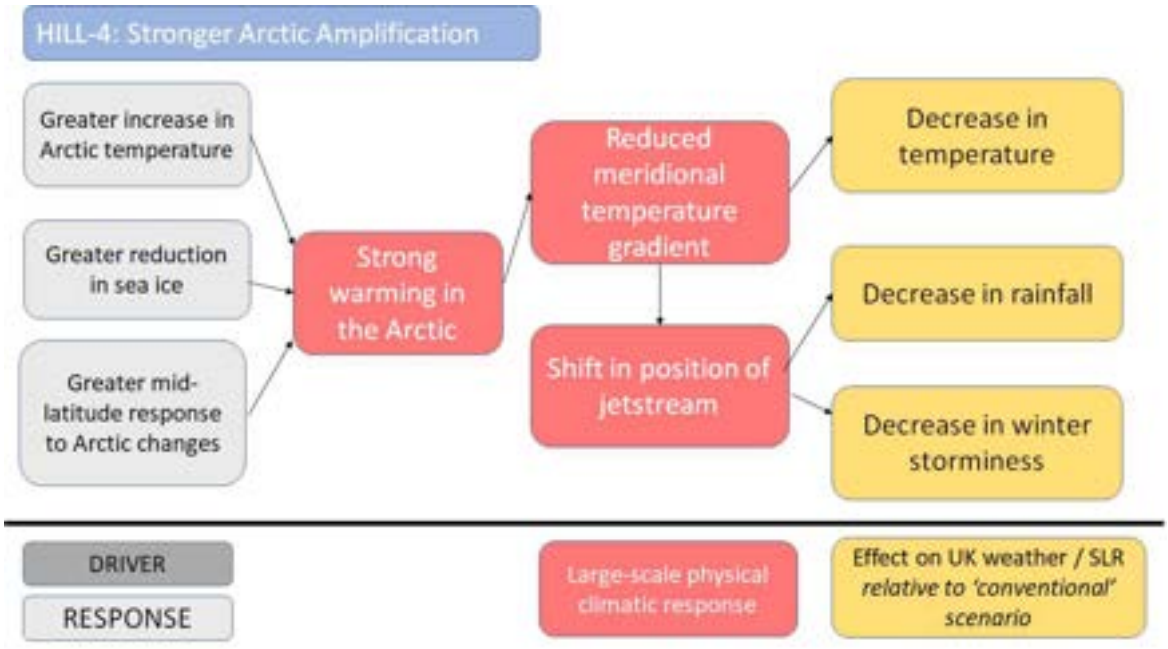

Figure 4.11: Causal loop diagram for the stronger Arctic Amplification scenario HILL-4. The red boxes describe the large-scale climate processes affected by the storyline, and the yellow boxes describe the consequences for the UK.

The scenario here assumes that the effects of Arctic Amplification on circulation patterns are *stronger* than currently represented in climate models, either because the rate of Arctic sea ice loss is stronger or because the modelled response is stronger. The scenario assumes a southward shift in the position of the jet stream and a weakening in jet stream strength throughout the year. During winter, a weakened jet stream leads to a greater forcing of planetary waves upwards into the stratosphere, leading to sudden stratospheric warmings, a weakening of the polar vortex, and at the surface, an outflowing of cold air from the Arctic towards the UK.

The scenario is developed from the UKCP18 PPE15 RCP8.5 projections. It is based on the difference between the monthly mean temperature, rainfall and windspeed in years with a weak southerly jet and all years, over the 30-year period 2069 to 2098. A weak southerly jet is defined here to occur in years when the mean monthly latitude and strength are both more than 0.5 standard deviations below the 30-year monthly mean. Figure 4.12 shows the absolute difference in change by the 2080s between weak southerly years and all years for eight example locations across the UK. There is considerable variability across the 15 ensemble members, largely because of the small size of the weak southerly composites, and all the years in the composite are weak and southerly – which would not necessarily be the case with enhanced Arctic amplification – but the plots do give an indication of the potential effect on mean monthly climate of a shift towards more frequent weak southerly jets. The effect on rainfall is lower than would be inferred from the theoretical considerations outlined above.

During the winter months, it is plausible for enhanced Arctic amplification to produce reductions in mean 30-year temperature of up to 1.5^{o}C relative to the increase that would be projected with conventional estimates of Arctic amplification by the 2080s. The change in mean monthly rainfall in winter months could be up to 20 percentage points lower than conventional estimates, and the change in mean monthly windspeed up to 15 percentage points lower.

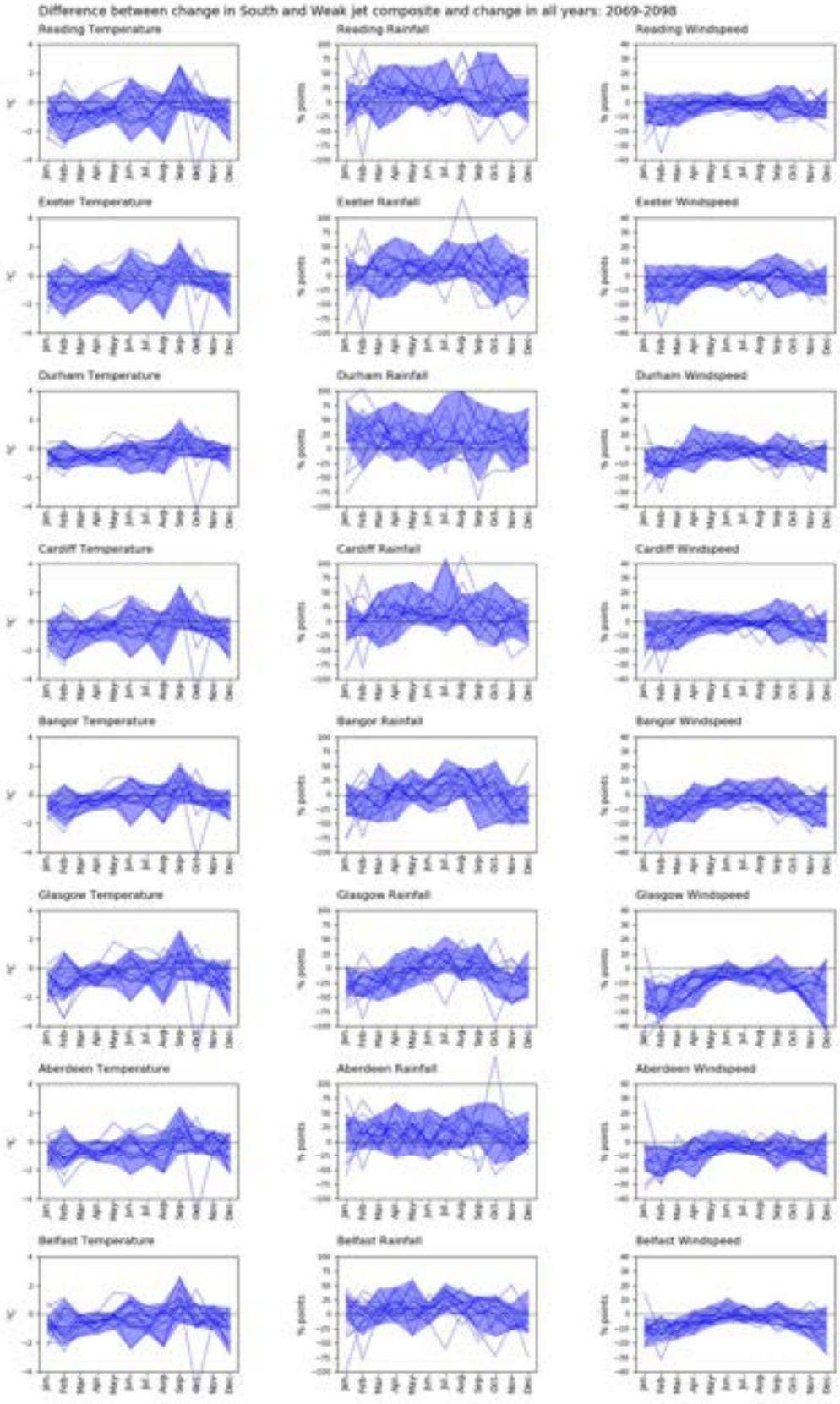

Figure 4.12: The difference in change in monthly mean temperature, rainfall and windspeed in years with southerly weak jet streams compared with all years over the period 2069-2098. The shaded area shows the range across all the UKCP18 PPE15 RCP8.5 members with at least three southerly weak years, and the thin lines show all 15 ensemble members.

4.6 HILL-5 Change in ocean circulation

The weather and climate of the UK are strongly influenced by the temperature of the North Atlantic Ocean. It affects the temperature of air masses reaching the UK, and gradients of temperature from south to north across the Atlantic Ocean affect the position and strength of storm tracks. The temperature of the North Atlantic Ocean depends on ocean circulation.

The dominant feature in the North Atlantic is the Gulf Stream, which brings warm water and therefore higher sea surface temperatures northwards from the tropical Atlantic Ocean. Temperatures in western Europe are therefore higher than the average for its latitude. The Gulf Stream is primarily driven by wind and is a part of the larger Atlantic Meridional Overturning Circulation (AMOC). The northward-flowing water is warm and salty, and as it travels northwards it cools. Because it is saltier than water from further north it is more dense, so it sinks as it cools and flows southwards at depth: it then rises slowly to the surface (primarily in the Southern Ocean). The strength of this circulation is essentially determined by salinity in the North Atlantic. The more saline the surface water, the stronger the circulation. A stronger AMOC enables the wind-driven Gulf Stream and its northerly branches (the North Atlantic Drift) to extend further north.

A warming climate is likely to increase freshwater inputs to the North Atlantic through additional precipitation, increased river runoff, and melting of sea ice and Greenland ice. This cool, fresh water reduces salinity in the North Atlantic and therefore reduces ocean density and reduces the rate at which water sinks (Figure 4.13). This weakens the AMOC and also therefore the Gulf Stream, meaning that warm northward flows are reduced and the North Atlantic therefore becomes cooler. There are some indications that the AMOC has reduced since the 19th century, but the IPCC AR6 (Fox-Kemper et al., 2021) has low confidence that it has weakened due to conflicting evidence from different sources, differences between climate models and strong year-to-year variability. Climate models – including those used to construct UKCP18 projections – generally simulate a decline in the AMOC during the 21st century (Weijer et al., 2020) and projected warming across the North Atlantic and western Europe is therefore slightly lower than would be the case without the AMOC weakening. The IPCC concludes that the AMOC is very likely to decline in the future, but there is low confidence in the rate and timing of decline. The Gulf Stream is projected to weaken during the 21st century (Fox-Kemper et al., 2021) but become warmer.

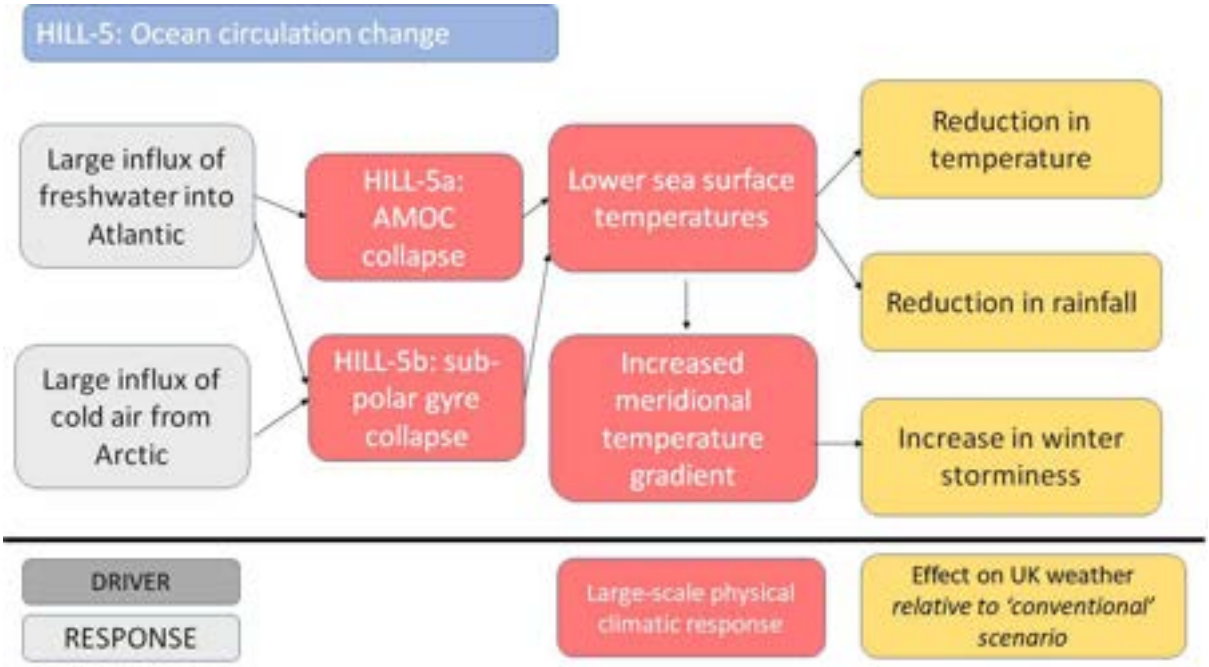

Figure 4.13: Causal loop diagram for the abrupt change in ocean circulation scenario HILL-5. The red boxes describe the large-scale climate processes affected by the storyline, and the yellow boxes describe the consequences for the UK.

Over sixty years ago it was first suggested that the AMOC has two equilibrium states – either 'on' (as now) or 'off' (e.g. Hawkins et al., 2011). A collapse, rather than a weakening, of the AMOC would lead to a reorganisation of ocean circulation and much cooler temperatures in the North Atlantic and western Europe. Such collapses have occurred in the past and have been linked to cold periods such as the Younger Dryas (12900 to 11700 years ago) which temporarily reversed warming following the most recent glacial period. AMOC collapse is the premise behind the 2004 Hollywood disaster movie 'The Day After Tomorrow'. However, there is considerable uncertainty over the likelihood of AMOC collapse, primarily due to uncertainty in both critical thresholds and the projected size of future change in AMOC and its drivers. Climate models run with plausible emissions scenarios simulate a weakening, but not collapse, in AMOC. The IPCC AR6 (Fox-Kemper et al., 2021) concluded with medium confidence that a collapse of AMOC was not anticipated before 2100, and Armstrong McKay et al. (2022)'s review of tipping points assigned medium confidence to AMOC collapse based on estimated critical temperature thresholds. Note that 'Gulf Stream Collapse' (a phrase often used in media reports) is a misnomer: the Gulf Stream is largely driven by winds, so will continue – albeit in a weaker form – even if AMOC collapses, and temperatures in the North Atlantic will remain higher than the latitudinal average. Although AMOC does not collapse under conventional scenarios, the effects of a collapse can be simulated using climate models run with large imposed inputs of fresh water or reductions in salinity. These

are known as ‘hosing experiments’ (e.g. Jackson et al., 2015; Mecking et al., 2016; Orihuela-Pinto et al., 2022; Jackson et al., 2022; van Westen et al., 2024).

If the AMOC were to collapse, the temperatures across the UK would decrease (by 5-6^{o}C), mean winter precipitation would increase in the north and west and decrease in the south and east, and summer rainfall would decrease across the whole of the UK – all relative to changes that would be expected if the AMOC did not collapse. Winter windspeeds and number of windstorms would increase. The scenario here assumes that collapse begins in 2030, its maximum effect is seen in 2050, and this effect persists to at least 2100. It is based on the hosing experiment reported by Jackson et al. (2015) and Mecking et al. (2016) using HadGEM3 GC2: this was also used by Ritchie et al. (2020). Like Ritchie et al. (2020), it is assumed that the difference between stable climates with and without AMOC collapse can be applied to conventional scenarios with any emissions pathway. The change in temperature assumed in the scenario is very similar to the change estimated for London by van Westen et al. (2024).

A collapse of the AMOC would also potentially lead to increased sea level in the Atlantic (Levermann et al., 2005) and around the UK, partly through changes to ocean currents and partly through changes in temperature and salinity and therefore the rate of thermal expansion. The magnitude of the effect around the UK are uncertain, because the estimated effects are model dependent and most analyses have been undertaken in the west Atlantic on the east coast of the US (see the review by Little et al., 2019). A plausible worst case would be for sea level to increase by up to 40cm above the level that would otherwise be assumed 20 years after AMOC collapse (i.e. increasing at a cumulative 2cm per year every year up to 40cm).

The AMOC (and Gulf Stream) is not the only circulation pattern affecting temperatures in the North Atlantic Ocean. The subpolar gyre (SPG) is a wind-driven circulation in the North Atlantic south of Greenland. Cold water from the Labrador and Irminger Seas sinks in the SPG through convection. However, increased precipitation and runoff from North America would lead to a reduction in salinity (and hence density), an increase in stratification in the Labrador and Irminger Seas and a reduction in convection. Cool water would be less likely to sink. This would lead to lower sea surface temperatures in the North Atlantic. Such a collapse of convection in the SPG has occurred in the past and is projected to occur in the future in a subset of climate models run with plausible emissions scenarios (Sgubin et al., 2017; 2019; Swingedouw et al., 2021). The AMOC and SPG are connected, but SPG collapse can occur much more rapidly than AMOC collapse and potentially occurs at lower levels of warming (Armstrong McKay et al., 2022). Swingedouw et al. (2021) found that four out of 35 CMIP6 models simulated rapid cooling in the SPG with

conventional climate scenarios and concluded that – because the models simulating cooling were amongst the models simulating the North Atlantic most accurately – the risk of encountering an abrupt cooling event during the 21st century was approximately one in three. There is some suggestion that the risk is lower with high emissions because the effect of higher temperatures on salinity offsets the effects of increased freshening.

A collapse of the SPG would have similar effects in principle to those of an AMOC collapse, although smaller. The scenario here assumes that collapse begins in 2030 with its maximum effect seen in 2050. It is assumed that there would be no additional effect on sea level rise around the UK. The scenario can be applied to any emissions pathway. The scenario is based on one of the CMIP6 models (CESM2-WACCM) that was shown by Swingedouw et al. (2021) to simulate a collapse in the SPG (Figure 4.14).

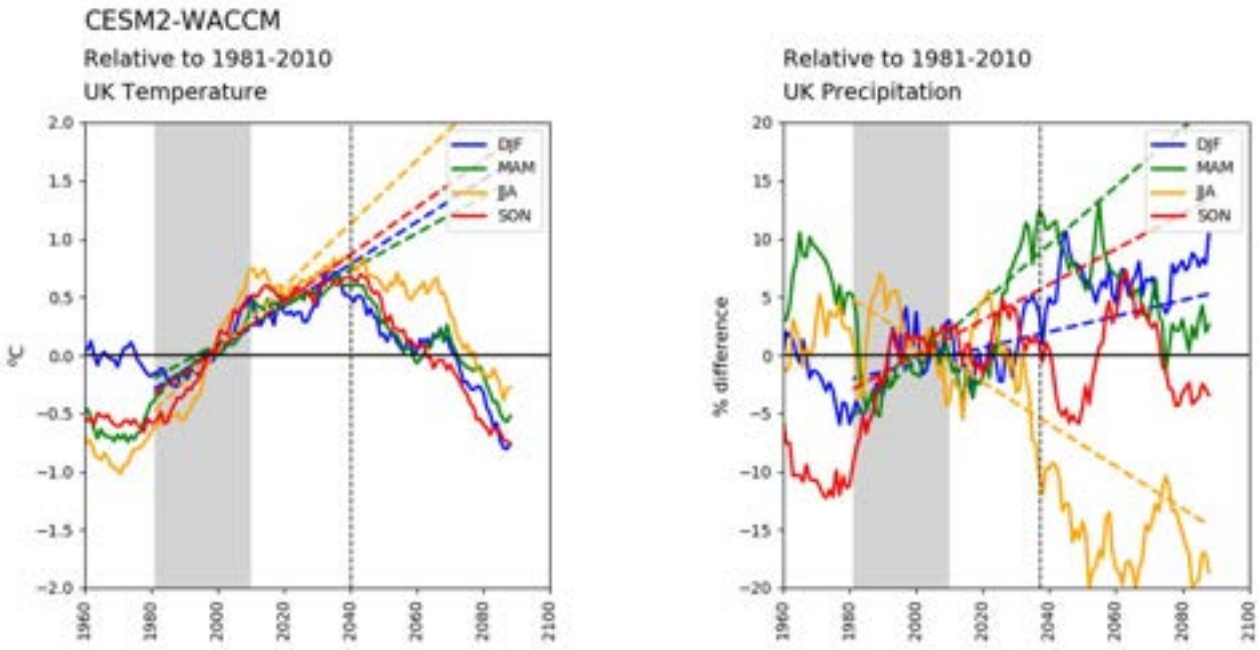

Figure 4.14: The effect of SPG collapse on UK average seasonal temperature and precipitation. CMIP6 model CESM2-WACCM with SSP1-2.6. The shaded area shows the 1981-2010 reference period, and the dotted lines show extrapolated trends calculated between 1981 and 2040 (the assumed date of collapse).

4.7 HILL-6 Enhanced sea-level rise

Global mean sea level will rise in the future due to the thermal expansion of sea water as it warms and inputs of water from melting glaciers and ice sheets and, to a much smaller extent, changes in terrestrial water storage (e.g. extraction of groundwater). The IPCC's Sixth Assessment Report (AR6; Fox-Kemper et al., 2021) concluded that global mean sea level would likely increase by between 0.63 and 1.01m by 2100, relative to the 1994-2015 mean, under very high SSP5-8.5 emissions. With emissions consistent with a 2°C increase in temperature, the likely increase in sea level would be between 0.32 and 0.55m.

However, it is possible that increased ice melt from Greenland and Antarctica could lead to substantially larger increases in sea level (Fox-Kemper et al., 2021) as summarised in Figures 4.15 and 4.16 – even with low emissions.

Large increases in ice melt from Greenland could potentially arise from accelerated feedbacks as climate warms around Greenland or due to increased calving from glaciers draining the ice sheet: changes in the surface mass balance are most important.

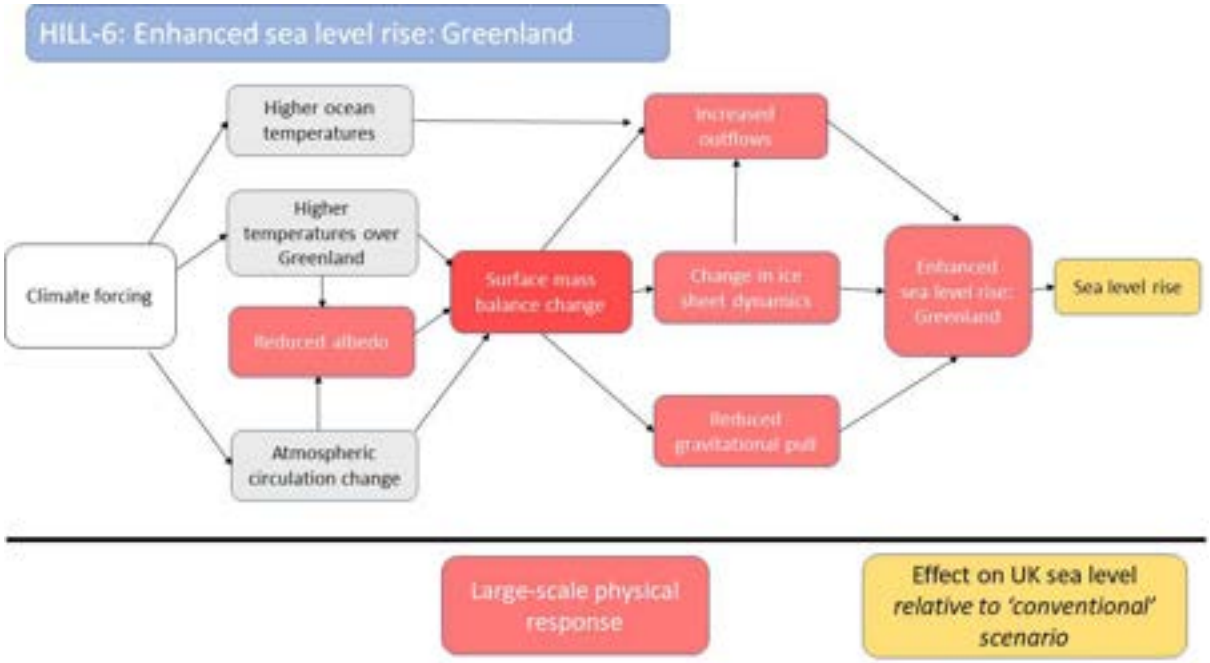

Figure 4.15: Causal relation between processes leading to a high-end contribution of Greenland to sea level rise. Based on van de Wal et al. (2022).

Large increases in ice melt from the Antarctic ice sheet could plausibly arise from Marine Ice Sheet Instability (MISI) – where ice sheets that are currently resting on the sea bed start to float and melt more rapidly – or Marine Ice Cliff Instability (MICI) – where ice cliffs become exposed to open water and fail leading to rapid ice loss (Fox-Kemper et al., 2021; Crawford et al., 2021; Golledge et al., 2019; Milillo et al., 2019). The Thwaites and Pine Island Glacier ice shelves could potentially disintegrate this century, potentially triggering MICI before 2100. In contrast to Greenland, ice sheet collapse is more important than changes in surface mass balance. There is considerable scientific uncertainty about whether or when these processes would be initiated, so there is therefore large uncertainty in their effect on sea level rise.

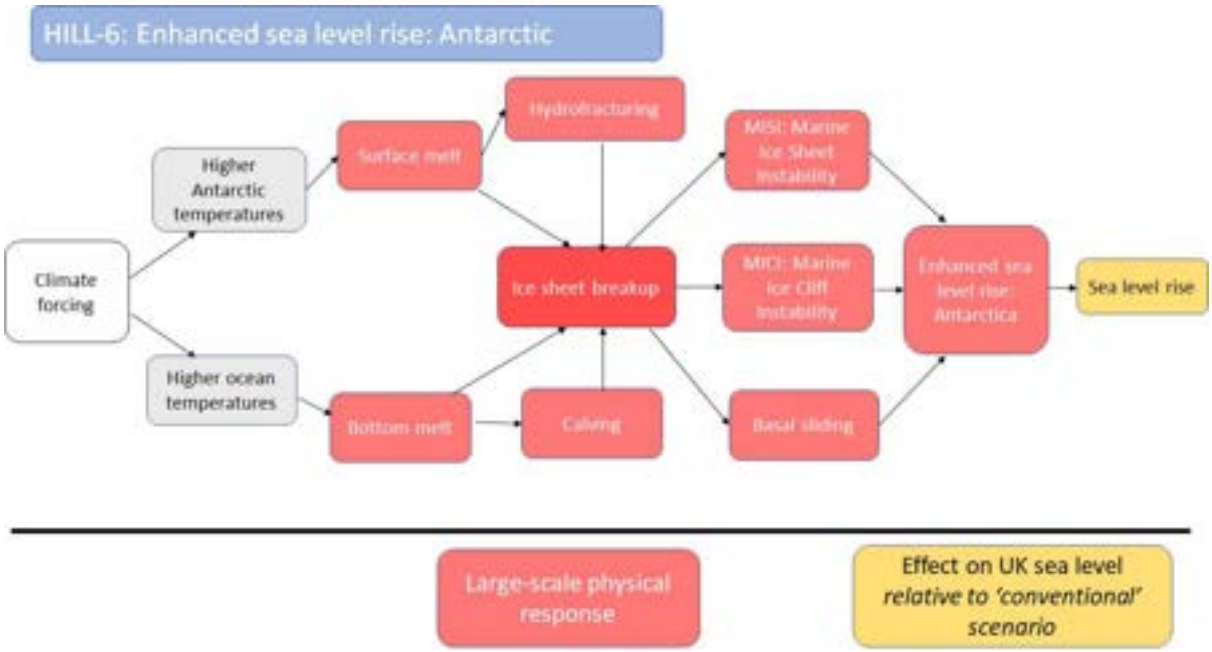

Figure 4.16: Causal relation between processes leading to a high-end contribution of Antarctica to sea level rise. Based on van de Wal et al. (2022).

The IPCC AR6 outlined a storyline (Box 9.4 in Fox-Kemper et al., 2021) which examined the potential for, and early-warning signals of, a high-end sea-level scenario unfolding within this century. In developing the storyline, emphasis was placed on understanding the driving factors involved that might lead to a high-end sea-level rise scenario, and the plausibility of those factors; no a priori probability is assessed. With high-end sea-level rise the main uncertainty is timing (i.e., when) rather than if it arises. Because it takes many hundreds of years for the cryosphere and the deepest parts of the ocean to adjust to increased air temperatures (i.e., the long-term committed sea-level), sea-levels beyond the upper limit of the likely range (1.01m for SSP5-8.5 scenario), will be exceeded in any future warming scenarios on century to millennial time scales. The AR6 storyline assumes a strong warming scenario and then considers faster-than-projected sea-level contributions from

Antarctica and Greenland. It considers processes in the models used to derive the projections that are not well represented or understand, and if adjusted could further enhance rates of sea-level rise. The quantified scenario was produced using a statistical emulator (Edwards et al., 2021) with parameters describing ice sheet behaviour. These parameters were based on a structured expert judgment study (Bamber et al., 2019) and – for MICI – one model simulation (DeConto et al., 2021). The IPCC AR6 concluded that a plausible high-impact low-likelihood increase in global average sea level by 2100 would be up to 2.3m above the 1995-2014 level with very high emissions (SSP5-8.5: 95th percentile of the emulator distribution) and 1.1m with emissions consistent with a 2^{o}C world (SSP1-2.6). The AR6 storyline has been used in the French, Swedish and Danish (DMI, 2024) extreme sea level rise scenarios.

An alternative framework for estimating global high-end sea level rise scenarios was developed by van de Wal et al. (2022). This took a co-produced approach between scientist and practitioners to provide high-end sea level estimates for practitioner application and is based on expert evaluation of physical evidence and approaches currently used in policy environments to understand high end risk. The authors developed a different approach to that used by Fox-Kemper et al. (2021) for projected sea level contributions from Greenland and Antarctic but highlight that their approach complements rather than replaces that of Fox-Kemper et al. (2021). van de Wal et al. (2022) estimated a global high-end sea level rise by 2100 of 1.6m with SSP5-8.5 and 0.8m with SSP1-2.6: these are both lower than the IPCC AR6 estimates. The van de Wal et al. (2022) estimates are used in the Dutch extreme sea level rise scenario (van Dorland et al., 2023).

A third approach was developed by Palmer et al. (2024), who defined five illustrative sea level storylines around the UK, based on an ensemble of simulations conducted for and subsequent to the UKCP18 sea level projections (Palmer et al., 2018a;b; 2020). In essence, the approach involves selecting individual ensemble members consistent with storylines describing specific increases in global mean sea level at specific times. Two of their illustrative storylines (H1 and H2) define ‘high-end’ estimates of sea level rise. H1 is based on the van de Wal et al. (2022) estimate. H2 is taken from the 83rd percentile of AR6 projections: it has a global mean sea level rise of 1.49m by 2100, rising to approximately 9.7m by 2200 and over 16m by 2300.

The HILL-6 scenario here is based on the AR6 high-impact low-likelihood projections rather than van de Wal et al. (2022) for two primary reasons. First, the estimates are higher so are more ‘risk averse’, and secondly corresponding projections for the UK coastline can be readily obtained from the NASA IPCC AR6 sea level projection tool (https://sealevel.nasa.gov/ipcc-ar6-sea-level-projection-tool; Garner et al., 2022; Kopp et al., 2023). It also differs from – and is higher than – the Palmer et al. (2024)

H2 projection because it is based on the 95th percentile from the AR6 high-impact low-likelihood projections rather than the 83rd percentile.

The rise in sea level around the UK coastline will be different to the global mean, for several reasons (see Palmer et al., 2018a). Two are particularly important. The average UK sea level rise will be *smaller* than the global average due to the reduced gravitational effect of a smaller Greenland ice sheet, and the land mass of the UK is slowly rising following the removal of ice sheets at the end of the most recent ice age (Glacial Isostatic Adjustment). Both the gravitational effect and the rate of rebound are greater in the north, so the increase in sea level is lower around the coastline of the north of the UK than the south (the rise in 2100 is around 0.2m higher in London than Edinburgh under UKCP18 RCP8.5: Palmer et al.,2018).

The H++ sea level rise scenario (Ranger et al., 2013; Lowe et al., 2009), which is currently specified to be a 'credible maximum scenario', assumes a maximum increase in sea level around the UK of 1.9m by 2095, relative to the 1981-2000 mean. This was based on an assumed increase in global mean sea level of 2.5m, taking into account the lower increase expected around the UK. The H++ sea level rise scenario does not explicitly define change in sea level over time.

The HILL-6 scenarios for the UK here are taken from the NASA sea level projection tool based on IPCC AR6 projections (the New York extreme sea level rise scenarios were taken from the same source: Braneon et al., 2024). These provide projections of sea level rise for 44 locations around the United Kingdom, including vertical land movement (Figure 4.17). The HILL-6 increase in sea level, relative to 1981-2000 (the baseline used in the UKCP18 marine projections), varies between 0.8 and 1.1m with emissions consistent with a 2°C world, and between 1.9 and 2.2m with very high emissions. The increase is highest along the southern and eastern coastline of the UK, and lowest in the north and west (northern and western Scotland, north west England, north Wales and Northern Ireland), and the HILL-6 scenario can be expressed as the average across sites in these two parts of the UK.

The increase in sea level continues beyond 2100, and with very high emissions the rate of increase accelerates: by 2300 the rise in sea level around the UK could be over 16m (Palmer et al., 2024). With low emissions accelerated loss of Greenland ice contributes more than accelerated loss of Antarctic ice, but with high emissions the contribution from Antarctic ice is greater.

The increase in UK mean sea level with very high emissions in HILL-6 is very close to the H++ scenario. The two sets of estimates were produced in different ways, and the projections based on IPCC AR6 results can therefore be seen as validating the earlier H++ scenario.

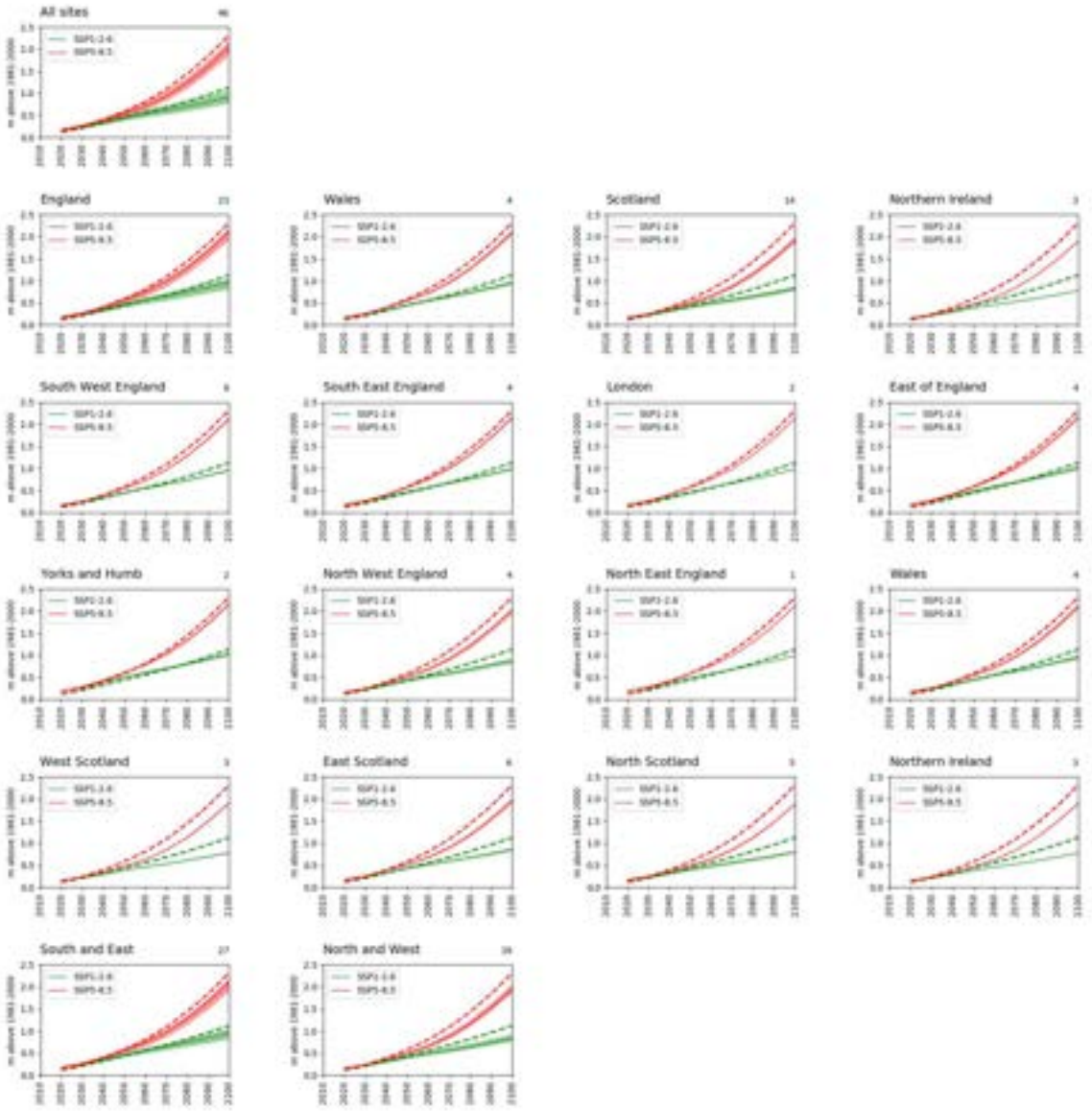

Figure 4.17: Increase in sea level around the UK under low and very high emissions relative to the 1981-2000 mean. Top row: all UK locations plus Isle of Man. Second row: locations grouped by country. Rows 3 to 5: locations grouped by region. Bottom row: locations grouped into two regions. In each plot, the dotted line represents the global average increase, the solid line is the regional average, and the shaded area defines the range across the region. The projections are taken from the NASA IPCC AR6 sea level projection tool (https://sealevel.nasa.gov/ipcc-ar6-sea-level-projection-tool), correcting for the difference in baselines (+0.041m, following Weeks et al., 2023).

4.8 Application of the scenarios: a summary

The enhanced global warming (HILL-1) and enhanced sea level rise (HILL-6) scenarios are defined here as specific applications of members of existing climate projections: the UKCP18 RCP8.5 ensemble and the IPCC AR6 projections respectively.

The other four scenarios are defined as perturbations to be applied to any of the UKCP18 climate and sea level projections. These perturbations can be applied to averages over time slices (for example 2041-2070) or to time series of climate variables which may be used to calculate impact indicators or used as input to an impact model. Figure 4.18 illustrates the application of HILL-2 to HILL-5 with a single UKCP18 climate projection for a single location. In this example, the perturbations are applied to temperature, rainfall and windspeed time series from one of the global strand HadGEM PPE-15 ensemble members, rescaled to correspond to an increase in global warming of 4^{o}C: the perturbations could in principle be applied to any individual projection. The differences between the perturbed and original time series can appear to be small compared with year-to-year variability and can be small compared with the range across ensemble members (compare with Figure 4.1). However, the differences are systematic. HILL-2 always leads to a more rapid increase in temperature, for example, HILL-3 always leads to a short-term fall in temperature, HILL-4 always leads to lower temperatures than anticipated in winter, and HILL-5 always leads to considerably lower temperatures through the year.

The climate scenarios here just define change in mean monthly temperature, rainfall and windspeed (and for some scenarios no change is assumed). Some risk assessments may require scenarios for other climate variables – such as humidity - or for changes at shorter durations – such as the frequency of storms. These can be inferred from the narrative storylines.

The quantifications of the storylines presented here should be regarded as indicative, based on interpretation of evidence currently available. As more information becomes available and further studies are published the quantifications of the storylines can be revised and updated.

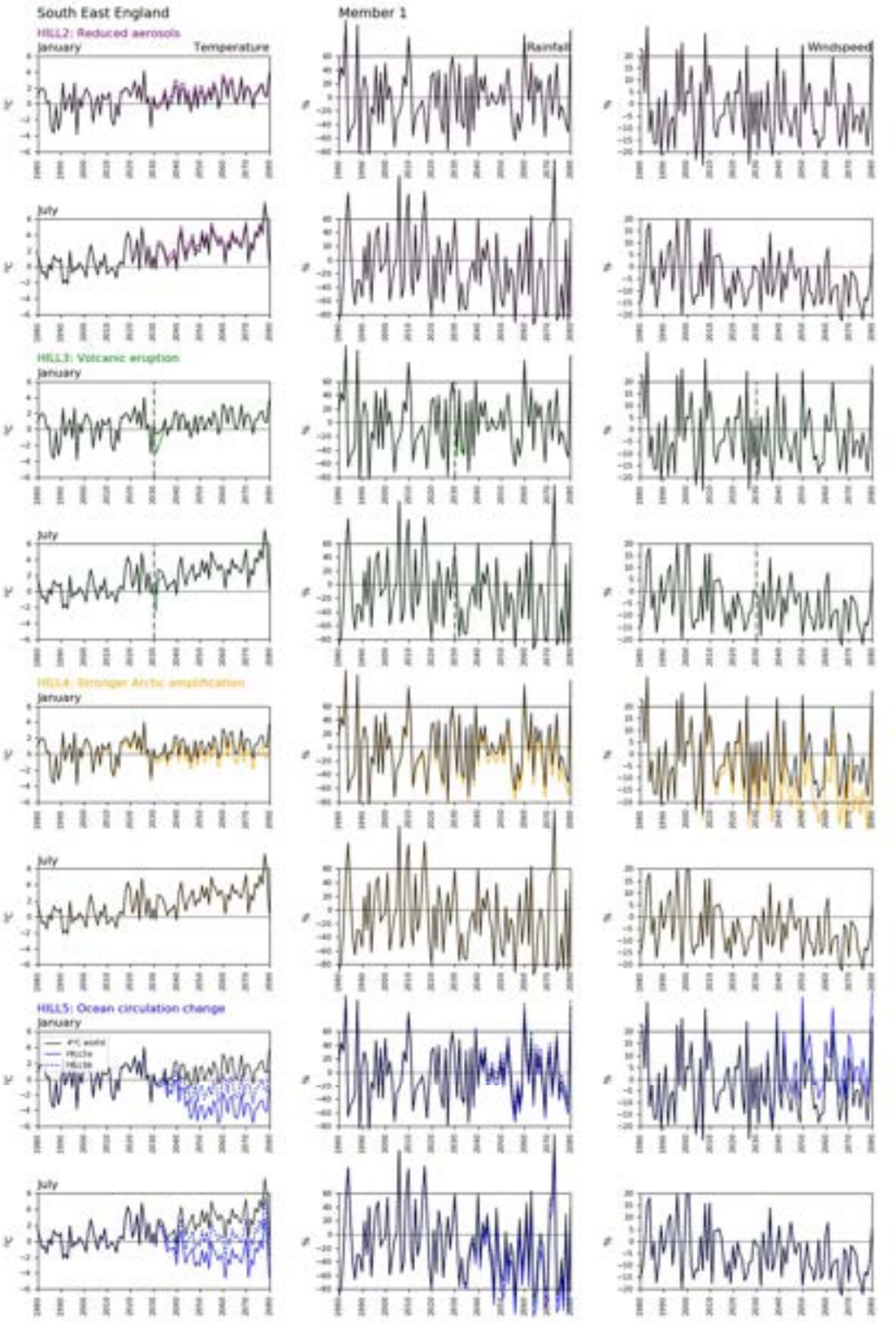

Figure 4.18: Illustration of the application of scenarios HILL-2 to HILL-5 to time series of monthly temperature, rainfall and windspeed. The plots show January and July for a location in south east England, and show changes relative to the 1981-2010 mean. The changes are applied to one member of the UKCP18 Global strand PPE-15 ensemble, rescaled to represent an increase in global average temperature of 4°C by 2100.

5. Extreme anomaly scenarios

5.1 Introduction

The extreme anomaly scenarios describe plausible extreme monthly and seasonal temperature, rainfall and windspeed anomalies, both individually and in combination as compound scenarios. They do not define short-duration events such as heatwaves, cold spells, rainstorms and windstorms, primarily because the user requirements for such events – in terms for example of duration and location - vary considerably between users. They are therefore not direct replacements for the H++ temperature, rain and wind scenarios or the Reasonable Worst Case Scenarios used in emergency planning. Extreme months or seasons do not necessarily include extreme short-duration events, and extreme short-duration events do not necessarily lead to an extreme month or season. The hot summer of 2018, for example, did not include any extended spells of extremely high temperatures, but temperatures were persistently above average (McCarthy et al., 2019).

The central concept behind the scenarios is that they are expressed as differences from a long-term mean and can be applied to a long-term mean representing any current or future time period. They are based on anomalies from a 30-year mean, but 'long-term' can be any period of at least 20 years. The concept assumes that the relative variability around a mean does not change as the mean changes. This assumption is explored in Section 5.5.2. The scenarios are defined at different spatial scales.

A conventional storyline approach to the creation of a scenario starts with the definition of motivations or drivers and follows through to evaluate consequences and outcomes. The approach followed here is the reverse: it starts with the outcome and works backwards to specify a 'backstory' consistent with the outcome. This is because the drivers behind extreme months and seasons in the UK are varied and complex, as outlined in Section 5.2.

The extreme scenarios are based on the analysis of historical observations and model simulations, coupled with theoretical reasoning. An overview of the methods used is given in Section 5.3 and Section 5.4 describes the data sources used. Section 5.5 summarises the analysis that informs the scenarios.

5.2 Drivers of extreme months and seasons

At the most basic level, weather in the UK varies with the direction of the airflow and the characteristics of air masses, which are determined by large-scale atmospheric

circulation patterns, the state of the Atlantic Ocean and the extent of snow and ice cover (Dong et al., 2025). Air masses from the west are typically wet and mild in winter but cool in summer because they come from across the Atlantic Ocean, whilst air from the north tends to be cold. Air from the east is usually dry because it comes from across the continent: it is often cold in winter but may be hot in summer. Air from the south is warm but may be dry or wet depending on the precise direction. The different types of weather affecting the UK can be grouped into classes such as the Lamb Weather Types (e.g. Jones et al., 2013) or Met Office Weather Patterns (Neal et al., 2016), each with distinctive temperature, rainfall and windspeed.

The weather patterns affecting the UK on any particular day are largely dependent on the ***dynamical characteristics*** of the atmosphere, and specifically on the characteristics of the jet stream. The 'polar eddy-driven jet' is a band of fast flowing air moving from west to east at around 9000m above the surface. It drives the progression of weather systems across the UK, but varies in strength, latitude and waviness from day to day, month to month and year to year (Woollings et al., 2010; 2014; 2018). When the jet stream is strong weather systems cross rapidly from west to east. Weather is then typically wet and windy: in winter it is milder than average, and in summer cooler. If the jet stream is to the north then weather systems pass across northern parts of the UK; if it is to the south they pass over more southerly regions. If the jet stream is weak then fewer weather systems pass across the UK. A weak jet stream can develop strong meanders, and these may create blocked conditions. Depending on where these blocks occur, weather across the UK can be much colder and drier than average in winter, or hotter and drier in summer.

The jet stream is a dimension of a complex and dynamic fluid system, and many indices are used to characterise its strength, latitude, waviness and the position (longitude) of meanders over different time scales. The North Atlantic Oscillation (NAO) is the most commonly used index to describe variability in weather across the North Atlantic and surrounding continents. It is characterised by variability in surface pressure across the Atlantic and is particularly important during winter. When this pressure gradient is high (positive NAO) the jet stream is strong: temperature and rainfall in winter across the UK are above average. Conversely, when the gradient is low (negative NAO) fewer weather systems cross the UK. In summer, a positive NAO is associated with higher temperatures across the UK (Folland et al., 2009) because the jet stream is to the north. The NAO is known to be influenced by temperatures in the North Atlantic Ocean (e.g. Sutton & Dong, 2012), the El Nino-Southern Oscillation (ENSO) and other modes of atmospheric variability (Hardiman et al., 2020), the extent of Arctic Sea ice (especially north of Europe), and interactions with the stratosphere (Scaife et al., 2016; Dunstone et al., 2016; 2018; Parker et al., 2019). However, variability in the jet stream from year to year, particularly in summer, is not just associated with variability in the NAO: it is also

linked to the East Atlantic Pattern (EAP), a pattern of variability characterised by high surface pressure over the east Atlantic (Woollings et al, 2010). A positive EAP is linked to high sea surface temperatures in the equatorial Pacific Ocean (El Nino), high rainfall over tropical oceans and a weakened Walker circulation in the tropics (Thornton et al., 2023). The penetration of oceanic westerly air flows into western Europe – steered by the jet stream – is also influenced by pressure over Scandinavia. When pressure over Scandinavia is high westerly flows are diverted to the north or south, and the UK is affected by air from the east. In winter this is cold, and in summer it is warm (Cassou & Cattiaux, 2016): the 'flip' in spring from cold to hot and in autumn from hot to cold is influenced by the extent of snow cover in Eurasia. Cold events in winter are typically associated with outflows of cold polar air from the Arctic and high latitude Eurasia. These outflows are often triggered by a weakening of the polar vortex and development of a large area of blocking high pressure, preceded by Sudden Stratospheric Warming events, themselves triggered by anomalous heating at the surface in high latitudes (Cohen et al., 2024). The Arctic Oscillation (AO) describes variability in pressure across the Arctic, and when the polar vortex is weak – with cold airflows across the UK – the AO index is strongly negative (Spaeth & Birner, 2022). Taken together, the jet characteristics and therefore weather regimes affecting the UK can be largely characterised by the NAO, the East Atlantic Pattern, the Arctic Oscillation and high pressure over Scandinavia (Madonna et al., 2017; Li et al., 2020) and are influenced by ocean characteristics (Dong et al., 2025), although there are major challenges in unpicking 'cause' and 'effect' and to a large extent the various indicators are measuring different dimensions of the same fundamental phenomena. The location in Europe and persistence of meanders in the jet stream, and therefore the location and persistence of atmospheric blocks, can be defined by quasi-stationary waves in the atmosphere, so that blocks are often part of a broader-scale wave pattern circling the Northern Hemisphere (Wolf et al., 2017; Mann et al., 2017) and occur in consistent locations. However, not all blocks are associated with quasi-stationary waves.

Adding to this dynamic complexity, the characteristics of a weather pattern may be influenced by ***thermodynamic*** properties, and in particular the characteristics of the surface over which the weather pattern has travelled. Sea surface temperatures not only influence atmospheric dynamics (the characteristics of the jet stream) but also the temperature and moisture content of the air: if the Atlantic Ocean is warmer than average, then air moving from the west will be warmer and wetter than average over the UK (Petch et al., 2020; Fereday & Knight, 2022). Similarly, dry or wet soils over Europe can lead – through positive feedbacks – to drier (and hotter) or wetter conditions respectively (Petch et al., 2020). Snow lying on the ground increases albedo and reduces radiation absorbed at the surface, so leads to further cooling.

Extreme months and seasons are typically characterised by persistent behaviour rather than the occurrence of a single extreme event (as in the summer of 2018). A persistently strong jet stream set at a specific latitude, for example, will generate a sequence of weather systems which together may bring high rainfall and high mean windspeeds (as in the winter of 2013/14, for example: Kendon & McCarthy, 2015). A persistently wavy and weak jet stream may lead to the development of a blocking high pressure anticyclone. Persistent behaviour, perhaps with gaps between long-duration events, may potentially persist for several weeks or even months (Richardson et al., 2019).

At the other extreme, it is plausible for weather regimes to 'flip' from one extreme state to another – flipping for example from very dry to very wet. Such flips are termed 'weather whiplash events' (Francis et al., 2023) and these are more likely under some sets of dynamic conditions than others. The potential for both long-term persistence and for 'flipping' implies that sequences of challenging months or seasons can be built up from any combination of extremes.

Finally, the geographical extent of an extreme month or season will depend on the geographical characteristics of the drivers. In principle most drivers are most likely to generate extremes in specific regions or extremes that are concentrated in part of the UK.

Taken together, the complexity of the drivers of variability in weather patterns in general and extreme months or seasons specifically, and uncertainty in how these drivers operate, mean that it is not feasible to define a storyline for extreme months and seasons from the drivers alone. Scenarios have to be developed 'backwards', starting from plausible extreme months and seasons.

5.3 Potential methods for identifying extreme months and seasons

5.3.1 Introduction

There are five groups of methods for identifying and characterising extreme months and seasons.

5.3.2 Historical experience

Historical extremes provide a guide to extreme months and seasons that could occur in the future. Not only can they describe quantitatively how monthly and seasonal temperature, rainfall and windspeed can differ from the long-term mean, but it is

often possible to identify the atmospheric and oceanic circumstances that generated the anomaly to help build up a narrative 'backstory'. Table 5.1 summarises some historical extreme events together with papers describing the associated climatic conditions.

Table 5.1: Some example historical extreme months and seasons

Year	Type of extreme	References
1963	Cold winter	Booth (1968); Greatbatch et al. (2014)
1976	Hot dry summer	Baker et al. (2021)
2003	Summer heatwave	Black et al. (2004)
2010	Cold winter	Cattiaux et al. (2010)
2013/14	Wet and stormy winter	Kendon & McCarthy (2015); Matthews et al. (2014)
2018	Summer heatwave	McCarthy et al. (2019); Drouard et al. (2019); Kornhuber et al. (2019); Petch et al. (2020); Li et al. (2020)
2018/19	Drought	Turner et al. (2021)
2019/20	Wet and stormy winter	Davies et al. (2021)
2022	Summer heatwave	Kendon (2022)

Historical extremes represent real experience and therefore provide a good indication of what could plausibly happen. Matthews et al. (2016) used 'memorable seasonal extremes' in Ireland to build a narrative describing the impacts of climate change. There are, however, a number of challenges with using historical experience.

The Central England Temperature (CET) record extends back to the late 17th century (Parker et al., 1992) and isolated long records exist (for example at Oxford and Durham), but systematic and consistent records across the UK only extend back to 1836 for rainfall and 1884 for temperature. Windspeed data across the UK are only available back to 1969 (see Section 5.4). Recent data rescue initiatives (Hawkins et al., 2023a) have added significantly to observed data sets and allowed their extension back in time. Reanalysis products – such as the 20CR (Compo et al., 2011) which extends back to 1806 – have been used to generate data further back in time, but there are potential inhomogeneities particularly for pressure and wind variables. Information on notable weather extremes extends further back – the TEMPEST archive (Endfield, 2016) contains records back to 1346 – but these tend to be short duration events.

Given that they have actually happened, historical extremes provide a lower bound on the most extreme month or season that could plausibly occur. It is also possible that the future might see types of extreme month or season that have not been physically plausible in the past; conversely, some types of past extreme months or seasons might not be physically plausible in the future.

On a more technical note, there is an issue over whether historical extremes should be expressed relative to a recent mean (for example 1981-2010), to an earlier mean, or whether the historical data should be detrended. A cold month in the early 1960s, for example, would appear more extreme when compared with a 1981-2010 mean than a mean centred around the 1960s due to the increase in temperature since then.

5.3.3 Statistical analysis

A conventional approach to identifying an extreme is to fit a statistical frequency distribution and calculate the T-year return period event. The problems with this approach are well known. The estimated T-year event depends on the distribution that is fitted, and it is often difficult to differentiate between candidate distributions from the data available. Estimating return periods of joint or compound extremes (for example hot plus dry, or hot followed by hot) is even more challenging. The statistical approach is therefore not employed here.

5.3.4 Stochastic simulation

Stochastic simulation has been used for many years, particularly in hydrology, to create long records where only short records are available and to estimate the magnitude of extremes. A large range of stochastic models have been produced, simulating point and multi-site weather and cross-correlated weather variables. The UKCP09 weather generator (Jones et al., 2010) is an example of a stochastic generator that simulates time series, whilst other generators create samples of extremes. Zhang et al. (2022), for example, created a stochastic generator for heatwaves in Australia. The flood scenarios used for Reasonable Worst Case Scenarios for the UK National Risk and Security Assessment are based on stochastic generation. All stochastic approaches need to make assumptions about distributions and correlations across space, time and weather variables, and are calibrated from observations. The robustness of the projected extremes depends on these assumptions. As with the statistical approach, different assumptions can produce very different extremes and it is generally difficult to discriminate between different sets of assumptions from the data available. The stochastic approach is not employed here.

5.3.5 Climate model simulation

Climate models produce simulated time series which sample a wider range of possible outcomes than represented by observations and potentially therefore generate more extreme monthly and seasonal anomalies. The realism of these outcomes, however, depends on the quality of the climate model and on the extent

to which the model reproduces observed and physically-realistic relationships between drivers and extremes.

There are two approaches to using climate model simulations to assess potential extreme events, months and seasons. The first uses large numbers of repetitions drawn from repeated application of a climate model, either with slightly different initial conditions (as in the UNSEEN methodology: Thompson et al., 2017) or from a very long simulation run (e.g. Gessner et al., 2021). The UNSEEN methodology developed for the National Flood Resilience Review (HM Government, 2016) uses a Met Office forecast model run with different initial conditions but a consistent set of boundary conditions to produce an ensemble of simulations and a larger distribution of climates than provided by observations. It has been applied to winter rainfall (Thompson et al., 2017), hot summers (Kay et al., 2020) and extreme daily rainfall in summer (Kent et al., 2022), with slightly different measures of extreme in each case – the magnitude of the largest winter rainfall total, the likelihood of exceeding the 2018 summer temperature, and the 1000-year return period daily rainfall respectively. A similar approach in principle was used by Chan et al. (2023) to extract samples with specific combinations and sequences of dry springs, summers, autumns and winters.

The second approach is a more tailored application of a climate model. It involves running a model with boundary conditions representing potential influences on extreme conditions and exploring how these generate extreme climatic outcomes: it has become known as the 'pseudo-global-warming' approach (Schar et al., 1996; Brogli et al., 2023). Variations on this approach (e.g. 'ensemble boosting': Fischer et al., 2023; Gessner et al., 2022; 2023 or 'spectral nudging': van Garderen et al., 2021; Sanchez-Benitez et al., 2022) use slightly different ways of defining initial conditions. The approach was used in the ExSamples project (Leach et al., 2022) to simulate extreme hot and wet winters across the UK from conditions which generated hot and wet winters in the UKCP18 projections in order to see whether even more extreme outcomes were feasible (they were). Hawkins et al. (2023b) suggested another variation using the 20th Century Reanalysis simulations to translate historical events into a model context.

Results from climate model simulation experiments are used here to help define the high-impact low-likelihood scenarios.

5.3.6 Empirical relationships with drivers of extreme anomalies

The fifth approach to estimating plausible extreme months and seasons is based on an empirical analysis of how past anomalies have varied with, or been influenced by, atmospheric and ocean drivers. There are three groups of methods.

The first uses empirical relationships – for example correlation or regression – between drivers and variability in climate from year to year across the UK. A very wide range of drivers (Section 5.2) have been used, including NAO indices, measures of jet stream variability and pressure variability (e.g. Baker et al., 2018; Hall & Hanna, 2018; Lavers et al., 2010; West et al., 2022; Harvey et al., 2023; Simpson et al., 2024; Cornes & Jones, 2024). A general conclusion from these studies is that empirical relationships vary between seasons and across the UK, and that relationships with single variables rarely fully capture variability over time. Empirical relationships are also best at general patterns rather than explaining extreme months or seasons which are often outliers. This is because the most extreme months and seasons are often a result of unusual combinations of drivers.

The second group of studies use composite analysis to define the mean and variability in climate behaviour for defined categories of driver behaviour – for example grouping all years with very high NAO values or high Atlantic sea surface temperatures (e.g. Sutton & Dong, 2012). These studies give a good indication of average behaviour when the driver is in a specific category, but the range in behaviour is a better measure of differences in extremes between categories. The smaller the number of years in a category the more the categorisation highlights extremes, but at the expense of a smaller sample size. Composites can be produced for combinations of driver categories (for example northerly jet plus strong jet), but this can lead to small sample sizes if observed or reanalysis data only are used. Chan et al. (2024) used this approach with the ECMWF probabilistic hindcast simulations (a total of 2850 plausible winters), yielding a much larger sample of combinations, and developed worst case winter drought scenarios based on the NAO and EAP.

The third group of studies seek to identify plausible extremes using empirical data on the weather associated with different circulation patterns – for example Met Office Weather Patterns (Neal et al., 2016). Richardson et al. (2018; 2020) used this approach to identify weather patterns associated with extreme rainfall and drought. Some of these studies examine how the properties of weather patterns have changed over time (e.g. Harrington et al., 2019; Baker et al., 2021) to see how climate change has affected the magnitude of extremes occurring with a given weather pattern. Yule et al. (2024) went a step further and assessed future changes in the magnitude of future UK heatwaves by looking at future temperature extremes during circulation pattern types that corresponded to historical extreme heatwaves.

Results from published and original empirical analysis of extreme months and seasons are used here to help define the high-impact low-likelihood scenarios.

5.4 Sources of data

5.4.1 Observed climate data

Observed average temperature, rainfall and windspeed data were primarily taken from the Met Office HadUK-Grid data set (Hollis et al., 2019), and specifically v1.2.0.ceda which extends to 2022. The monthly temperature, rainfall and windspeed data extend back to 1884, 1836 and 1969 respectively, and daily temperature and rainfall extend back to 1960 and 1891 respectively. The analysis here used monthly and daily data at the 5x5km, 12x12km, 25x25km, 60x60km, administrative region and national scales. The HadUK-Grid monthly mean windspeed data were disaggregated to the daily scale using daily windspeeds from the ERA5 reanalysis (Copernicus Climate Service, 2017). The HadUK-Grid data set has undergone rigorous quality control, but a few anomalous values remain at the finest 1x1km scale which can influence regional extremes (e.g. for rainfall North Hebrides June 1877, Tiree June 1891 and South Uist June 1907 and for windspeed Cairngorms September 1983: some anomalous windspeed data in v1.2.0.ceda are removed in v1.3.0.ceda): these may reflect either erroneous input data or effects of gridding in areas of complex terrain. The specific magnitudes of extreme anomalies are therefore not to be interpreted too literally.

These data are supplemented by the Met Office historic station data (https://www.metoffice.gov.uk/research/climate/maps-and-data/historic-station-data) for a number of locations (data back to 1853 for the earliest sites), and daily temperature and rainfall data from long records at Oxford (Burt & Burt, 2019: temperature from 1815, rainfall from 1767) and Durham (Burt & Burt, 2022: temperature and rainfall from 1843). The Central England Temperature (CET) record (Parker et al., 1992) extends back to 1659 and is representative of an area of England bounded by Lancashire, London and Bristol. The HadUKP England and Wales average precipitation data set begins in 1766 (Alexander & Jones, 2001).

The HadUK-Grid windspeed data start in 1969. Bett et al. (2017) reconstructed time series of mean windspeed across Europe back to 1850 using reanalysis products. Their results (their Figure 10) show that the highest and lowest annual average windspeeds across England and Wales have occurred since 1969 (although 1929 had a very high mean windspeed), implying that the period since 1969 does give a good indication of the range in extreme monthly average windspeeds (if not extreme windstorms). Over a longer period, Cornes & Jones (2024) concluded from long pressure data records that mean windspeeds in the English Channel were on average higher during the late 18th and early 19th century than the recent windy period since the 1990s and that summer windspeeds were higher in the late 18th

century, implying that larger extreme months may have been experienced in the historical past.

The long-term observed data sets exhibit trends and multi-decadal variability around a long-term mean (Kendon et al., 2023). These trends and variability are directly related to both the thermodynamic effects of global warming (air is warming and able to hold more water) and variability in atmospheric dynamics and circulation: some of this dynamical variability is internal to the climate system, and some is forced by increasing greenhouse gas concentrations. The thermodynamic effect is dominant for temperature (the pattern of increase in temperature across the UK is similar to the pattern of global increase, although the increase is larger: Kendon et al., 2023), but the dynamic effect is dominant for rainfall and windspeed. Whilst warmer air can hold more water, year-to-year variability in rainfall is largely determined by year-to-year variability in atmospheric dynamics and circulation.

Some of the analysis below uses the raw data, but some analysis of temperature variability and extremes uses detrended data in order to reduce the contribution of the thermodynamic effect to variability over time. Temperature data series are detrended using a triangular weighted kernel filter with 14 terms either side of each target point: this is the same as used by Kendon et al. (2023) in annual State of the UK Climate reports. Published studies examining historical extremes and linking year to year variability in weather with potential drivers use a range of approaches. Some use raw data but most undertake some form of detrending. Most of these use linear detrending, but the magnitude of the trend depends on the period used, and trends are not necessarily linear.

5.4.2 Drivers of variability and extremes

Data on weather regimes affecting the UK were taken from two sources. One is the set of 30 Met Office Weather Patterns (Neal et al., 2016, Neal, 2022; Harrison et al., 2022), based on pressure across the North Atlantic region and western Europe. These describe circulation types affecting the UK and can be grouped into eight summary classes. Available data span the period 1950 to 2020. The other is the set of Lamb Weather Types (Jones et al., 2013) which categorise weather regimes into 26 classes based on direction of flow and whether circulation patterns are anticyclonic or cyclonic. Data extend back to 1871.

The strength and latitude of the jet stream (Figure 5.1a) were taken from the estimates produced by Harvey et al. (2023), based on the 20CR Reanalysis and calculated between 1836 and 2015. Different studies have used slightly different definitions for the position of the jet stream, have averaged over different areas and have used different data sources.

There are several indices of the NAO. Some are based on differences in pressure between specific weather stations (e.g. Jones et al., 1997) or specific regions in a gridded pressure data set (e.g. Scaife et al., 2014; Dunstone et al., 2016; 2023; Wang & Ting, 2022; Kendon et al., 2020), whilst others are defined as the first mode from Empirical Orthogonal Function (EOF) analysis of gridded pressure data across much of the North Atlantic (e.g. Vallis & Gerber, 2008; Woollings et al., 2015; Parker et al., 2019). The primary disadvantage of the point- or regional-based indicators is that the geographical characteristics of the NAO vary through the year: some studies get round this by using different regions in different seasons (e.g. Kendon et al., 2020). The EOF-based indicators use different patterns in each month so account for this variation. The analysis here uses the monthly Hurrell EOF-based measure of NAO (Hurrell et al., 2024; https://climatedataguide.ucar.edu/climate-data/hurrell-north-atlantic-oscillation-nao-index-pc-based; Schneider et al., 2013), calculated from NCAR observed gridded sea level pressure data. This time series extends back to 1899 (Figure 5.1a). NAO shows considerable variability from year-to-year and decade-to-decade, with no clear underlying trend.

The East Atlantic Pattern (EAP) is generally defined as the second mode from an EOF of gridded pressure data. It is here taken from the NOAA-CPC monthly teleconnections data set https://www.cpc.ncep.noaa.gov/products/precip/CWlink/teleconnections/monthly/scn/ based on NCEP reanalysis (https://www.cpc.ncep.noaa.gov/data/teledoc/ea.shtml), which extends back to 1950 (Figure 5.1a). The EAP shows an increasing trend over time.

Anomalously high pressure over Scandinavia affects the penetration of weather systems across the UK. It is variously characterised by the frequency of occurrence of specific Euro-Atlantic regime types (e.g. Day et al. (2019) and Grams et al. (2017) using four- and seven-class classifications respectively), by one of the EOFs of gridded pressure data (for example in the NOAA-CPC monthly teleconnections data set https://www.cpc.ncep.noaa.gov/data/teledoc/telecontents.shtml), or simply as a pressure anomaly over Scandinavia (Cassou & Cattiaux, 2016). Here both the NOAA-CPC index is used (back to 1950) and a pressure anomaly (Figure 5.1a). The monthly pressure anomaly is (following Cassou & Cattiaux, 2016) calculated from daily surface pressure taken from 20CR reanalysis data (Compo et al., 2011) over the region 0 to 20ºE and 50 to 65ºN and expressed relative to the 1981-2010 mean pressure: it is calculated from 1960 to 2015. The two indices are not well correlated. One of the composite 8-class Met Office weather patterns (Neal et al., 2016) is described as ‘Scandinavian high’.

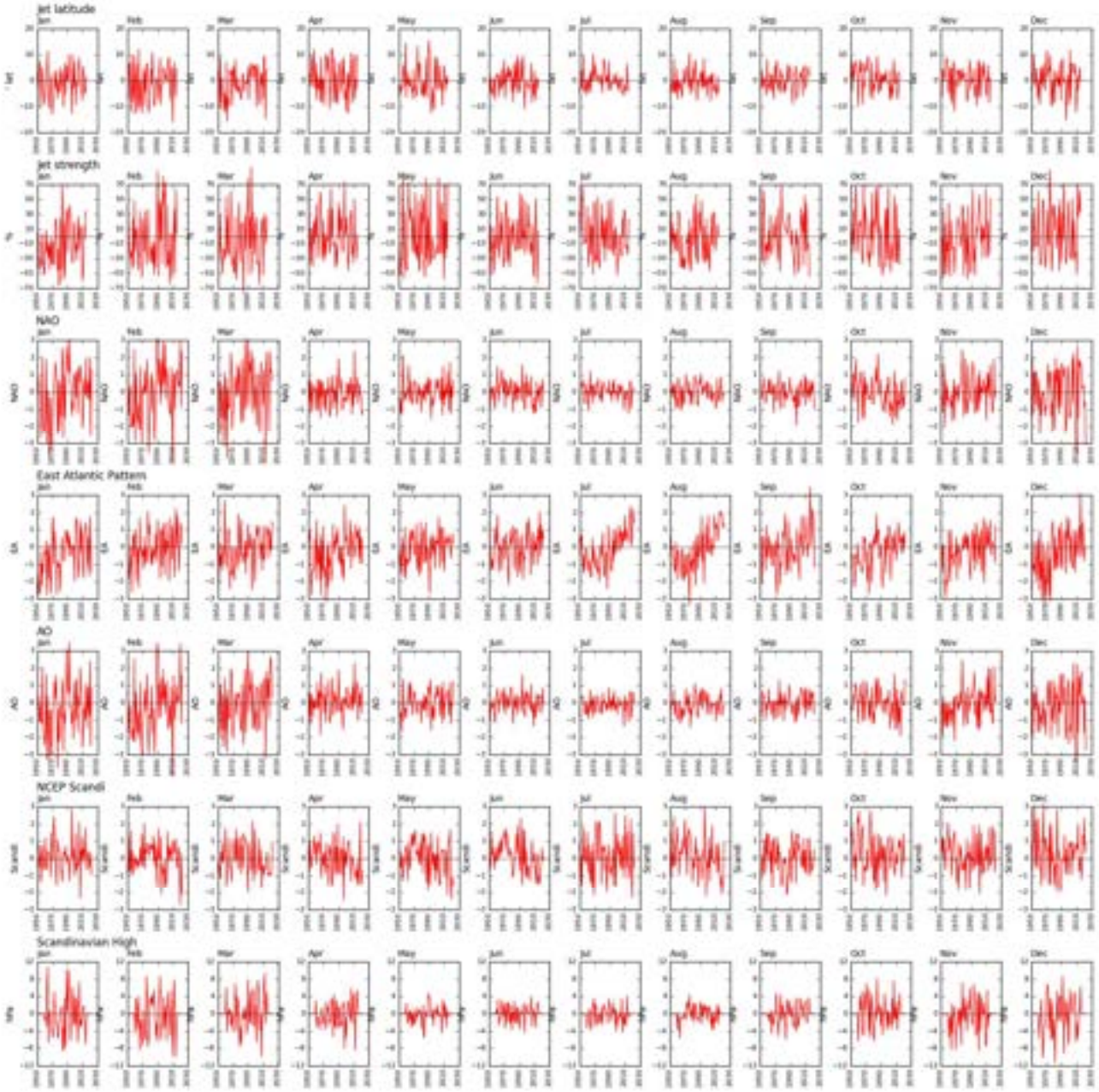

Figure 5.1a: Variability over time in potential drivers of climatic variability: 1950 to end of available data.

The Arctic Oscillation (AO) describes variability in air pressure over the Arctic which influences the latitude of the jet stream particularly in winter and is itself influenced by the strength of the Stratospheric Polar Vortex (SPV: Thompson et al., 2002). It is here (Figure 5.1a) characterised by the NOAA-CPC monthly teleconnections AO index (https://www.cpc.ncep.noaa.gov/products/precip/CWlink/daily_ao_index/history/method.shtml#eof). It shows greatest year-to-year variability in winter, and a strongly negative AO is associated with cold air flows.

The Lamb Weather Types (Jones et al., 2013) are calculated from surface pressure data. The CRU data set containing the daily weather types also includes the strength

of airflow across the UK, the shear vorticity of the flow (the degree of 'spin' or cyclonicity) and the direction of flow. It also contains a gale index (Jenkinson & Collinson, 1977; Jones et al., 1993) calculated from flow strength and shear vorticity (Figure 5.1b).

Variability in Atlantic Ocean sea surface temperatures is characterised by the Atlantic Multi-decadal Oscillation (AMO), calculated from sea surface temperature anomalies across the North Atlantic (Kerr, 2000). The AMO index is taken from the NCAR climate index data set (Trenberth & Shea, 2006; Trenberth et al., 2023; https://climatedataguide.ucar.edu/climate-data/atlantic-multi-decadal-oscillation-amo; Schneider et al., 2013). This extends back to 1870 and has been detrended to remove the effect of increasing global sea surface temperatures. The unsmoothed AMO index is used here (Figure 5.1b). The AMO describes multi-decadal variability in sea surface temperatures across the North Atlantic Ocean as a whole, although there is some year-to-year variability. Year-to-year variability more locally around the UK potentially affects temperature (Petch et al., 2020) and rainfall extremes. It is indexed here (Figure 5.1b) by the monthly average sea surface temperature anomaly around the UK (between 12°W and 5°E and 48 to 60°N) calculated from the HadSST4.0.1.0 gridded data set (Kennedy et al., 2019). Only the grid locations with a continuous record from 1950 to 2022 are used.

Several of the indicator data sets exhibit multi-decadal variability or a trend (there is a poleward trend in jet stream position, for example, and an increase in sea surface temperatures). The analysis here is based on the raw indicators without removal of trends.

5.4.3 Climate model data

The UKCP18 global strand projections (Lowe et al., 2018) are used to characterise current and future extreme monthly anomalies in temperature, rainfall and windspeed, specifically the 15-member HadGEM3-GC3.05 ensemble (Sexton et al., 2021; Yamazaki et al., 2021). This is an ensemble of simulations using variations of model parameters (a perturbed parameter ensemble PPE) designed to summarise the range of scientific uncertainty. The ensemble consists of equally plausible simulations from December 1899 to November 2098. The analysis here uses the projections at the national and administrative region scales. The climate simulations are used for two purposes: to see how observed extreme anomalies compare with simulated extreme anomalies over a consistent historical period (does the larger number of 'observations' from additional synthetic worlds expand the range?), and to test the assumption that anomalies from a long-term mean can be assumed to be relatively constant with a changing mean.

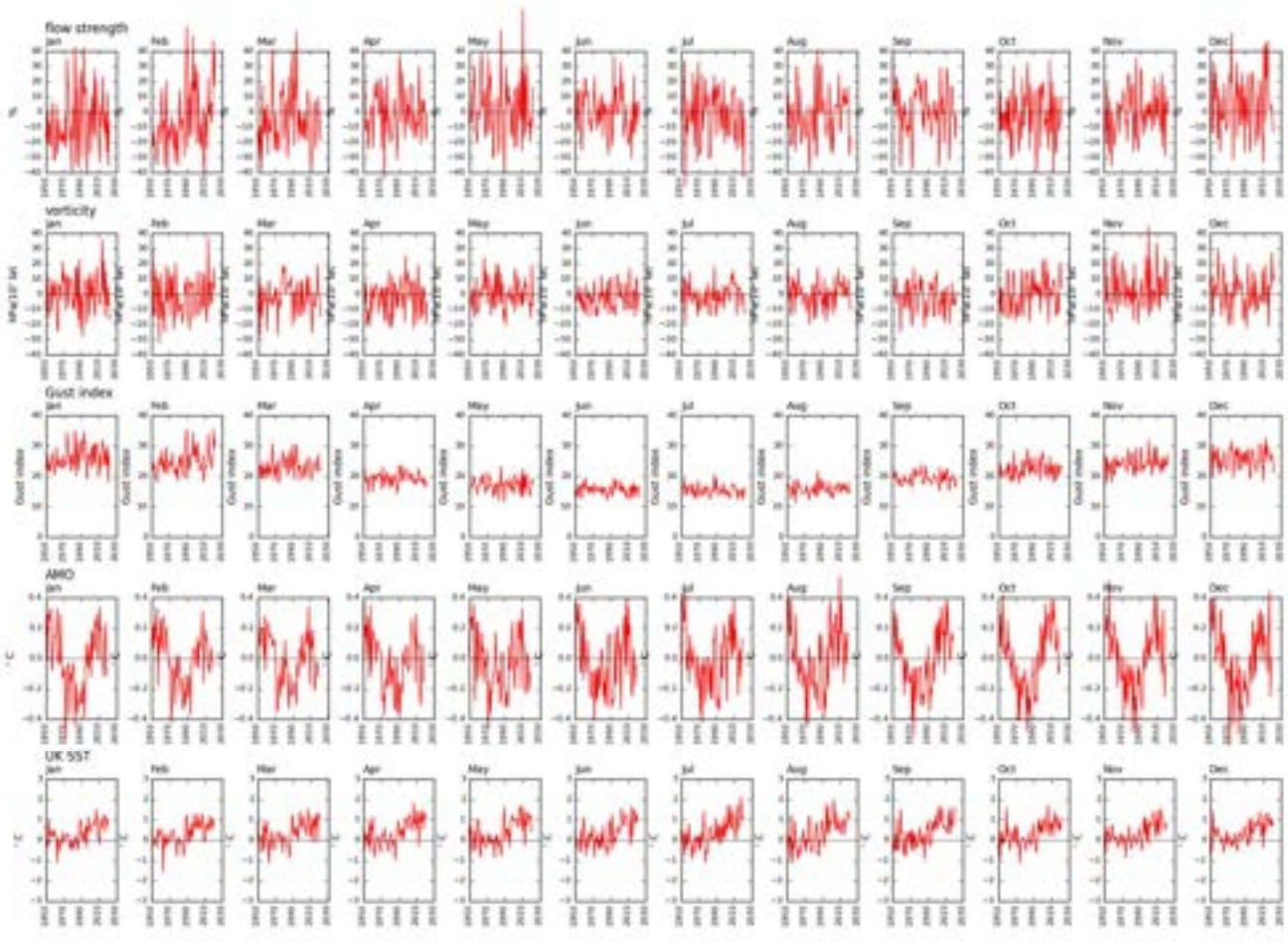

Figure 5.1b: Variability over time in potential drivers of climatic variability: 1950 to end of available data.

Whilst the HadGEM3-GC3.05 climate model ensemble simulates well the physical processes generating weather and climate, as is the case with all climate models the simulations are not perfect and do not necessarily accurately reproduce observed historical behaviour. Climate model projections therefore need to undergo some form of bias adjustment. The simplest is to rescale the simulations so that the mean over some time period (e.g. 1981-2010) matches the observed mean or, equivalently, to express the simulations as an anomaly from a specific period. However, this assumes that the model simulates year-to-year variability accurately and this is important when considering extreme behaviour. It is straightforward to adjust the variance of simulated data so that it matches the observed variance, but this does not adjust for bias in the shape of the distribution. A variety of quantile-mapping bias adjustment methods has therefore been developed and applied which adjust climate model data so that the shapes of distributions match. There are, however, two problems with quantile-mapping bias adjustment, one practical and the other conceptual. The main practical problem is that the rescaled model simulations are dependent on the assumed distribution describing variability from year to year and

how well the distribution fits the data, and this is particularly important when estimating extreme anomalies. As with the statistical analysis of observed data described in Section 5.3.3, it can be difficult to distinguish between distributions with very different tail properties from the available data. The conceptual problem is that the results of bias adjustment are dependent on what aspects of bias it is assumed need to be adjusted. If the aim is to adjust the simulated data so that it looks exactly like real data – which is the aim of bias adjustment when used for weather forecasting – then a 'perfect' bias adjustment would produce an identical distribution, and therefore extreme anomalies, to the observed data over the calibration period. The distributions would be different over different time periods, depending on how robust the calibration was (the longer the calibration period, the more robust the calibration). However, a perfect bias adjustment assumes that the observations are fully representative of possible experience, which defeats the purpose of using a model to explore plausible but unrealized outcomes. A 'less perfect' bias adjustment would seek to match some key statistical properties of the observations, such as the mean or the mean and variance, which may be assumed to be more robustly defined by both observations and simulations. But the key point is that these are choices, so there is no one 'correct' bias adjustment method, or indeed assumed distribution for quantile-mapping.

The analysis here applies a bias adjustment to the UKCP18 global strand projections which just matches mean and variance over the period 1981 to 2010, because otherwise the results are dependent on the assumed distribution used for quantile-mapping. The UKCP18 global strand projections tend to overestimate the standard deviation of monthly temperature throughout the year, underestimate relative variability in monthly rainfall between November and June but overestimate it in summer, and slightly underestimate relative variability in monthly mean windspeed (Figure 5.2).

5.5 Extreme months and seasons in the UK

5.5.1 Introduction

This section describes extreme months and seasons in the UK and evaluates the influence of drivers outlined in the previous section. First, however, the assumption that extreme anomalies from a long-term mean do not vary as the mean changes is tested.

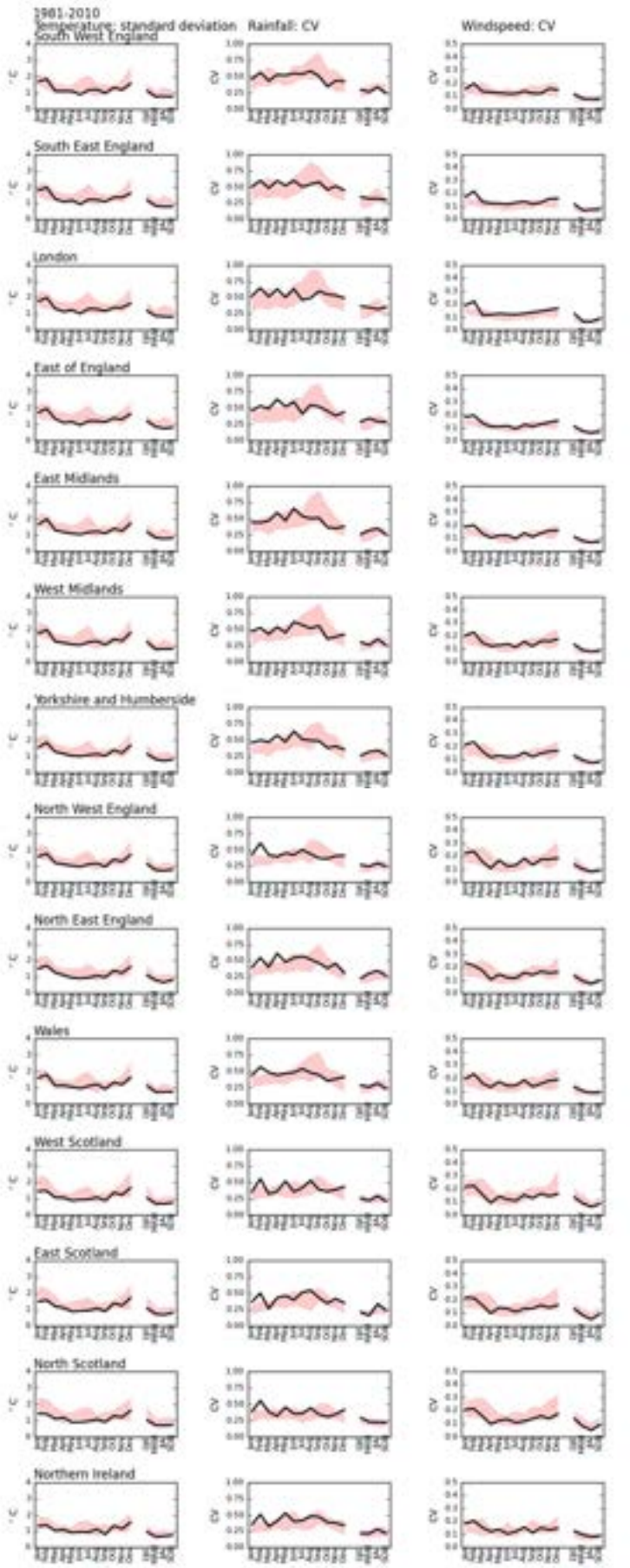

Figure 5.2: Observed (black) and simulated (pink) variability in regional temperature, rainfall and windspeed, over the period 1981-2010. Simulated from UKCP18 global strand.

5.5.2 Change in variability around the mean due to climate change

As global climate changes, mean temperature, rainfall and windspeed across the UK averaged over several years will also change, and this is well characterised in the UKCP18 climate projections. Potential changes in variability from year to year, however, are much less well understood. The high-impact low-likelihood scenarios defined here therefore explicitly assume that the (relative) variability around this mean in monthly and seasonal weather does not change substantially over time, so that the scenarios can be applied to any time period and associated long-term mean.

This assumption is tested in Figure 5.3, which shows (averaged over England) change by month over the 21st century in variability and extreme annual anomalies for temperature, rainfall and windspeed. The figure shows the 15 ensemble members of the UKCP18 global strand with very high RCP8.5 emissions, without bias adjustment. Patterns of change are broadly the same across the regions of the UK, with slightly larger changes in summer rainfall variability in the south and east.

The temperature plots show that there is a small increase in variability (standard deviation) in summer and a small decrease in winter. There is a very small increase over time in the maximum anomaly expressed as a difference from the 30-year mean in summer, and a very small increase in the coldest anomaly in summer: there is a very small opposite pattern in winter. There is no change in the most extreme anomaly when expressed as a multiple of standard deviation. For monthly (and seasonal) temperature, it is therefore feasible to assume that the magnitude of the maximum annual anomaly is constant over time.

The rainfall plots show no change in the coefficient of variation in winter but an increase in summer. There is also a very large change in the magnitude of the largest anomaly in summer (expressed as a percentage difference from the long-term mean), particularly after the 2050s. This arises because the UKCP18 projections simulate that a greater proportion of summers will be dominated by dry anticyclonic conditions: ‘wet’ summers will still occur but be less frequent. There is little change in the absolute magnitude of the wettest summers. Mean rainfall therefore falls in summer months and variability increases. There is no clear change over time when the maximum anomaly is expressed as standard deviations from the mean. The assumption of a constant maximum anomaly (as a percentage difference from the mean) therefore holds for rainfall in autumn, winter and spring, but is less appropriate in summer. In summer, the anomaly increases over time, particularly after the 2050s. The assumption holds in summer if the anomaly is expressed as a multiple of the standard deviation. However, this is not so useful in practice as the standard deviation is rarely provided in standard climate scenarios.

The windspeed plots show that the assumption of consistent anomalies over time is plausible.

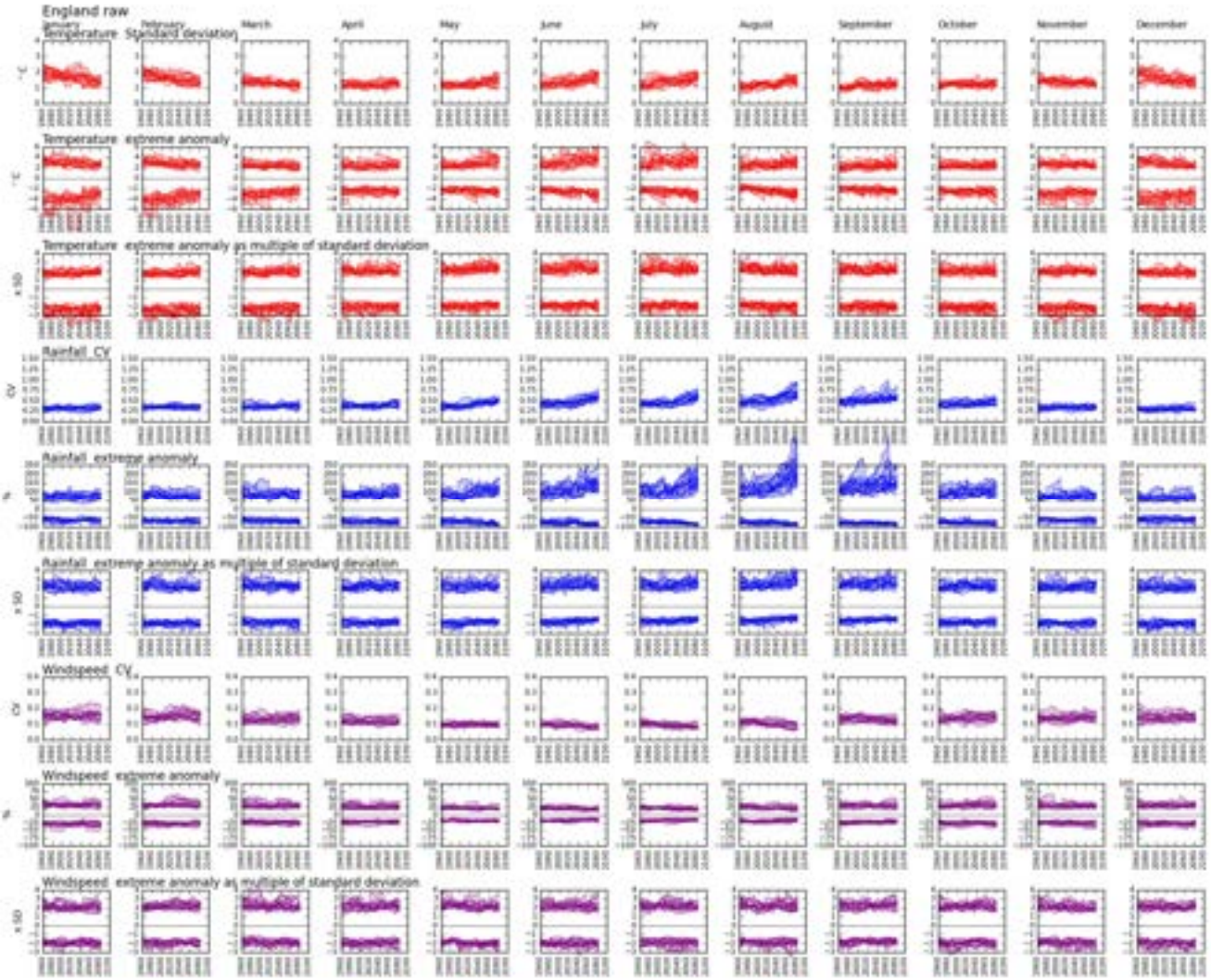

Figure 5.3: Simulated variability in monthly mean temperature, rainfall and windspeed: England. UKCP18 global strand RCP8.5. For each climate variable, the first row shows standard deviation (temperature) or coefficient of variation (rainfall and windspeed) calculated over a running 30-year period. The second row shows the maximum anomaly (high and low) over a running 30-year period, expressed as a difference (°C for temperature and % for rainfall and windspeed) from the 30-year mean. The third row shows the maximum anomaly expressed as a number of standard deviations away from the mean. In each case, the individual lines show the 15 ensemble members.

5.5.3 Historical extremes

5.5.3.1 Extreme historical monthly and seasonal anomalies

The most extreme historical monthly and seasonal anomalies – relative to the 1981-2010 average – vary across the UK, between months and seasons, and with spatial resolution (Figure 5.4).

Tables 5.2 to 5.7 show the largest historical anomalies on record at the regional average scale. The largest monthly temperature anomalies are typically between plus and minus 4°C, with larger anomalies – up to 6°C in some winter months, particularly in the south and east. Detrending the data has no material effect on the magnitude of extremes. Some of the earlier cold events are slightly less cold and some of the recent hot events are more extreme, but the effect is small. Maximum monthly regional rainfall can be over three times the mean across England, and the driest months have only 10% of the average rainfall at the regional scale. The windiest months can be up to 1.8 times windier than the average in winter at the regional scale, and 1.5 times windier in summer: the calmest months have average windspeeds as low as 40% of the mean.

The variation across the UK in the magnitude of the most extreme anomalies largely reflects the geographic location of the most extreme events on record but is influenced to a certain extent by small variations across the UK in the 'inherent' variability in climate from year to year. Figure 5.5 shows the standard deviation of temperature and coefficient of variation (CV) of rainfall and windspeed by region, calculated over 30-year periods starting every ten years from 1891, 1841 and 1971 for temperature, rainfall and windspeed respectively. The vertical lines represent the range across locations in the region. The variability in standard deviation and CV between time slices in each month is generally larger than the variability between regions (reflecting the occurrence or not of extreme events). However, there are indications that the standard deviation of monthly temperature in December, January and February is larger in most of the English regions and Wales than in Scotland or Northern Ireland, and the CV of rainfall in most months is slightly lower in Scotland and Northern Ireland than in the English regions or Wales. There is no clear variability in the CV of monthly windspeed across the regions of the UK.

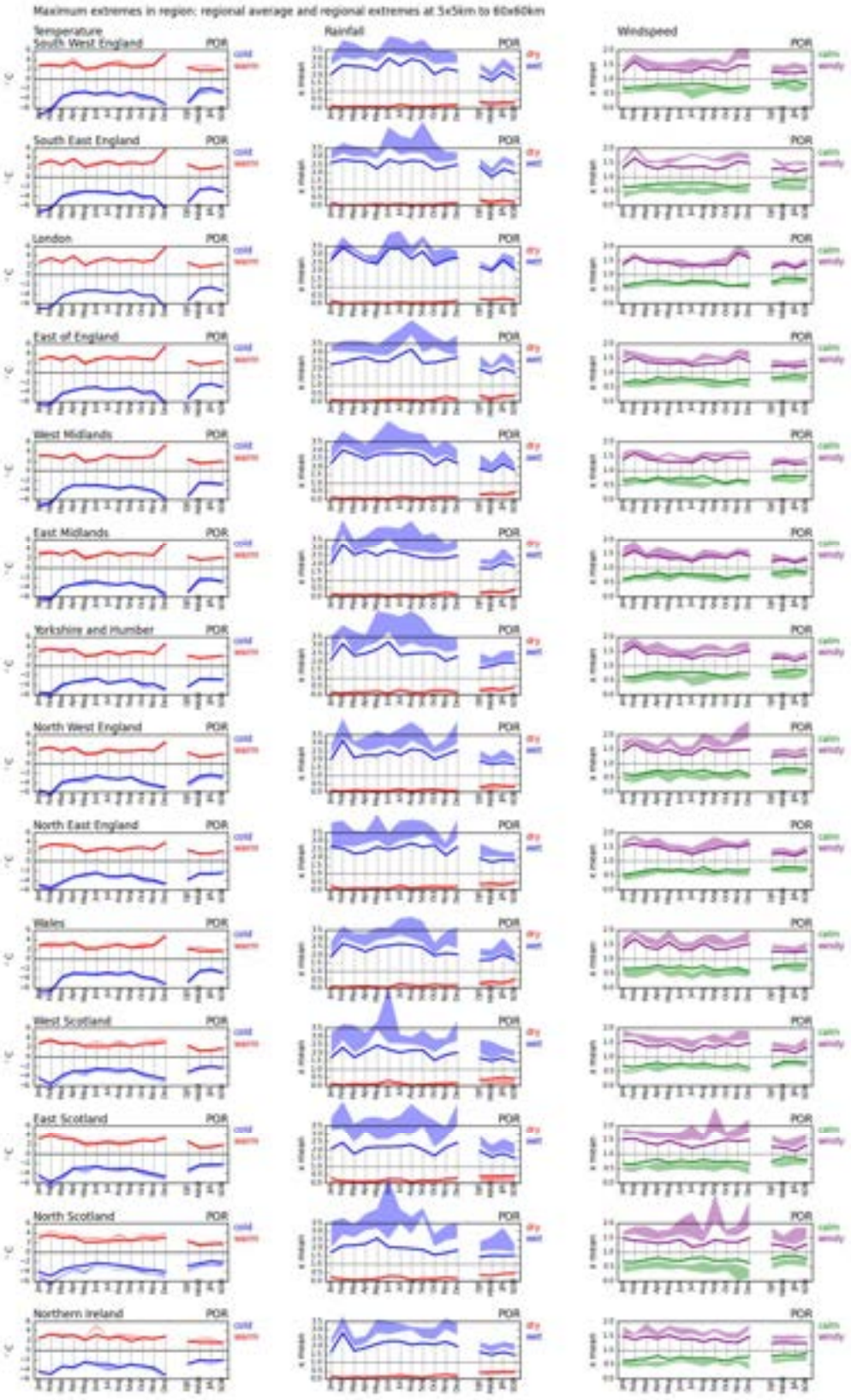

Figure 5.4: Maximum historical temperature, rainfall and windspeed anomalies, relative to the 1981-2010 mean, by region. The solid line shows the largest regional average anomaly, and the shaded area shows the largest anomaly in a region at scales ranging from 5x5km (most extreme) to 60x60km (closest to the regional average). Note that the large anomalies in June rainfall in west and north Scotland, and the large anomalies in windspeed in north Scotland are erroneous.

Table 5.2: Historical monthly and seasonal hot extremes: maximum ºC difference from 1981-2010 mean, over the period 1884-2022

		South West England	South East England	London	East of England	East Midlands	West Midlands	Yorkshire and Humb.	North West England	North East England	Wales	West Scotland	East Scotland	North Scotland	Northern Ireland
Jan	year	1916	2007	2007	2007	1916	1916	1916	1916	1916	1916	1989	1989	1989	1898
	anom	2.7	2.57	2.6	2.75	2.84	3.05	3.02	2.9	2.77	2.8	2.78	3.23	3.07	2.45
Feb	year	1990	1990	1990	1990	1998	1998	1998	1998	1998	1998	1998	1998	1998	1998
	anom	2.84	3.35	3.4	3.33	3.16	3.07	3.45	3.29	3.49	2.82	3.4	3.95	3.55	3.27
Mar	year	1957	2017	2017	1938	1938	1957	1938	1957	1938	1957	2012	1938	2012	1938
	anom	2.56	2.51	2.62	2.58	2.7	2.55	2.96	2.52	3.31	2.84	2.68	3.22	2.91	2.72
Apr	year	2011	2011	2011	2011	2011	2011	2011	2011	2011	2011	2011	2011	2011	2011
	anom	3.33	3.67	3.85	3.48	3.52	3.41	3.27	3.1	3.2	3.24	2.86	3.02	2.97	3.03
May	year	2008	2008	1992	1947	2022	1992	2018	2008	2017	2008	2008	2018	1889	2008
	anom	1.98	2.01	1.98	1.89	1.88	1.85	1.95	1.91	1.92	2.09	2.11	1.92	2.03	2.1
Jun	year	1976	1976	1976	1976	1976	1976	1976	1940	1940	2018	1940	1940	1970	1887
	anom	2.23	2.6	2.98	2.76	2.48	2.22	2.13	2.02	2.41	2.15	2.12	2.1	2.05	2.9
Jul	year	1983	2006	2006	2006	2006	2006	2006	2006	2006	1983	2006	2006	2006	2013
	anom	3.07	3.13	3.43	3.23	3.22	3.18	2.91	2.83	2.74	2.63	2.13	2.39	2.22	2.38
Aug	year	1995	1995	1997	1997	1997	1995	1975	1995	1975	1995	1947	1995	1947	1995
	anom	2.96	2.55	2.78	2.82	2.55	2.7	2.22	2.46	2.14	2.99	2.49	2	2.4	2.68
Sep	year	2006	2006	2006	2006	2006	2006	2006	2006	2006	2006	2006	2006	2006	2021
	anom	2.48	2.92	3.12	3.12	3.01	2.66	2.76	2.57	2.72	2.33	2.09	2.32	2.36	1.84
Oct	year	2001	2001	2001	2001	2001	2001	2001	2001	2001	1995	2001	2001	1908	1969
	anom	2.47	2.69	2.69	2.86	2.8	2.76	2.82	2.84	2.86	2.45	2.62	2.86	2.75	2.45
Nov	year	1994	1994	1994	1994	1994	1994	2011	1994	2011	1994	1994	2011	2011	1994
	anom	2.87	3.03	2.97	2.67	2.61	2.98	2.37	2.59	2.46	2.86	2.62	2.68	2.61	2.34
Dec	year	2015	2015	2015	2015	2015	2015	2015	2015	2015	2015	1988	1988	1988	1934
	anom	5.13	5.59	5.63	5.42	5.13	5.25	4.44	4.3	3.86	4.7	3.07	3.28	2.91	2.82
DJF	year	2016	2016	2016	2016	2016	2016	1989	1989	1989	2016	1989	1989	1989	1989
	anom	2.33	2.51	2.46	2.43	2.31	2.33	2.04	2.22	2.25	2.11	2.25	2.49	2.18	1.83
MAM	year	1893	2017	2017	2017	2011	2017	2011	2017	2017	1893	2017	2014	2003	1893
	anom	1.71	1.57	1.65	1.62	1.68	1.48	1.55	1.35	1.56	1.65	1.23	1.3	1.38	1.52
JJA	year	2018	2022	2022	2022	2022	2018	2022	1995	2022	1995	1995	2003	2003	1995
	anom	1.71	1.73	1.9	1.9	1.84	1.67	1.75	1.41	1.54	1.59	1.32	1.38	1.6	1.5
SON	year	2006	2006	2006	2006	2006	2011	2006	2006	2006	2011	2006	2006	2006	2021
	anom	1.86	2.23	2.29	2.32	2.17	1.94	2.05	1.98	2.07	1.73	1.73	1.8	1.66	1.5

The extremes are calculated from regional HadUK-Grid observed data

Table 5.3: Historical monthly and seasonal cold extremes: maximum ºC difference from 1981-2010 mean, over the period 1884-2022

		South West England	South East England	London	East of England	East Midlands	West Midlands	Yorkshire and Humb.	North West England	North East England	Wales	West Scotland	East Scotland	North Scotland	Northern Ireland
Jan	year	1963	1963	1963	1963	1963	1963	1940	1940	1940	1963	1895	1895	1895	1963
	anom	-7.49	-7.24	-7.04	-6.67	-6.26	-7.12	-5.59	-5.61	-4.98	-6.76	-4.51	-4.59	-4.22	-4.48
Feb	year	1895	1895	1895	1947	1947	1895	1947	1895	1895	1895	1895	1895	1895	1895
	anom	-6.39	-6.57	-6.89	-6.45	-6.42	-6.78	-5.79	-6.27	-5.49	-6.79	-5.65	-5.83	-5	-4.98
Mar	year	1962	1892	1892	1892	1962	1962	1892	1892	1947	1962	1947	1947	1947	1892
	anom	-3.71	-4.07	-4.52	-4.29	-4.07	-4.06	-3.98	-3.85	-4.34	-3.74	-3.85	-4.67	-3.69	-3.39
Apr	year	1986	1917	1917	1917	1917	1922	1917	1917	1917	1986	1917	1922	1917	1922
	anom	-2.86	-3.36	-3.72	-3.68	-3.52	-3.06	-3.46	-3.41	-3.3	-2.96	-3	-3	-3.1	-3.52
May	year	1941	1902	1902	1902	1902	1885	1902	1885	1902	1885	1902	1902	1923	1885
	anom	-2.72	-3.02	-3.33	-3.15	-2.95	-3.01	-3.05	-3.18	-2.79	-3.07	-2.94	-2.91	-2.81	-2.53
Jun	year	1972	1916	1916	1916	1916	1972	1916	1972	1916	1972	1927	1927	1927	1927
	anom	-3.22	-3.1	-3.35	-3.03	-2.91	-3.02	-2.69	-2.59	-2.4	-3.16	-2.52	-2.6	-2.29	-2.87
Jul	year	1922	1888	1919	1919	1888	1922	1888	1922	1888	1922	1922	1965	1888	1922
	anom	-2.79	-3.19	-3.64	-3.55	-3.36	-3.3	-3.69	-3.08	-3.17	-2.86	-2.58	-3.14	-2.53	-2.9
Aug	year	1912	1912	1912	1912	1912	1912	1912	1912	1912	1912	1956	1912	1912	1912
	anom	-3.48	-3.66	-3.85	-3.4	-3.58	-3.69	-3.29	-3.3	-3.2	-3.18	-2.83	-3.08	-2.78	-3.53
Sep	year	1986	1912	1912	1952	1952	1952	1952	1952	1952	1952	1918	1918	1918	1918
	anom	-2.85	-3.19	-3.36	-3.15	-3.08	-3.27	-2.95	-2.87	-2.86	-2.71	-2.63	-3.04	-3.08	-2.97
Oct	year	1892	1905	1887	1905	1905	1892	1896	1896	1896	1896	1896	1896	1885	1896
	anom	-3.55	-4.09	-4.39	-4.14	-3.85	-3.7	-3.81	-3.9	-3.65	-3.8	-3.54	-3.6	-3.65	-3.37
Nov	year	1919	1923	1923	1923	1910	1915	1910	1915	1910	1915	1910	1919	1919	1919
	anom	-3.93	-4.19	-4.33	-3.93	-3.97	-4.24	-3.89	-4.55	-3.99	-4.08	-4.08	-4.2	-3.77	-3.73
Dec	year	1890	1890	1890	1890	1890	1890	2010	2010	2010	1890	2010	2010	2010	2010
	anom	-5.35	-6.46	-6.86	-6.23	-5.46	-5.76	-4.89	-4.97	-4.73	-5.21	-4.61	-4.71	-4.15	-5.15
DJF	year	1963	1963	1963	1963	1963	1963	1963	1963	1963	1963	1963	1895	1895	1963
	anom	-4.96	-5.3	-5.32	-5.19	-5	-5.25	-4.35	-4.16	-3.85	-4.71	-3.16	-3.42	-2.86	-2.91
MAM	year	1887	1888	1887	1887	1891	1887	1891	1891	1891	1887	1891	1891	1891	1979
	anom	-2.22	-2.62	-2.93	-2.57	-2.38	-2.51	-2.84	-2.64	-2.59	-2.52	-2.24	-2.36	-2.43	-2.12
JJA	year	1922	1888	1888	1907	1922	1922	1888	1888	1888	1922	1922	1888	1922	1912
	anom	-2.02	-2.35	-2.6	-2.34	-2.42	-2.55	-2.8	-2.34	-2.62	-2.16	-2.01	-2.25	-1.95	-2.19
SON	year	1887	1887	1887	1887	1919	1919	1887	1887	1887	1887	1885	1952	1885	1919
	anom	-2.77	-3.09	-3.36	-2.97	-2.88	-2.82	-2.97	-2.71	-2.44	-2.76	-2.32	-2.23	-2.18	-2.12

The extremes are calculated from regional HadUK-Grid observed data

Table 5.4: Historical monthly and seasonal wet extremes: maximum ratio to 1981-2010 mean, over the period 1836-2022

		South West England	South East England	London	East of England	East Midlands	West Midlands	Yorkshire and Humb.	North West England	North East England	Wales	West Scotland	East Scotland	North Scotland	Northern Ireland
Jan	year	2014	2014	2014	1939	2014	2014	2008	1928	1948	1948	1928	2016	1993	1877
	anom	2.05	2.59	2.63	2.26	2.01	2.19	2.11	2.03	2.58	1.91	1.71	2.05	1.74	1.7
Feb	year	1923	1951	1951	1916	1977	2020	2020	2020	1848	2020	1990	1848	1990	2020
	anom	2.61	2.79	3.36	2.31	3.21	2.92	3.01	3.08	2.48	2.62	2.29	2.36	2.14	2.72
Mar	year	1947	1947	1947	1947	1947	1947	1981	1981	1979	1981	1994	1903	1990	2019
	anom	2.53	2.7	3.01	2.57	2.51	2.73	2.35	2.09	2.19	2.47	1.7	1.73	2.15	1.7
Apr	year	2000	2000	2012	1998	2012	2000	2012	1843	1998	1920	1947	1947	1947	1961
	anom	2.48	2.65	2.58	2.68	2.77	2.41	2.44	2.28	2.27	2.2	2.05	2.11	2.24	1.91
May	year	2021	1843	1843	2007	1932	1886	1967	1967	1924	2021	2011	1906	2011	1916
	anom	2.25	2.27	2.39	2.42	2.51	2.77	2.7	2.22	2.59	2.5	2.44	2.17	2.58	2.14
Jun	year	1860	1860	1903	1997	2007	2007	2007	2012	2012	2012	1872	1838	1872	2012
	anom	2.99	2.79	3.23	2.43	2.84	2.78	3.12	2.5	2.43	2.57	2.2	2.17	2.03	2.35
Jul	year	1936	1888	1855	1875	1880	2007	1920	1988	1940	1939	1988	1940	1940	1936
	anom	2.55	2.59	3.32	2.83	2.69	2.74	2.4	2.24	2.58	2.67	1.99	2.2	2	2.29
Aug	year	1912	1912	1878	1912	1912	1912	1956	1956	1956	1917	2009	1948	1992	2008
	anom	2.95	2.75	2.75	3.16	2.5	2.82	2.49	2.6	2.83	2.59	2.15	2.29	1.94	2.13
Sep	year	1866	1896	1968	1918	1883	1976	1918	1918	1976	1918	1950	1950	1950	1950
	anom	2.78	2.7	3.03	2.31	2.33	2.69	2.52	2.52	2.54	2.44	2.14	2	1.87	2.15
Oct	year	1960	1865	1880	1865	1903	1903	1903	1967	1903	1903	1995	1903	1983	1870
	anom	2.03	2.19	2.29	2.37	2.31	2.05	2.5	2.01	2.71	1.94	1.53	1.62	1.58	2.07
Nov	year	1929	1940	1940	1940	1852	1852	2009	2009	2009	1929	2009	1984	1981	1852
	anom	2.39	2.3	2.64	2.51	2.31	2.46	2.06	2.28	2.11	2.09	1.86	2.14	1.7	2.1
Dec	year	1934	1914	1914	1914	1868	1914	1868	2015	1876	2015	2015	2015	2015	1876
	anom	2.23	2.49	2.77	2.66	2.47	2.19	2.26	2.54	2.58	2.04	1.99	2.42	1.84	2.01
DJF	year	2014	2014	2014	1915	1877	1990	1915	2016	2016	2014	2014	2016	1989	1877
	anom	1.96	2.35	2.2	1.93	1.72	1.86	1.62	1.87	1.88	1.68	1.68	1.88	1.44	1.67
MAM	year	1947	1979	1979	1981	1979	1932	1979	1920	1947	1920	1986	1947	1990	1986
	anom	1.62	1.7	1.99	1.67	1.7	1.67	1.71	1.69	1.69	1.72	1.5	1.55	1.53	1.45
JJA	year	1879	1879	1903	1879	1912	1912	1912	2012	2012	1879	1985	1877	2019	1912
	anom	2.16	2.21	2.61	2.03	2.03	2.12	1.94	1.81	1.84	2.03	1.69	1.75	1.51	1.65
SON	year	1960	2000	2000	1852	2019	1960	2000	1954	1872	2000	1954	1984	1981	2000
	anom	1.73	1.99	2.07	1.78	1.86	1.78	1.92	1.72	1.76	1.67	1.48	1.49	1.55	1.46

The extremes are calculated from regional HadUK-Grid observed data

Table 5.5: Historical monthly and seasonal dry extremes: minimum ratio to 1981-2010 mean, over the period 1836-2022

		South West England	South East England	London	East of England	East Midlands	West Midlands	Yorkshire and Humb.	North West England	North East England	Wales	West Scotland	East Scotland	North Scotland	Northern Ireland
Jan	year	1855	1880	1880	1880	1880	1855	1880	1997	1880	1997	1963	1997	1881	1855
	anom	0.1	0.16	0.16	0.1	0.15	0.12	0.12	0.1	0.21	0.08	0.11	0.25	0.18	0.15
Feb	year	1932	1891	1891	1891	1891	1891	1891	1932	1891	1932	1932	1932	1963	1932
	anom	0.02	0.02	0.02	0.04	0.08	0.07	0.07	0.05	0.05	0.03	0.02	0.09	0.1	0.06
Mar	year	1840	1929	1929	1929	1929	1929	1929	1840	1929	1840	1840	1856	1856	1837
	anom	0.06	0.04	0.02	0.05	0.11	0.11	0.13	0.11	0.1	0.07	0.09	0.07	0.04	0.13
Apr	year	1938	1893	1912	2007	1938	1938	1938	1980	2020	1938	1842	1842	1842	1842
	anom	0.05	0.03	0.04	0.02	0.07	0.06	0.12	0.09	0.08	0.11	0.06	0.07	0.08	0.07
May	year	1896	2020	2020	2020	2020	2020	1844	1836	1859	1844	1836	1859	1859	1844
	anom	0.06	0.09	0.05	0.06	0.12	0.1	0.17	0.06	0.11	0.05	0.07	0.08	0.12	0.11
Jun	year	1925	2018	2018	1962	1925	1925	1925	1925	1925	1925	1921	1865	1889	1921
	anom	0.02	0.05	0.01	0.1	0.04	0.04	0.05	0.09	0.08	0.03	0.29	0.23	0.28	0.14
Jul	year	1911	2022	2022	2022	1911	1911	1868	1868	1868	1911	1863	1863	1955	1898
	anom	0.17	0.1	0.08	0.1	0.11	0.17	0.27	0.18	0.26	0.24	0.15	0.21	0.26	0.21
Aug	year	1940	1940	1995	1947	1947	1940	1995	1947	1947	1995	1947	1947	1947	1947
	anom	0.07	0.04	0.04	0.09	0.08	0.13	0.13	0.06	0.09	0.14	0.02	0.04	0.05	0.13
Sep	year	1865	1959	1959	1959	1959	1959	1959	1910	1865	1959	1894	1972	1894	1894
	anom	0.05	0.06	0.04	0.03	0.05	0.06	0.11	0.15	0.18	0.11	0.05	0.15	0.13	0.07
Oct	year	1978	1969	1978	1978	1947	1969	1978	1946	1969	1947	1946	1946	1946	1838
	anom	0.09	0.06	0.06	0.1	0.13	0.14	0.25	0.16	0.22	0.19	0.1	0.12	0.11	0.24
Nov	year	1879	1945	1945	1867	1945	1945	1945	1945	1867	1945	1945	1867	1945	1855
	anom	0.14	0.13	0.09	0.29	0.21	0.15	0.23	0.09	0.18	0.14	0.12	0.21	0.2	0.25
Dec	year	1926	1840	1926	1843	1843	1840	1843	1844	1844	1844	1853	1843	1927	1844
	anom	0.16	0.16	0.18	0.15	0.14	0.14	0.12	0.09	0.2	0.16	0.14	0.28	0.14	0.2
DJF	year	1964	1992	1992	1858	1858	1858	1858	1891	1858	1964	1964	1964	1838	1891
	anom	0.35	0.34	0.28	0.35	0.2	0.3	0.27	0.29	0.35	0.28	0.34	0.39	0.33	0.38
MAM	year	1893	1893	1893	2011	1852	1938	1852	1984	2020	1893	1840	1852	1852	1837
	anom	0.27	0.22	0.22	0.2	0.32	0.37	0.34	0.43	0.41	0.38	0.39	0.38	0.29	0.41
JJA	year	1995	1995	1921	1921	1995	1995	1976	1976	1995	1976	1869	1955	1955	1983
	anom	0.32	0.34	0.31	0.35	0.23	0.32	0.27	0.38	0.33	0.3	0.51	0.41	0.43	0.43
SON	year	1978	1978	1978	1978	1964	1978	1964	1915	1867	1922	1915	1972	1894	1837
	anom	0.3	0.21	0.22	0.35	0.43	0.46	0.46	0.35	0.48	0.52	0.41	0.42	0.47	0.46

The extremes are calculated from regional HadUK-Grid observed data

Table 5.6: Historical monthly and seasonal windy extremes: maximum ratio to 1981-2010 mean, over the period 1969-2022

		South West England	South East England	London	East of England	East Midlands	West Midlands	Yorkshire and Humb.	North West England	North East England	Wales	West Scotland	East Scotland	North Scotland	Northern Ireland
Jan	year	1974	1974	1983	1983	1983	1983	1993	1983	1983	1974	1974	1983	1974	1993
	anom	1.36	1.35	1.36	1.37	1.41	1.4	1.44	1.45	1.54	1.46	1.51	1.5	1.85	1.48
Feb	year	1990	1990	1990	1990	1990	1990	1990	1990	1990	1990	1990	1990	1997	1990
	anom	1.6	1.65	1.6	1.55	1.58	1.62	1.67	1.63	1.52	1.64	1.52	1.48	1.39	1.5
Mar	year	1994	1979	1979	1994	1994	1994	1994	1994	1994	1994	1994	1990	1979	1990
	anom	1.3	1.37	1.43	1.35	1.37	1.43	1.43	1.42	1.43	1.4	1.4	1.42	1.41	1.38
Apr	year	1972	1972	1972	1972	1977	1972	1977	1977	1977	1972	1977	1977	1991	1973
	anom	1.41	1.47	1.44	1.36	1.39	1.37	1.43	1.37	1.48	1.34	1.31	1.3	1.26	1.35
May	year	1972	1977	1977	1972	1986	1986	1986	1986	1986	1986	1986	1986	1970	2011
	anom	1.34	1.38	1.45	1.36	1.32	1.34	1.36	1.58	1.38	1.59	1.42	1.44	1.44	1.45
Jun	year	2012	2012	1977	1981	1981	1994	1981	1981	1981	1981	1981	1994	1994	1981
	anom	1.27	1.33	1.29	1.34	1.32	1.3	1.3	1.29	1.35	1.28	1.27	1.32	1.3	1.29
Jul	year	1974	1974	1974	1974	1974	1970	1970	1970	1974	1988	1970	1969	1970	1970
	anom	1.3	1.37	1.4	1.29	1.31	1.37	1.28	1.37	1.23	1.35	1.36	1.26	1.31	1.32
Aug	year	1985	1985	1992	1985	1985	1985	1985	1985	1985	1985	1985	1985	1982	1985
	anom	1.41	1.37	1.29	1.3	1.38	1.48	1.37	1.55	1.34	1.56	1.37	1.25	1.22	1.34
Sep	year	1974	1974	1974	1978	1978	1978	1978	1978	1978	1978	1978	1978	1978	1980
	anom	1.4	1.42	1.45	1.31	1.37	1.32	1.37	1.43	1.45	1.41	1.28	1.32	1.32	1.33
Oct	year	1998	1998	1998	1998	1998	1998	1983	1983	1983	1998	1983	1983	1977	1983
	anom	1.3	1.33	1.33	1.37	1.33	1.45	1.31	1.41	1.5	1.32	1.38	1.39	1.36	1.24
Nov	year	2009	1980	1977	1977	1977	1977	1977	1986	1977	1977	1986	1978	1971	1986
	anom	1.48	1.52	1.75	1.54	1.51	1.45	1.43	1.45	1.46	1.4	1.34	1.34	1.4	1.35
Dec	year	1974	1974	1974	1974	1974	1974	1974	1974	1974	2015	1974	1974	1974	1974
	anom	1.53	1.56	1.69	1.55	1.61	1.63	1.62	1.64	1.68	1.53	1.64	1.6	1.62	1.56
DJF	year	1990	1990	1975	1995	1990	1990	1990	1995	1976	1990	1974	1989	1974	1981
	anom	1.25	1.28	1.26	1.21	1.2	1.22	1.24	1.22	1.26	1.22	1.25	1.25	1.4	1.22
MAM	year	1972	1972	1977	1977	1977	1994	1994	1986	1994	1986	1994	1994	1970	1986
	anom	1.26	1.31	1.39	1.26	1.28	1.29	1.27	1.26	1.25	1.28	1.23	1.22	1.23	1.22
JJA	year	1985	1974	1974	1977	1977	1985	1985	1985	1981	1985	1974	1974	1974	1986
	anom	1.21	1.23	1.28	1.2	1.18	1.22	1.15	1.24	1.17	1.26	1.21	1.12	1.13	1.17
SON	year	1980	1974	1980	1980	1977	1980	1977	1977	1977	1980	1977	1977	1977	1980
	anom	1.24	1.28	1.39	1.27	1.29	1.28	1.28	1.28	1.31	1.26	1.3	1.24	1.3	1.26

The extremes are calculated from regional HadUK-Grid observed data

Table 5.7: Historical monthly and seasonal calm extremes: minimum ratio to 1981-2010 mean, over the period 1969-2022

		South West England	South East England	London	East of England	East Midlands	West Midlands	Yorkshire and Humb.	North West England	North East England	Wales	West Scotland	East Scotland	North Scotland	Northern Ireland
Jan	year	2022	2017	2017	1997	1997	1997	1997	1997	1997	1997	1997	1997	2001	1997
	anom	0.68	0.65	0.63	0.66	0.59	0.64	0.57	0.55	0.5	0.66	0.6	0.58	0.65	0.61
Feb	year	1993	1993	1993	1975	1975	1985	1975	2010	2010	2010	2010	2010	2010	2010
	anom	0.72	0.68	0.7	0.73	0.71	0.71	0.59	0.58	0.6	0.65	0.56	0.6	0.6	0.54
Mar	year	2012	2012	2011	2012	2012	2011	2011	2011	2011	2011	2011	1991	1991	2011
	anom	0.72	0.72	0.76	0.7	0.72	0.65	0.7	0.67	0.71	0.69	0.71	0.69	0.69	0.65
Apr	year	2007	1996	2009	1996	1984	2021	2021	2021	1974	2021	1974	1974	1974	1974
	anom	0.79	0.76	0.8	0.83	0.84	0.76	0.79	0.74	0.62	0.77	0.71	0.65	0.6	0.76
May	year	1989	2004	2004	2004	2004	2004	2004	1990	1990	2004	1990	1990	1990	1990
	anom	0.78	0.75	0.76	0.75	0.74	0.72	0.76	0.7	0.68	0.71	0.7	0.71	0.73	0.7
Jun	year	2006	1993	1993	1993	1993	1993	2014	2014	2014	2014	2014	2014	1991	2016
	anom	0.79	0.78	0.75	0.81	0.81	0.75	0.75	0.75	0.7	0.76	0.78	0.76	0.76	0.81
Jul	year	1983	1983	1994	1983	1983	1983	1994	2021	2021	1983	2021	2021	2021	2021
	anom	0.8	0.77	0.79	0.79	0.78	0.73	0.76	0.68	0.67	0.67	0.7	0.72	0.79	0.7
Aug	year	1981	1981	2002	2002	2002	1984	1983	2002	1997	1976	1976	2000	2000	1983
	anom	0.82	0.78	0.77	0.76	0.79	0.81	0.75	0.78	0.76	0.76	0.77	0.79	0.8	0.72
Sep	year	2014	2003	2003	2014	1971	2014	2014	2014	2014	2014	1972	1972	2002	2014
	anom	0.76	0.74	0.76	0.71	0.74	0.68	0.66	0.65	0.65	0.64	0.65	0.66	0.75	0.66
Oct	year	2007	2007	2007	2007	2007	2007	2007	1993	1993	2007	1993	1993	2012	1993
	anom	0.66	0.66	0.64	0.67	0.65	0.6	0.66	0.62	0.67	0.64	0.65	0.73	0.68	0.63
Nov	year	1988	1988	1988	1988	1988	1988	1983	2016	1993	1988	2019	1993	2019	2016
	anom	0.7	0.69	0.64	0.73	0.71	0.69	0.74	0.74	0.7	0.71	0.73	0.73	0.72	0.74
Dec	year	2016	2016	1984	2016	2010	2010	2010	2010	2010	2010	2010	2010	2010	1976
	anom	0.73	0.7	0.67	0.77	0.73	0.66	0.7	0.58	0.71	0.58	0.61	0.67	0.62	0.74
DJF	year	2010	2017	2017	2017	2010	1985	2010	2010	2010	2010	2010	2010	2010	2010
	anom	0.83	0.77	0.76	0.81	0.81	0.73	0.75	0.69	0.72	0.72	0.66	0.7	0.71	0.7
MAM	year	1971	2004	2022	2004	1984	2010	1984	1984	2021	1971	1984	1984	2010	2010
	anom	0.88	0.87	0.88	0.86	0.86	0.84	0.81	0.81	0.79	0.79	0.81	0.85	0.86	0.81
JJA	year	1999	1996	1987	2002	1999	2021	1983	2021	2021	1983	2021	2021	1991	1983
	anom	0.89	0.89	0.85	0.9	0.9	0.82	0.85	0.81	0.79	0.84	0.83	0.85	0.89	0.81
SON	year	2007	2007	2007	2014	1993	1993	1993	1993	1993	1993	1993	1993	1993	1993
	anom	0.79	0.84	0.85	0.86	0.84	0.79	0.84	0.79	0.78	0.78	0.81	0.78	0.81	0.83

The extremes are calculated from regional HadUK-Grid observed data

Figure 5.5: Variation in standard deviation (temperature) and coefficient of variation (rainfall and windspeed) across regions, by month and season. The standard deviation and coefficient of variation are calculated over 30-year periods starting at 10-year intervals beginning in 1891 (temperature), 1841 (rainfall) and 1971 (windspeed). For each time slice, the vertical lines show the range across all 12x12km cells within a region, and the regional median is shown by a dot.

The variation in the magnitude of the most extreme temperature anomalies through the year in a region largely reflects variation in inherent variability from year to year (Figure 5.6). The standard deviation of temperature is largest in most regions in January and February and, to a lesser extent in December, and the standard deviation is typically smallest in summer months. There is much less variability between months in the CV of monthly rainfall (Figure 5.6), with much larger variation between different time periods, suggesting that the inherent relative variability in monthly rainfall is consistent across the year. The CV of monthly windspeed is generally higher in winter months than summer months (Figure 5.6), particularly in the north of England and in Scotland.

The finer the spatial scale of interest, the more extreme (in relative terms) the anomaly. This is shown by the shaded areas in Figure 5.4 and also by Figure 5.7. The effect for temperature is relatively small (Figure 5.7a), and the most extreme anomaly at the 5x5km or 25km^2 scale is at most 1^{o}C larger than the most extreme anomaly in the regional average temperature: it is often far less. This is because high and low temperature anomalies typically cover a large geographic area. For rainfall (Figure 5.7b), however, the spatial scale effect can be very large because extreme months are more geographically restricted. The largest anomaly at the 25km^2 scale can be twice the largest anomaly at the regional scale (four times the mean, rather than twice the mean), and whilst months with zero rainfall have never occurred at the regional average scale, they have at the 25km^2 and 144km^2 scales. The effect for windspeed (Figure 5.7c) is smaller than for rainfall, but the windiest month at the 25km^2 scale can have an anomaly up to 1.5 times the anomaly at the regional scale.

The largest temperature and rainfall anomalies for specific point locations with long records are shown in Figure 5.8. Extreme monthly rainfall at these points has been around 3.5 times the 1981-2010 mean, but these long record sites do not necessarily have the most extreme local anomalies. Larger anomalies can be found in the HadUK-Grid data (Figure 5.4).

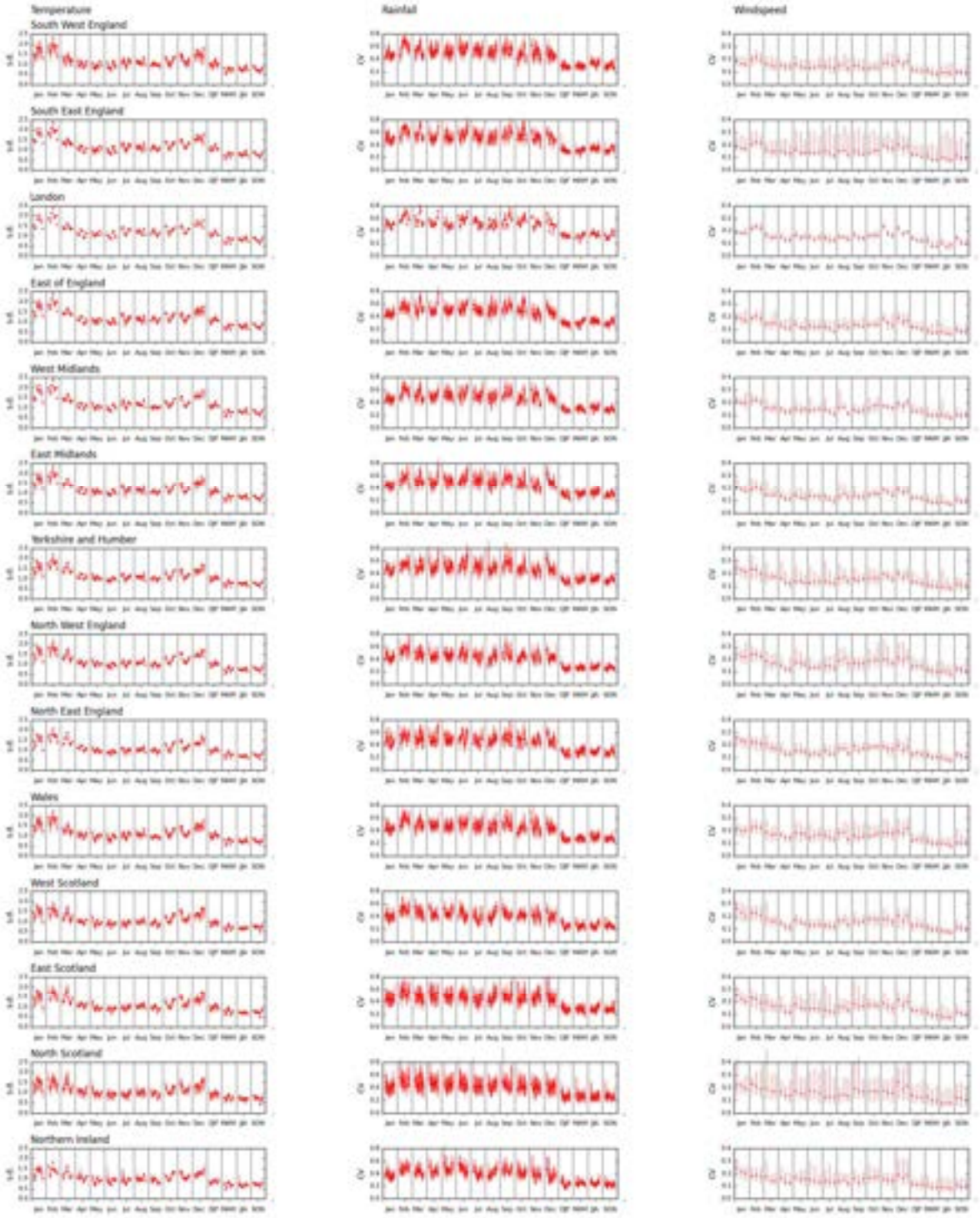

Figure 5.6: Variation in standard deviation (temperature) and coefficient of variation (rainfall and windspeed) across months and seasons, by region.

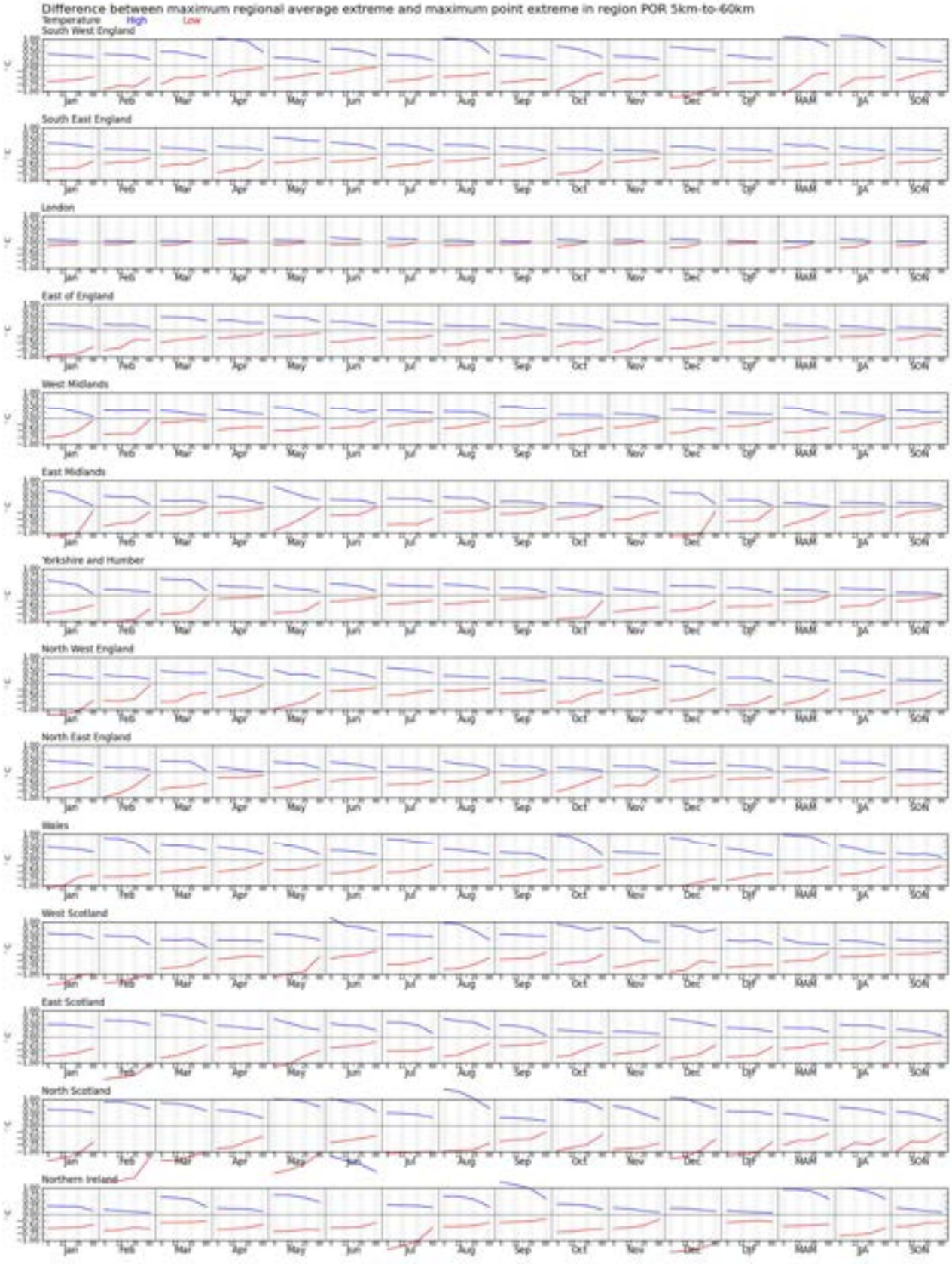

Figure 5.7a: Difference between the largest temperature anomaly within a region and the largest anomaly in regional average temperature, at scales between 5x5km and 60x60km. Note that the regions vary in size.

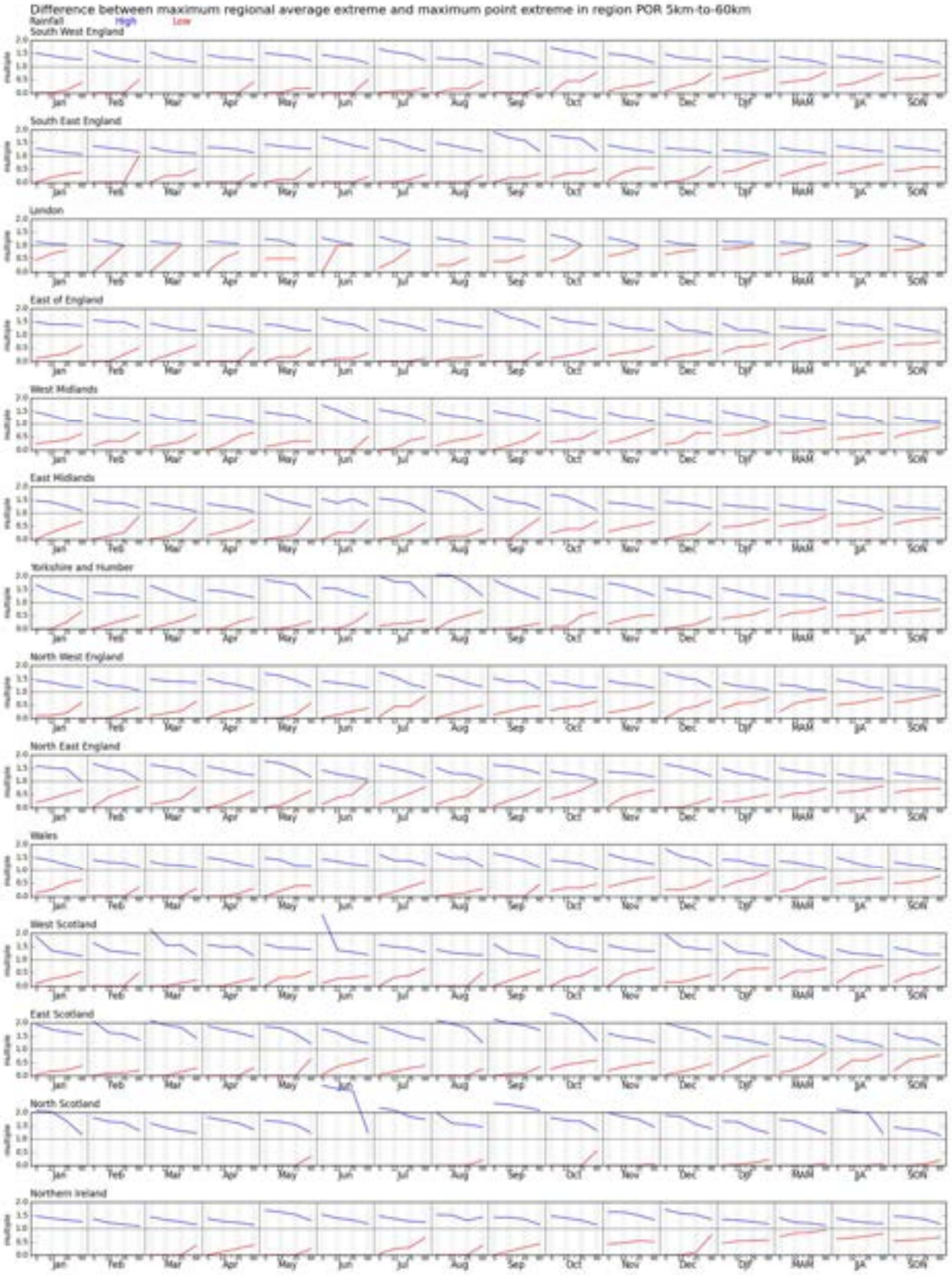

Figure 5.7b: Ratio of the largest rainfall anomaly within a region to the largest anomaly in regional average rainfall, at scales between 5x5km and 60x60km. Note that the regions vary in size. The large ratios for June in west and north Scotland are erroneous

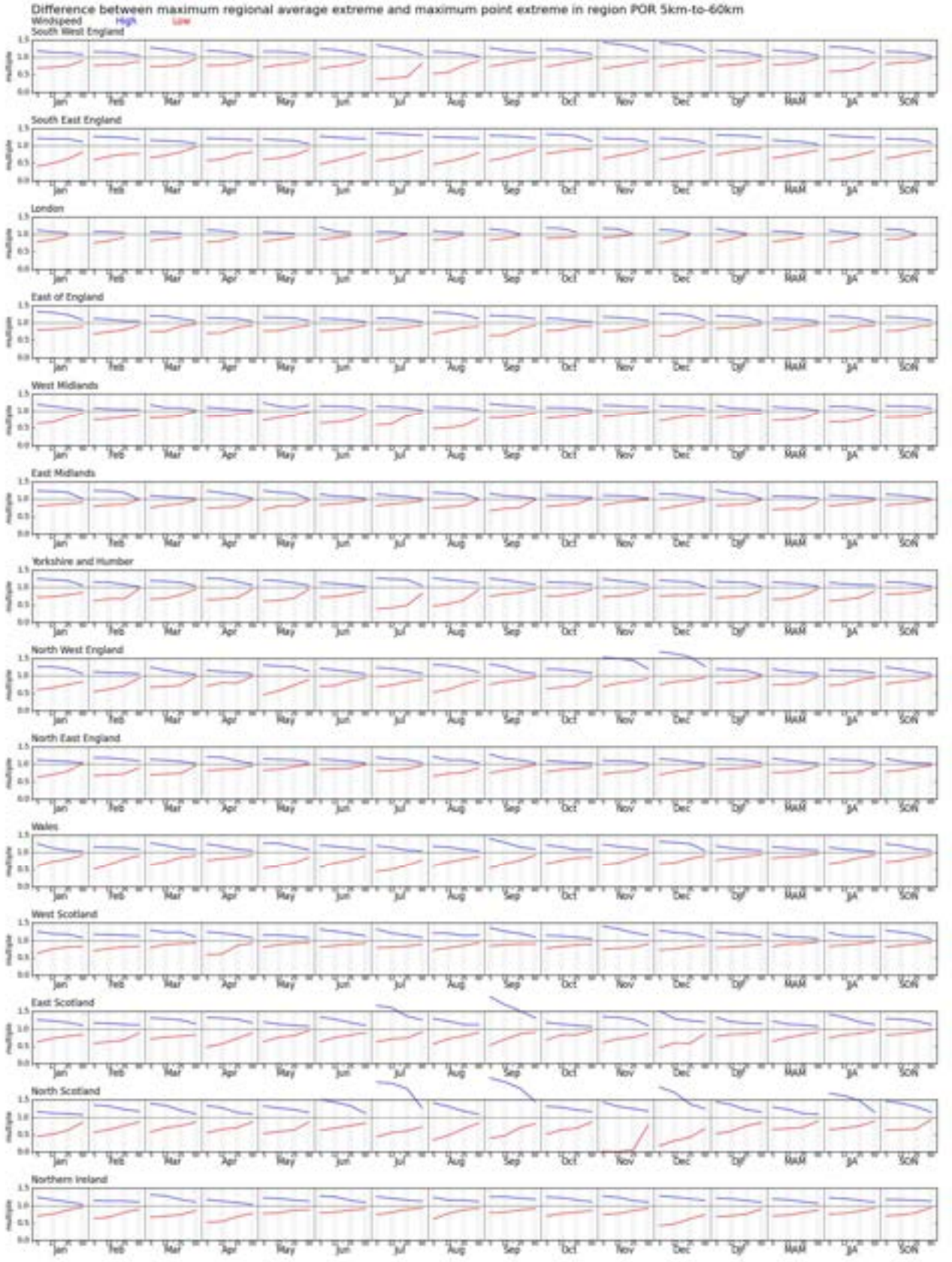

Figure 5.7c: Ratio of the largest windspeed anomaly within a region to the largest anomaly in regional average windspeed, at scales between 5x5km and 60x60km. Note that the regions vary in size. The large ratios for some months in north Scotland are erroneous

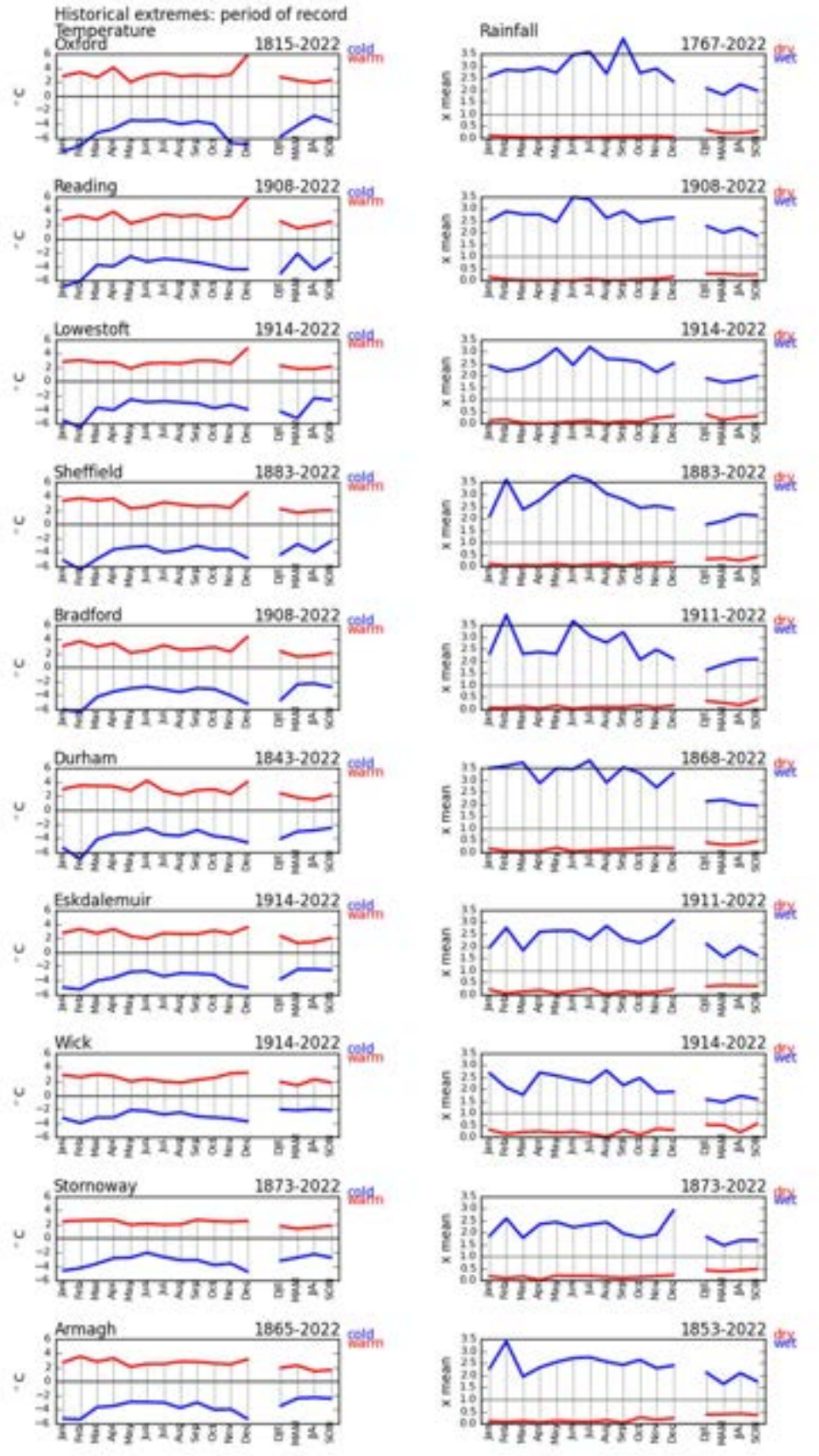

Figure 5.8: Maximum historical temperature and rainfall, relative to the 1981-2010 mean, for point locations with long records. Data from Met Office Long Record data set, and site records for Oxford, Durham and Reading.

Taking a longer-term perspective (Figure 5.9), most of the coldest months in the Central England Temperature record are before the HadUK-Grid records start in 1884 (January 1795, March 1674, April 1701, May 1698, June 1675, July 1816, September 1674, October 1740 and November 1782). Only two of the hottest months (February 1779 and June 1846) date from before 1884. Five of the driest months in the England and Wales HadUKP precipitation record date from before 1836 (January 1766, March 1781, July 1825, October 1781 and December 1788). Only two of the wettest months (May 1773 and July 1828) are before 1836. However, the historical extreme anomalies over these longer time scales are not substantially different to those over the HadUK-Grid period (compare the temperature extremes in Figure 5.9 with those for the West and East Midlands in Figure 5.4: the HadUKP rainfall data are averaged over a larger region than shown in Figure 5.4 but are similar to extremes from national averages calculated from HadUK-Grid).

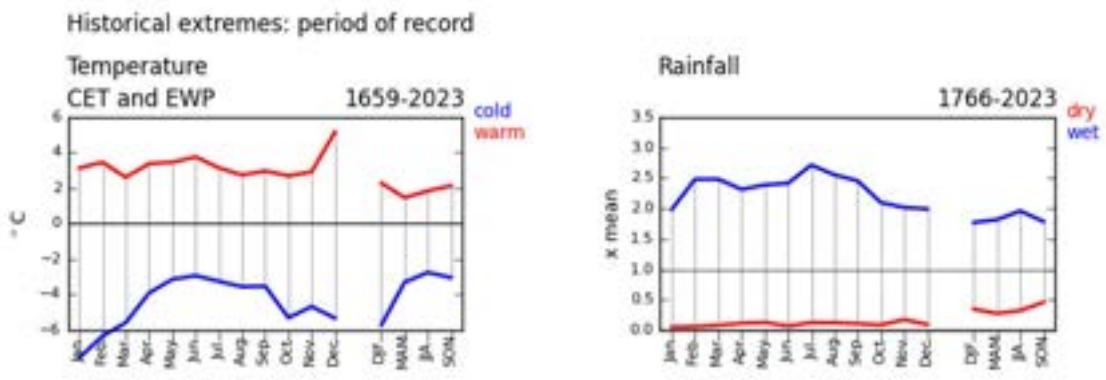

Figure 5.9: Maximum historical temperature and rainfall anomalies in the Central England Temperature and HadUKP England and Wales precipitation data, as differences from the 1981-2010 mean.

It is clear from the figures that there is typically a smooth pattern in the magnitude of the historical extreme through the year for temperature – with greater anomalies in winter – but there is much more variability from month to month in historical high rainfall and windspeed extremes. This does not necessarily imply that the plausible most extreme anomaly will vary from month to month. It probably reflects greater year-to-year variability in rainfall and windspeed than temperature and the smaller footprint of extreme rainfall and windspeed anomalies than temperature anomalies. It is therefore plausible to assume that extreme anomalies in rainfall and windspeed that occur in one month could have occurred in another month. For temperature, rainfall and windspeed, the largest observed differences between the regional and local anomaly (as plotted in Figures 5.4 and 5.6) reflect the spatial variability in

actual extreme events. It is plausible to assume that events with similar spatial variability could occur in other months or regions.

5.5.3.2 Observed and simulated extreme anomalies

The observed record represents one realisation of a plausible historical climate: other pasts, and particularly past extremes, could have occurred. This sampling effect is seen in the variation in extremes from month to month in Figure 5.4. An ensemble of computer simulations of current climate gives an indication of extremes that could have occurred but did not. The UNSEEN methodology (Thompson et al., 2017; Kay et al., 2020) applies this approach. Thompson et al. (2017) generated 2800 plausible sequences of winter rainfall across south east England, based on different sets of initial conditions simulated by forecast models. Their results (their Figure 3) show that the largest monthly rainfall in winter could be between approximately 3 and 3.6 times the average (anomaly of 200 to 260%), which is larger than the maximum historical regional anomalies shown in Figure 5.4. Leach et al. (2022) took a different approach to generate samples of extreme winters, generating winters from initial conditions characteristic of unusually hot or wet winters. Although they focused on the chance of experiencing winters above defined thresholds rather than absolute extremes, they did give the example of a simulated extreme hot winter anomaly (average across December to February temperatures over the UK) of approximately 4.5^{o}C (inferred from their Figures 3 and 6).

The regional extreme anomalies over the period 1900 to 2022 from the 15 UKCP18 global strand ensemble members are shown in Figure 5.10, along with the observed extreme regional scale anomalies. There is variation across the 15 ensemble members – some have smaller extreme anomalies than the observations – but the largest simulated anomalies are greater than the largest observed anomalies, particularly for rainfall where the wettest months may be over four times larger than the mean. Note that the largest rainfall anomalies in winter in south east England are similar to Thompson et al.'s (2017) UNSEEN anomalies. The simulations in Figure 5.10 are bias-adjusted so that the simulated standard deviation (temperature) and coefficient of variation (rainfall and windspeed) matches the observed over the period 1981-2010, but the results are similar with simulations that have not been bias adjusted.

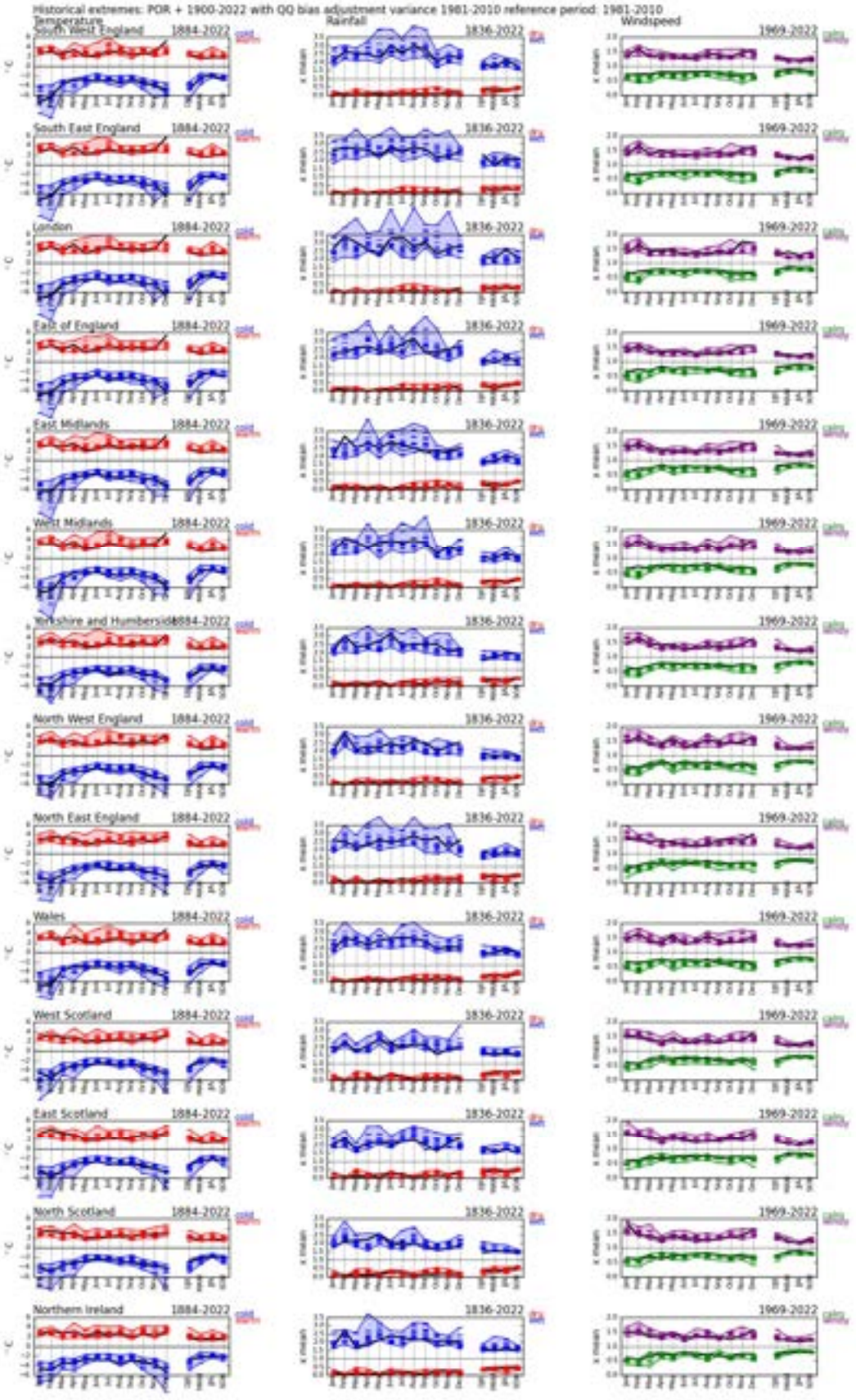

Figure 5.10: Observed and simulated maximum historical temperature, rainfall and windspeed anomalies, relative to the 1981-2010 mean, by region. Simulated data are from the UKCP18 global strand ensemble, adjusted so that standard deviation or coefficient of variation are the same as observed over 1981-2010. Simulated extremes calculated over 1900-2022.

5.5.3.3 Compound extremes

It is possible that extreme temperature, rainfall or windspeed anomalies can occur at the same time.

Figure 5.11 summarises regional compound temperature and rainfall extreme anomalies, based on regional average temperature and rainfall. A compound extreme anomaly is defined as one where both the temperature and rainfall extremes are among the top ten most extreme over a specific period – here 1884 to 2022. Compound extremes do not occur in every month, but different combinations appear in different months. Compound extremes in winter months are either ‘hot and wet’ or ‘cold and dry’, and in summer are either ‘hot and dry’ or ‘cold and wet’. There are very few occasions where other combinations occur. Combinations in spring and autumn can follow the winter or summer pattern. There is regional variability in when compound extremes have occurred, but the broad patterns of combinations are consistent across the UK.

Compound rainfall and windspeed anomalies are either ‘wet and windy’ or ‘dry and calm’ throughout the year. Compound temperature and windspeed anomalies are either ‘mild and windy’ or ‘cold and calm’ in winter, and ‘hot and calm’ or ‘cool and windy’ in summer. Compound temperature, rainfall and windspeed anomalies are rare, but are either ‘mild, wet and windy’ or ‘cold, dry and calm’ in winter and ‘hot, dry and calm’ or ‘cool, wet and windy’ in summer.

Table 5.8 shows the months and seasons by region with extreme compound regional temperature and rainfall anomalies: it also indicates which of these months and seasons also had an extreme windspeed anomaly. It is based on the most extreme five anomalies over the period 1884 to 2022, rather than the most extreme ten as shown in Figure 5.11.

Figure 5.11: Regional compound temperature and rainfall extremes. A compound extreme has an extreme anomaly within the largest ten over the period 1884-2022. The left three panels show the average temperature, rainfall and windspeed anomaly in these compound events (windspeed only over the events occurring after 1969), and the right panel shows the timing of the compound events (month/season on vertical axis, and year on horizontal axis).

Table 5.8: Historical compound extreme monthly and seasonal anomalies, as a difference from the 1981-2010 mean (temperature) and a ratio to the 1981-2010 mean (rainfall).

Region	Compound	Month	Year	Temp	Rain	Year	Temp	Rain	Year	Temp	Rain
South West England	cold+dry	Feb	1895	-6.39	0.05						
	cold+dry	Nov	1896	-3.36	0.27						
	cold+dry	DJF	1891	-3.08	0.48						
	cold+wet	May	1979	-2.34	1.87						
	cold+wet	Jul	1888	-2.38	2.35						
	cold+wet	Aug	1912	-3.48	2.95						
	cold+wet	Sep	**1974**	-2.23	2.52						
	hot+dry	Mar	1938	1.69	0.12						
	hot+dry	Apr	1893	2.64	0.09						
	hot+dry	Jun	2018	2.2	0.14						
	hot+dry	Aug	1995	2.96	0.17	**2003**	2	0.27			
	hot+dry	Sep	1929	1.99	0.2						
	hot+dry	MAM	1893	1.71	0.27	2011	1.37	0.35			
	hot+dry	JJA	1976	1.65	0.36	**1983**	1.44	0.46	1995	1.53	0.32
	hot+wet	Feb	**1990**	2.84	2.42						
	hot+wet	Aug	1997	2	2.14						
	hot+wet	Nov	2002	1.8	1.86						
	hot+wet	Dec	1934	3.08	2.23						
	hot+wet	DJF	**1990**	1.68	1.71						
South East England	cold+dry	Feb	1895	-6.57	0.12						
	cold+dry	Dec	1933	-4.07	0.19						
	cold+dry	DJF	1891	-3.86	0.39						
	cold+wet	Jun	**1991**	-2.42	2.22						
	cold+wet	Jul	1888	-3.19	2.59						
	cold+wet	Aug	1912	-3.66	2.75						
	hot+dry	Apr	**2007**	3.07	0.04	2011	3.67	0.07			
	hot+dry	Jun	2018	1.68	0.05						
	hot+dry	Jul	2022	1.93	0.1						
	hot+dry	Aug	1947	2.08	0.19	1995	2.55	0.08	2003	2.19	0.31
	hot+dry	MAM	2011	1.51	0.28						
	hot+dry	JJA	1976	1.62	0.4	2022	1.73	0.46			
	hot+dry	SON	2011	1.87	0.49						
	hot+wet	Feb	**1990**	3.35	2.43						
	hot+wet	Nov	**2009**	1.94	2.15	2022	2.44	2.17			
	hot+wet	Dec	1934	3.16	2.35						
	hot+wet	DJF	**1990**	2.07	1.81						
London	cold+dry	Feb	1895	-6.89	0.12						
	cold+dry	Dec	1933	-4.01	0.18						
	cold+dry	DJF	1891	-4.27	0.39						
	cold+wet	Jul	1888	-3.6	2.99						
	cold+wet	Aug	1912	-3.85	2.32						
	cold+wet	JJA	1888	-2.6	1.98	1903	-2.2	2.61			
	hot+dry	Apr	**2007**	3.03	0.06	2011	3.85	0.08			
	hot+dry	May	1989	1.79	0.09						
	hot+dry	Jun	2018	1.8	0.01						
	hot+dry	Jul	2022	2.18	0.08						
	hot+dry	Aug	1995	2.49	0.04	2003	2.44	0.21			
	hot+dry	Sep	1929	2.47	0.12						
	hot+dry	Dec	1988	2.21	0.22						

	hot+dry	MAM	2011	1.6	0.26						
	hot+dry	JJA	1976	1.73	0.34						
	hot+dry	SON	2011	1.93	0.44						
	hot+wet	Feb	**1990**	3.4	2.3						
	hot+wet	Dec	1934	3.12	2.13						
	hot+wet	DJF	**1990**	2.11	1.82	2020	1.87	1.58			
East of England	cold+dry	Dec	1890	-6.23	0.28	1933	-3.37	0.25			
	cold+dry	DJF	1891	-3.79	0.42						
	cold+wet	Jul	1888	-3.24	2.24						
	cold+wet	Aug	1912	-3.4	3.16						
	cold+wet	Oct	1892	-3.73	2.13						
	hot+dry	Feb	1998	2.73	0.17						
	hot+dry	Apr	2007	2.67	0.02	2011	3.48	0.1			
	hot+dry	Jun	1976	2.76	0.22						
	hot+dry	Jul	2022	2.12	0.1						
	hot+dry	Aug	1995	1.87	0.14						
	hot+dry	MAM	2011	1.6	0.2						
	hot+dry	JJA	2022	1.9	0.46						
	hot+dry	SON	2011	2	0.45						
	hot+wet	DJF	**1990**	2.03	1.6						
East Midlands	cold+dry	Feb	1895	-6.37	0.19						
	cold+dry	Dec	1890	-5.46	0.28						
	cold+wet	Jul	1888	-3.36	2.29						
	cold+wet	Aug	1912	-3.58	2.5	1956	-3.16	2.06			
	cold+wet	JJA	1956	-2.03	1.64						
	hot+dry	Mar	1938	2.7	0.17						
	hot+dry	Apr	2007	2.79	0.11	2011	3.52	0.11			
	hot+dry	Jun	1976	2.48	0.2	**2006**	1.81	0.22			
	hot+dry	Aug	1995	1.96	0.12						
	hot+dry	MAM	2011	1.68	0.35						
	hot+dry	JJA	1976	1.4	0.33						
	hot+dry	SON	2011	2.02	0.53						
West Midlands	cold+dry	Feb	1895	-6.78	0.12						
	cold+dry	Sep	1986	-2.86	0.2						
	cold+dry	Dec	1890	-5.76	0.31	1933	-3.28	0.17			
	cold+wet	Jul	1888	-3.08	2.42						
	cold+wet	Aug	1912	-3.69	2.82						
	hot+dry	Mar	1938	2.35	0.18						
	hot+dry	Apr	2011	3.41	0.1						
	hot+dry	Aug	1995	2.7	0.15						
	hot+dry	MAM	1893	1.43	0.47	2011	1.45	0.43			
	hot+dry	JJA	**1976**	1.54	0.41	1995	1.46	0.32	2018	1.67	0.53
Yorkshire and Humb.	cold+dry	Dec	1890	-4.23	0.32						
	cold+wet	Mar	1947	-3.97	2.06						
	cold+wet	Apr	1986	-2.74	1.78						
	cold+wet	Jul	1888	-3.69	2.3						
	cold+wet	Aug	1956	-3.15	2.49						
	cold+wet	Oct	1892	-3.77	2.06						
	hot+dry	Mar	1938	2.96	0.22						
	hot+dry	Apr	2007	2.73	0.16	2011	3.27	0.16			
	hot+dry	Jun	1976	2.13	0.17						
	hot+dry	Aug	1947	1.59	0.13	1995	1.82	0.13			
	hot+dry	MAM	2011	1.55	0.44						
	hot+dry	JJA	1976	1.2	0.27						
	hot+wet	Jan	2008	2.11	2.11						
	hot+wet	Nov	2015	2.1	1.8						
	hot+wet	Dec	**2015**	4.44	1.96						
	hot+wet	DJF	2016	1.9	1.57						

North West England	cold+dry	Jan	1941	-4.22	0.34	1963	-5.23	0.18				
	cold+dry	Feb	1986	-4.69	0.08							
	cold+dry	Mar	1892	-3.85	0.31							
	cold+dry	Sep	1894	-2.4	0.16	1986	-2.44	0.21				
	cold+dry	Dec	1890	-4.31	0.13	**2010**	-4.97	0.29				
	cold+dry	DJF	1963	-4.16	0.41							
	cold+wet	Jul	1888	-3.05	1.98							
	cold+wet	Aug	1956	-2.95	2.6							
	hot+dry	Aug	1947	2.23	0.06	**1995**	2.46	0.18				
	hot+dry	JJA	**1976**	1.38	0.38	1995	1.41	0.45				
	hot+wet	Feb	**1990**	2.5	2.19							
	hot+wet	Nov	2015	2.13	2.01							
	hot+wet	Dec	**2015**	4.3	2.54							
	hot+wet	DJF	2016	1.85	1.87							
North East England	cold+wet	Mar	1888	-3.7	1.73	1947	-4.34	1.98				
	cold+wet	Aug	1956	-3.17	2.83	1986	-2.96	2.1				
	cold+wet	Sep	1918	-2.67	2.22							
	hot+dry	Mar	**2012**	2.7	0.22							
	hot+dry	Jul	2006	2.74	0.29							
	hot+dry	Aug	**1995**	1.86	0.15							
	hot+dry	Oct	1969	2.33	0.22							
	hot+dry	Dec	1971	2.7	0.34							
	hot+dry	JJA	2022	1.54	0.56							
	hot+wet	Feb	**1990**	2.17	2.02							
	hot+wet	Dec	**2015**	3.86	2.52							
	hot+wet	DJF	2016	1.52	1.88							
Wales	cold+dry	Jan	1963	-6.76	0.18							
	cold+dry	Feb	1895	-6.79	0.09	1986	-5.48	0.07				
	cold+dry	Sep	1986	-2.64	0.16							
	cold+dry	Nov	1896	-3.12	0.28							
	cold+dry	Dec	1890	-5.21	0.25	1933	-3.39	0.29				
	cold+dry	DJF	1917	-3.07	0.47	1963	-4.71	0.43				
	cold+wet	Jul	1888	-2.46	2.11	1920	-2.16	2.15				
	cold+wet	Aug	1912	-3.18	2.34							
	hot+dry	Apr	1893	2.25	0.15							
	hot+dry	Jun	2018	2.15	0.24							
	hot+dry	Jul	**1983**	2.63	0.34							
	hot+dry	Aug	1947	2.26	0.18	**1995**	2.99	0.14				
	hot+dry	Oct	1969	2.29	0.26							
	hot+dry	MAM	1893	1.65	0.38							
	hot+dry	JJA	**1976**	1.37	0.3	1995	1.59	0.42				
	hot+wet	Jan	1990	2	1.64							
	hot+wet	Feb	**1990**	2.75	2.1							
	hot+wet	Dec	1934	3.04	1.72	**2015**	4.7	2.04				
	hot+wet	DJF	**2016**	2.11	1.66							
West Scotland	cold+dry	Jan	1895	-4.51	0.3	1941	-4.14	0.16	1963	-4.14	0.11	
	cold+dry	Feb	1895	-5.65	0.19	1947	-5.26	0.13	1986	-3.83	0.05	
	cold+dry	Mar	1892	-3.18	0.21							
	cold+dry	Dec	**2010**	-4.61	0.32							
	cold+dry	DJF	1895	-3.09	0.45	1963	-3.16	0.43				
	hot+dry	Jul	**2021**	1.94	0.34							
	hot+dry	Aug	1947	2.49	0.02	**1995**	2.33	0.26				
	hot+dry	Oct	1908	2.37	0.28							
	hot+dry	JJA	1976	1.09	0.52	1995	1.32	0.56	**2021**	1.2	0.55	
	hot+wet	Oct	**1995**	2.13	1.53							
	hot+wet	Dec	**2015**	2.91	1.99							
	hot+wet	DJF	**2014**	1.4	1.68							
	hot+wet	SON	**2011**	1.6	1.41							

East Scotland	cold+dry	Dec	1892	-2.72	0.41						
	hot+dry	Feb	1993	2.06	0.26						
	hot+dry	Mar	2012	3.09	0.29						
	hot+dry	May	1896	1.53	0.35						
	hot+dry	Jun	1887	1.65	0.3	1940	2.1	0.3			
	hot+dry	Aug	1947	1.86	0.04	**1995**	2	0.24			
	hot+wet	Nov	2022	1.9	1.57						
	hot+wet	Dec	**2015**	2.94	2.42						
	hot+wet	SON	2022	1.53	1.36						
North Scotland	cold+dry	Jan	1963	-3.74	0.2						
	cold+dry	Feb	1947	-4.89	0.16	**1986**	-3.49	0.11			
	cold+dry	DJF	1963	-2.39	0.47						
	hot+dry	May	**2008**	1.86	0.25						
	hot+dry	Aug	1947	2.4	0.05	1955	1.54	0.3	1995	2.01	0.36
	hot+dry	Oct	1908	2.75	0.27						
	hot+dry	JJA	1976	1.11	0.62	**2021**	1.12	0.64			
	hot+wet	Feb	**1998**	3.55	1.88						
	hot+wet	Oct	2001	2.58	1.48						
	hot+wet	DJF	**1989**	2.18	1.44						
Northern Ireland	cold+dry	Jan	1963	-4.48	0.34						
	cold+dry	Feb	1986	-3.71	0.07						
	cold+dry	Mar	1892	-3.39	0.26						
	cold+wet	Aug	1956	-2.32	1.82						
	cold+wet	JJA	1912	-2.19	1.65						
	hot+dry	Mar	2012	2.27	0.27						
	hot+dry	May	2008	2.1	0.26						
	hot+dry	Jun	1887	2.9	0.26						
	hot+dry	Jul	**1983**	1.79	0.28						
	hot+dry	Aug	1947	2.19	0.13	1995	2.68	0.14			
	hot+dry	Sep	1895	1.55	0.21						
	hot+dry	MAM	1893	1.52	0.48						
	hot+dry	JJA	1995	1.5	0.49						
	hot+wet	Dec	**2015**	2.43	1.94						
	hot+wet	SON	**2011**	1.41	1.43						

The extremes are calculated from regional HadUK-Grid observed data over the period 1884-2022. A compound extreme has both a temperature and a rainfall anomaly in the largest five over 1884-2022. **Bold** years are also windy or calm (when wet or dry respectively): note that wind extremes are not available before 1969.

5.5.3.4 Persistence and whiplash

Persistent extreme months and seasons arise when an anomalous month or season is followed by another (for example a hot month is followed by another hot month). In contrast, a ‘whiplash’ occurs when one extreme is followed by the opposite (for example a hot month is followed by a cold month). Here, ‘extreme’ months and seasons are defined as the largest or smallest 5% over the period of record (starting in 1884, 1836 and 1969 for temperature, rainfall and windspeed respectively).

Figures 5.12a and 5.12b show the occurrence of persistent and whiplash months and seasons, at the regional scale, for temperature and rainfall respectively. Persistent hot or cold months are more frequent than whiplash months but whiplashes have occurred in the past. Whiplashes are less frequent at the seasonal scale but have occurred in autumn. Persistent wet or dry months are relatively less frequent than persistent hot or cold months, and whiplash months are relatively more frequent. Whiplash rainfall seasons are as frequent as whiplash rainfall months. The record length for windspeed is much shorter, but both persistent and whiplash events (not shown) have occurred.

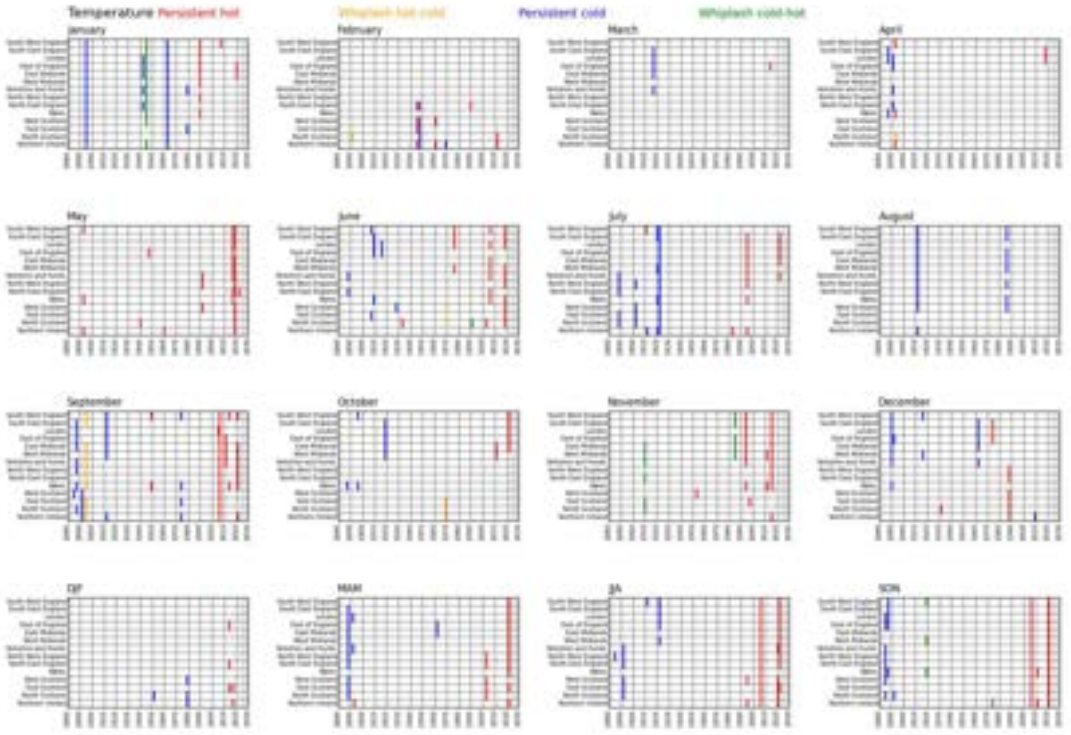

Figure 5.12a: Persistent and whiplash hot and cold months and seasons. An 'extreme' month or season is in the most extreme 5th percentile over the period of record (1884 to 2022). The persistent and whiplash events are plotted by the first month of the pair.

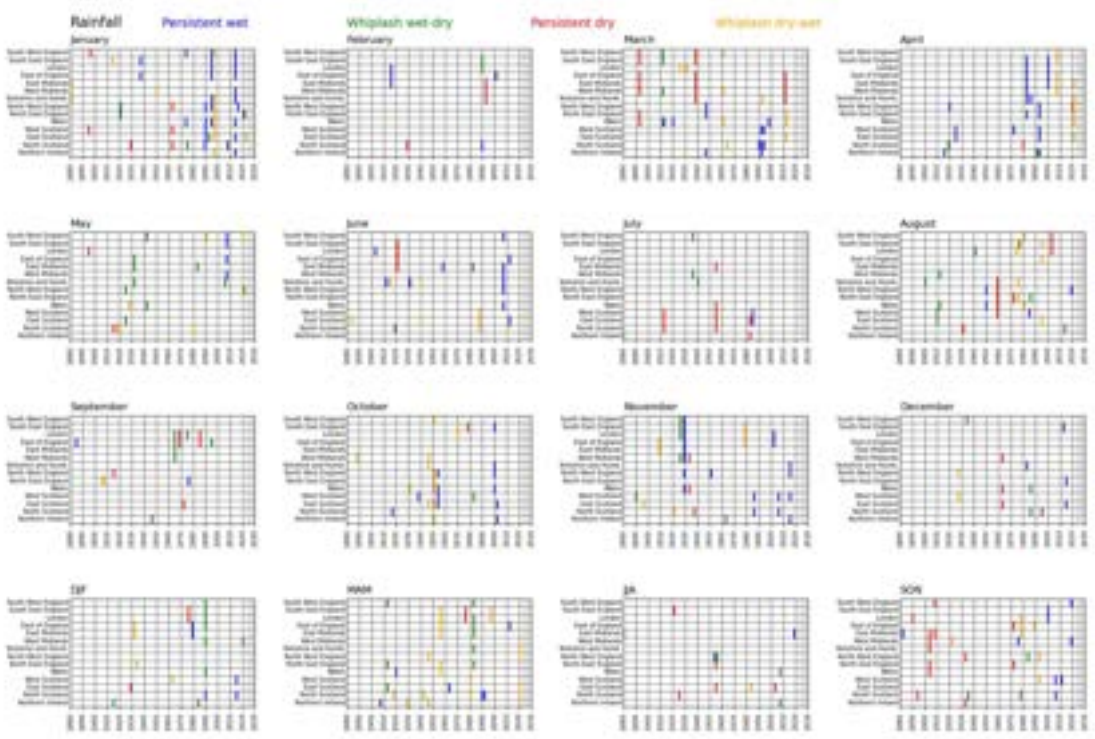

Figure 5.12b: Persistent and whiplash wet and dry months and seasons. An 'extreme' month or season is in the most extreme 5th percentile over the period of record (1836 to 2022). The persistent and whiplash events are plotted by the first month of the pair. For consistency with Figure 5.11a, only events over the period 1880-2022 are plotted.

5.5.4 What do extreme months and seasons look like?

Extreme months and seasons are generally characterised by prolonged periods with anomalous weather. They do not necessarily include the largest short-duration extremes (such as heatwaves, cold spells, rainstorms or windstorms), and the largest short-duration extremes do not necessarily occur in extreme months.

Figure 5.13 plots the years with the most extreme monthly temperature, rainfall and windspeed alongside the years with the most extreme daily temperature, rainfall and windspeed. The comparison is over the period 1960 to 2022 for temperature and rainfall (the HadUK-Grid daily rainfall data only go back to 1960), and between 1969 and 2022 for windspeed. The hottest monthly temperatures rarely occur in the same year as the hottest daily temperatures (Figure 5.13a). Notable exceptions are February 1998 in northern parts of the UK, March 2012 in Scotland, March 2017 in parts of southern England, June 1976 in southern England, and December 2015 in much of England. Similarly, the coldest months rarely coincide with the months with the coldest daily temperatures (Figure 5.13b), with the most widespread coincidence in July 1964, August 1966 and December 2010. Monthly and daily rainfall extremes coincide less frequently (Figure 5.13c), with the most extensive coincidence in February 2020. The most extreme monthly and daily windspeeds (Figure 5.13d) also coincide in February 2020 across most of the UK and November 1977 across central and northern England. Note that short-duration windstorms with high peak speeds (e.g. October 1987) are not picked up at this level of analysis.

The variation in daily weather during example extreme months is illustrated in Figure 5.14. In each case, the extreme months consist of long spells of weather (temperature, rainfall or windspeed) well above the monthly mean, interspersed with shorter spells close to or even below the mean. Some of the example extreme rainfall months have many days with above average rainfall, but others – specifically July 2007 – are generated by very high short duration rainfall.

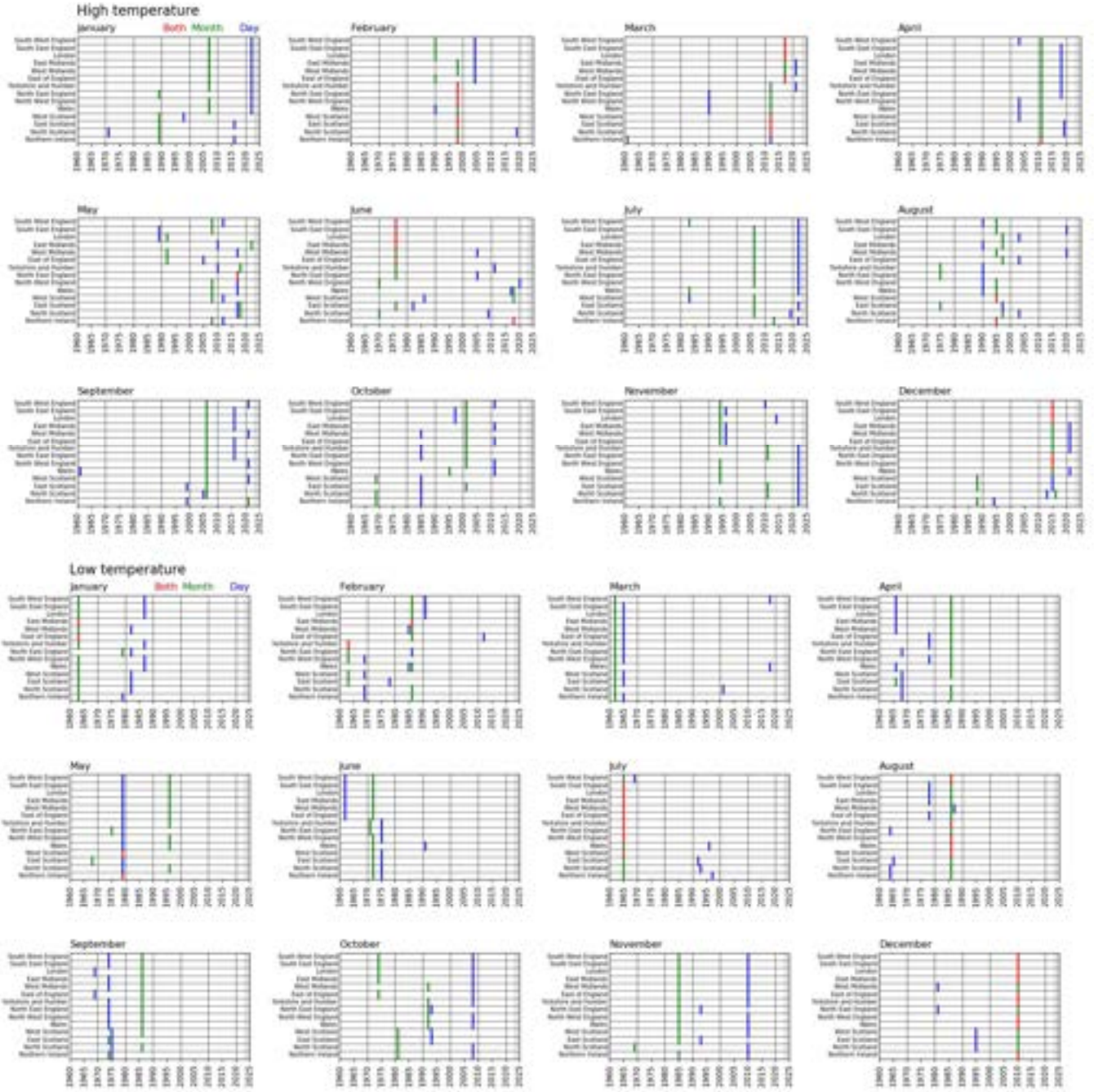

Figure 5.13a/b: Years with record monthly and daily extremes. Monthly extreme: green, daily extreme: blue, Both monthly and daily extreme: red. a) High temperature extremes (1960-2022). b) Low temperature extremes (1960-2022).

Figure 5.13c/d: Years with record monthly and daily extremes. Monthly extreme: green, daily extreme: blue, Both monthly and daily extreme: red. c) High rainfall extremes (1960-2022). d) high windspeed extremes (1969-2022).

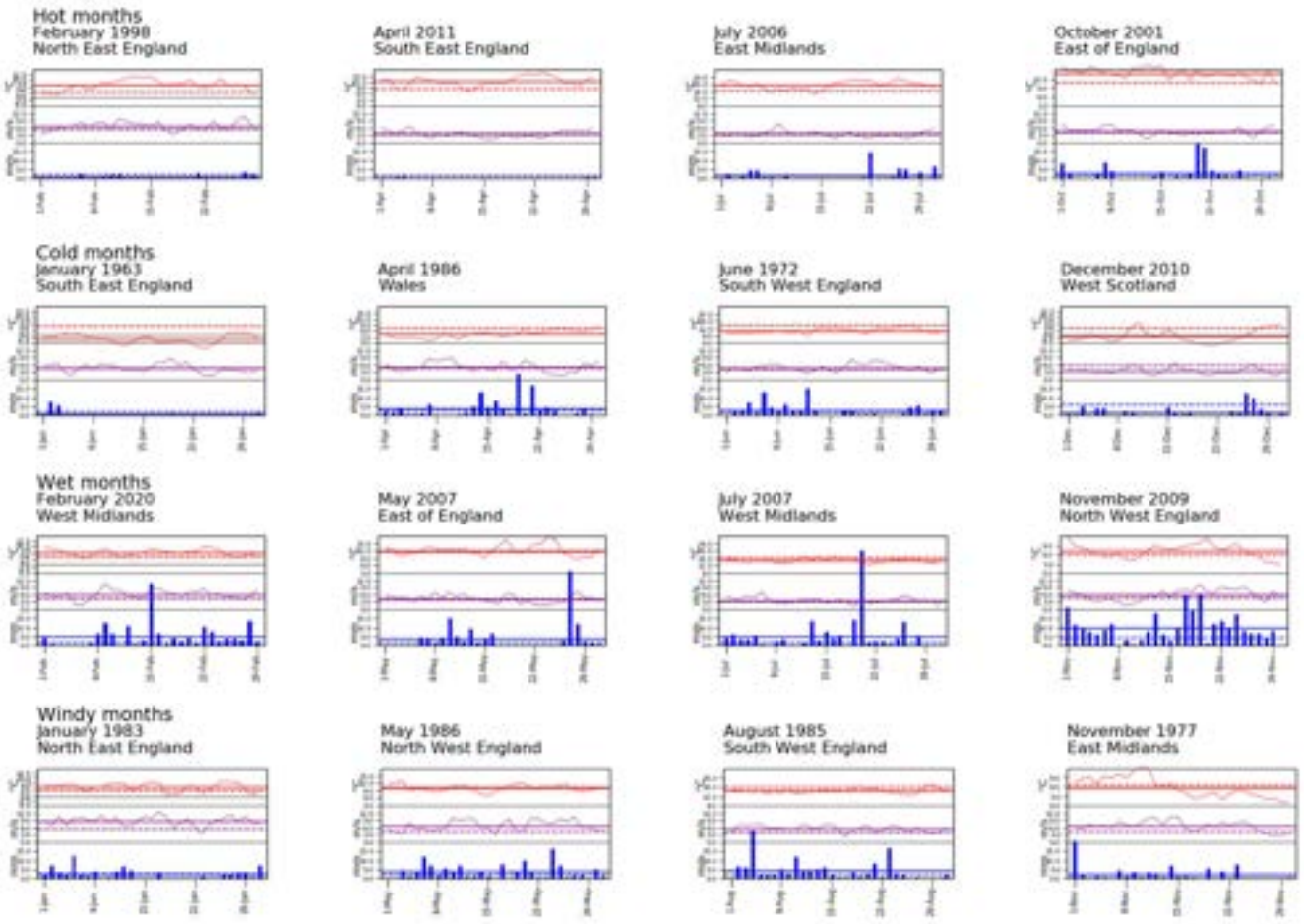

Figure 5.14: Daily temperature, rainfall and windspeed during example extreme months. Red: temperature, blue: rainfall, purple: windspeed. In each case the solid horizontal line is the monthly mean for the specific month, and the dotted horizontal line is the 1981-2010 mean.

Whilst some historically-extreme months and seasons are confined to specific parts of the UK, some events in some months have affected virtually all of the UK (Figure 5.13) – and even if they were not record-breaking everywhere they were extreme. The geographic distribution of anomalies (at the 60x60km scale) from the 1981-2010 mean are shown for example extreme months in Figure 5.15, highlighting the potential for extreme events to impact the whole of the UK at the same time.

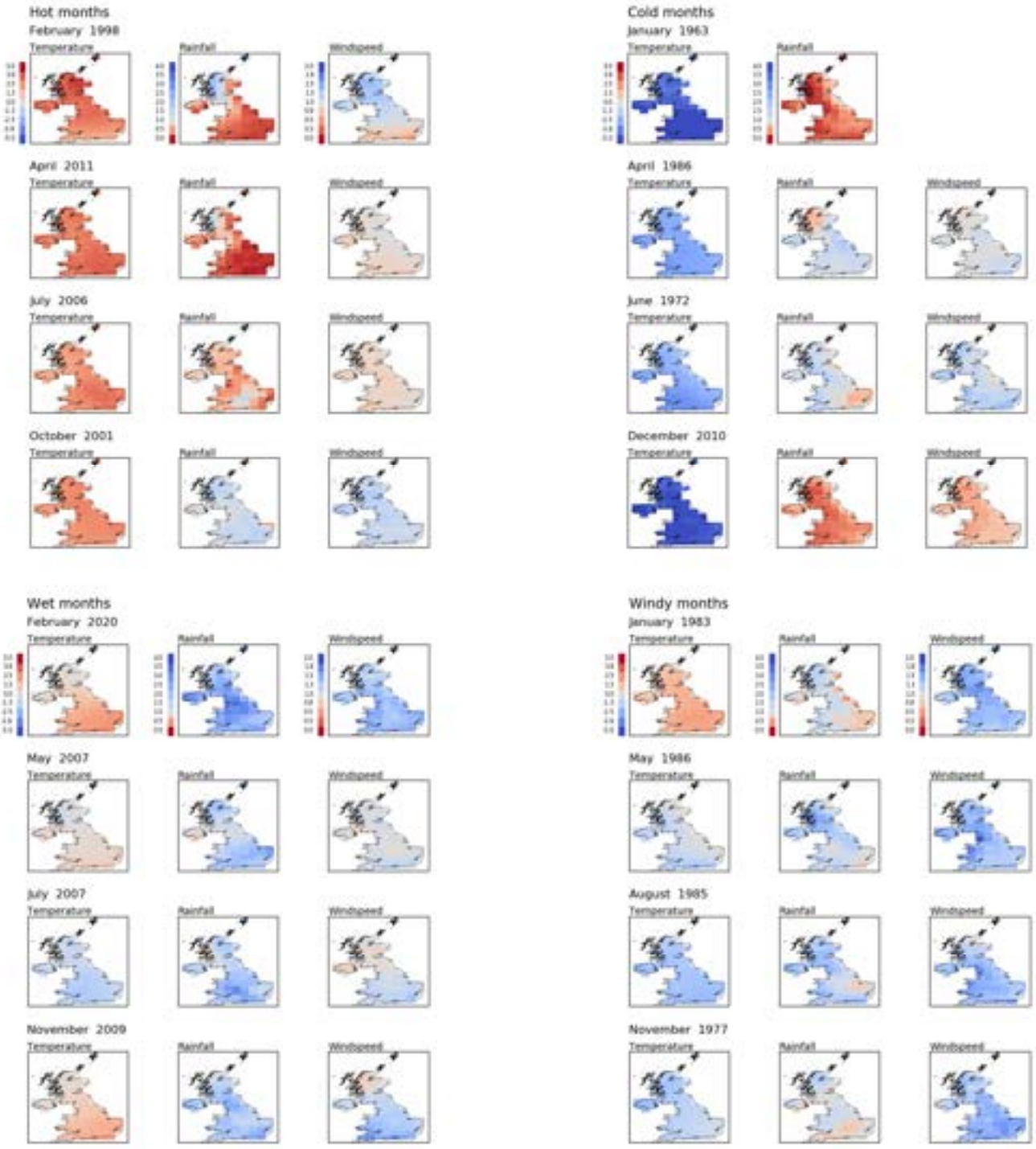

Figure 5.15: Geographic distribution of temperature, rainfall and windspeed anomalies for example extreme months. Anomalies are relative to the 1981-2010 mean. 60km spatial resolution

5.5.5 Weather by weather pattern

The temperature, rainfall and windspeed on any given day is influenced by the weather patterns affecting the UK: they describe the direction the air is coming from (which affect its temperature and moisture content) and the strength of the air flow. Figures 5.16 to 5.18 show the average temperature, rainfall and windspeed (60x60km resolution) respectively on days classified according to the Met Office 8 and 30-class weather patterns (Neal et al., 2016), averaged over the period 1981-2010. The 30-class patterns are grouped by row into the 8-class summary patterns. There is considerable variation in temperature, rainfall and windspeed for a given weather pattern. The maps therefore do not show the largest possible anomalies with each weather pattern, but they do indicate which patterns are more likely to generate extreme weather and the geographic variability in the effect of a given pattern on temperature, rainfall and windspeed. Figure 5.19 shows the correlation (over the period 1981-2010) between national average monthly temperature, rainfall and windspeed anomaly and the proportion of the month in each weather pattern. The use of national average temperature, rainfall and windspeed hides some regional variation as shown in Figures 5.16 to 5.18.

Particularly hot summer days are associated with weather patterns 16, 17, 27 and, to a lesser extent, 12, which all describe anticyclonic conditions. This is consistent with the conclusions of Huang et al. (2020) based on heat mortality. These patterns all affect the UK consistently. Cool summer days are associated with weather patterns 1, 14, 24 and 30, all describing cyclonic conditions and all with a consistent effect across the UK.

Cold winter days are associated with weather patterns 19, 24, 27 and 28 (again consistent with Huang et al., 2020), and to a lesser extent 5 and 19. These all describe either anticyclonic conditions or flow from the north. The mildest winter days across the UK typically occur with the cyclonic patterns 4, 15, 20, 21 and 23, and mild days in the south occur with pattern 30.

High rainfall days typically occur with cyclonic weather patterns, with some difference between winter and summer and more geographical variation in effect. Patterns 20, 21, 29 and 30 are associated with particularly high winter rainfall, whilst 8, 11 and 29 are associated with generally high summer rainfall. This is consistent with the conclusions of Richardson et al. (2020).

Dry days are associated with anticyclonic patterns, particularly 17, 18. 25 and 27: 16 is also associated with dry days in winter. Again this is consistent with previous analyses (Richardson et al., 2018).

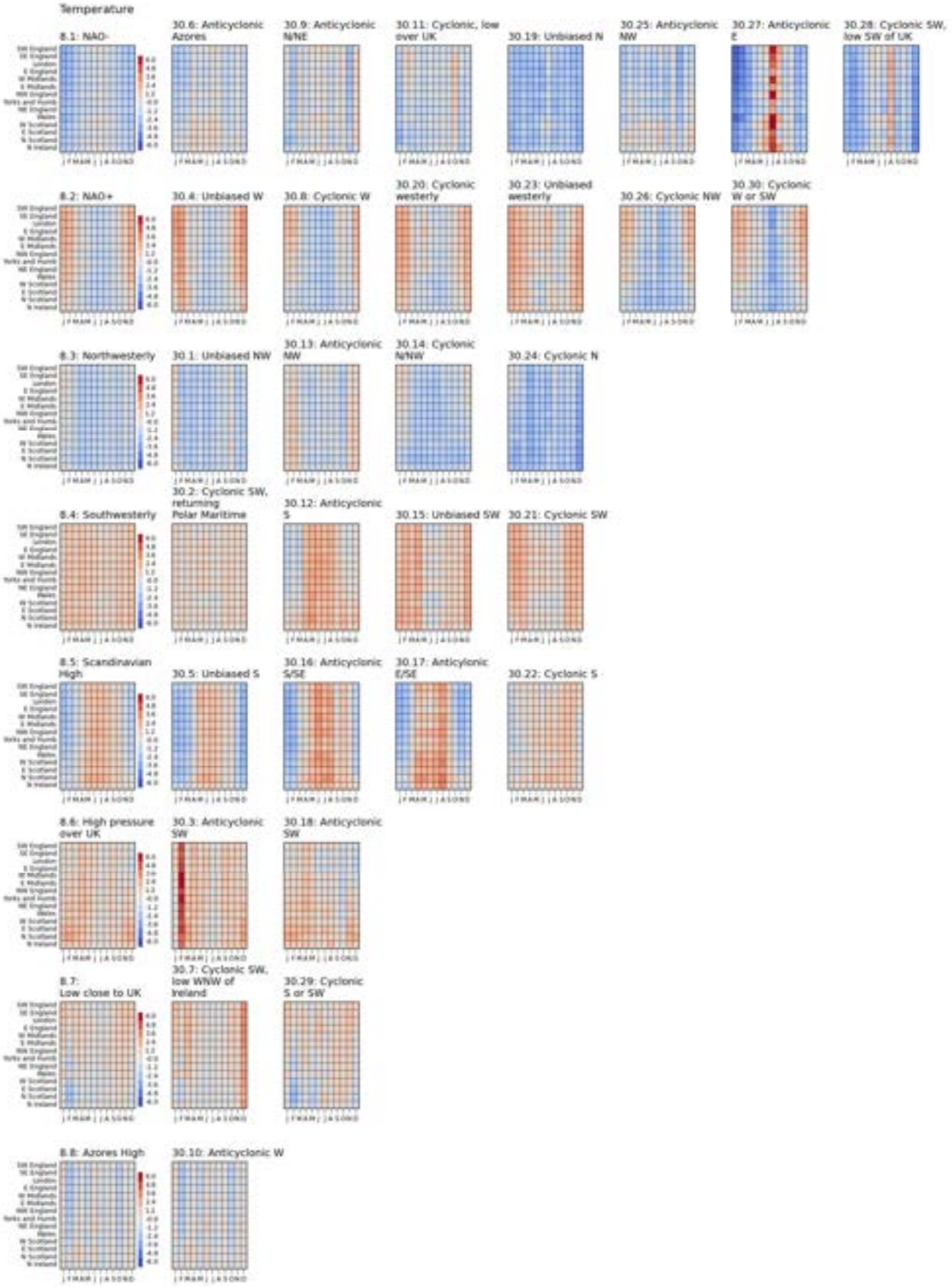

Figure 5.16: Regional average temperature by weather pattern, as anomaly from 1981-2010 mean across all patterns. The rows show the patterns in the 8 summary classes, and the first graph in each row shows the average across the summary classes.

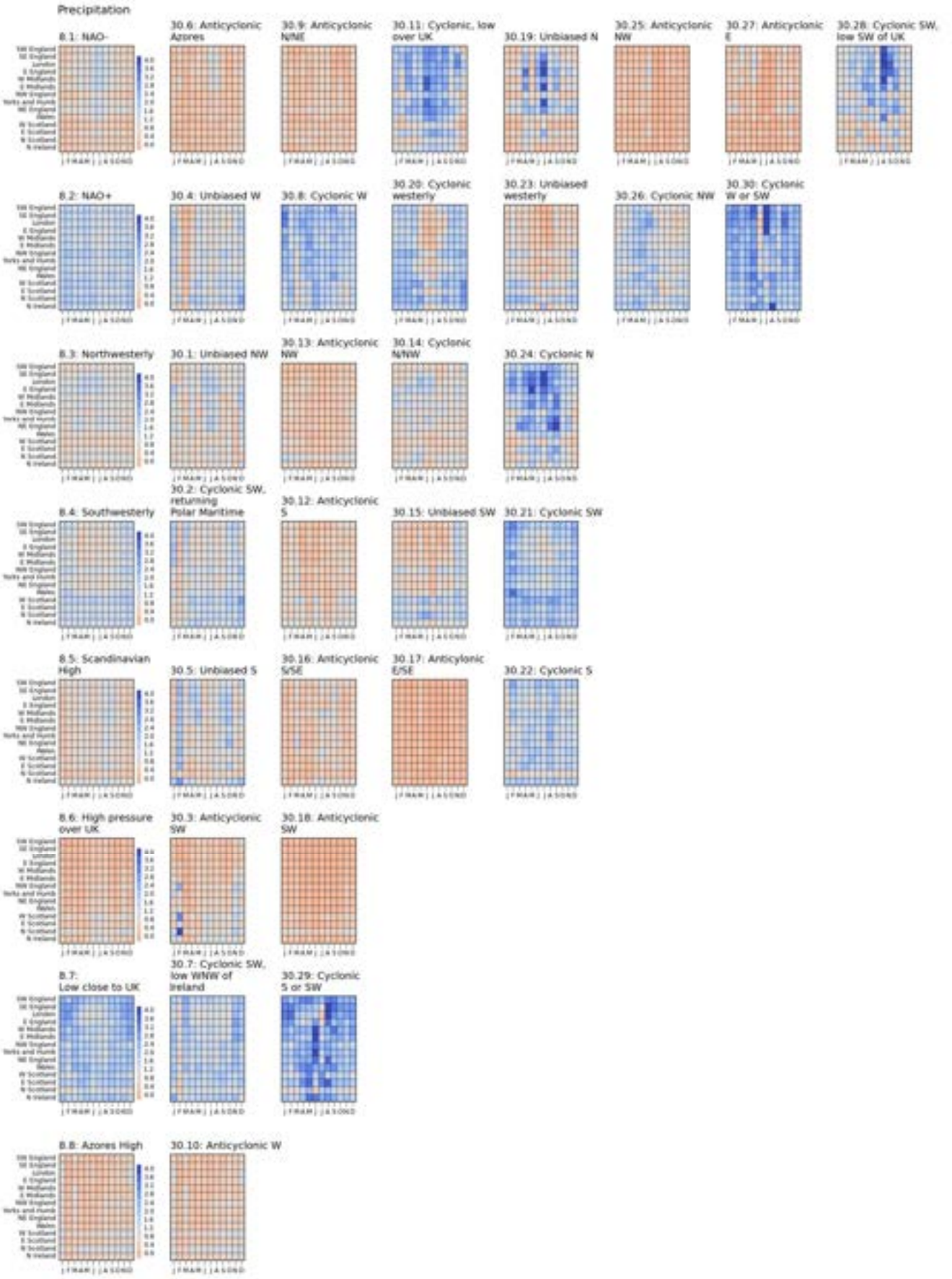

Figure 5.17: Regional average rainfall by weather pattern, as a ratio of the 1981-2010 mean across all patterns. The rows show the patterns in the 8 summary classes and the first graph in each row shows the average across the summary classes

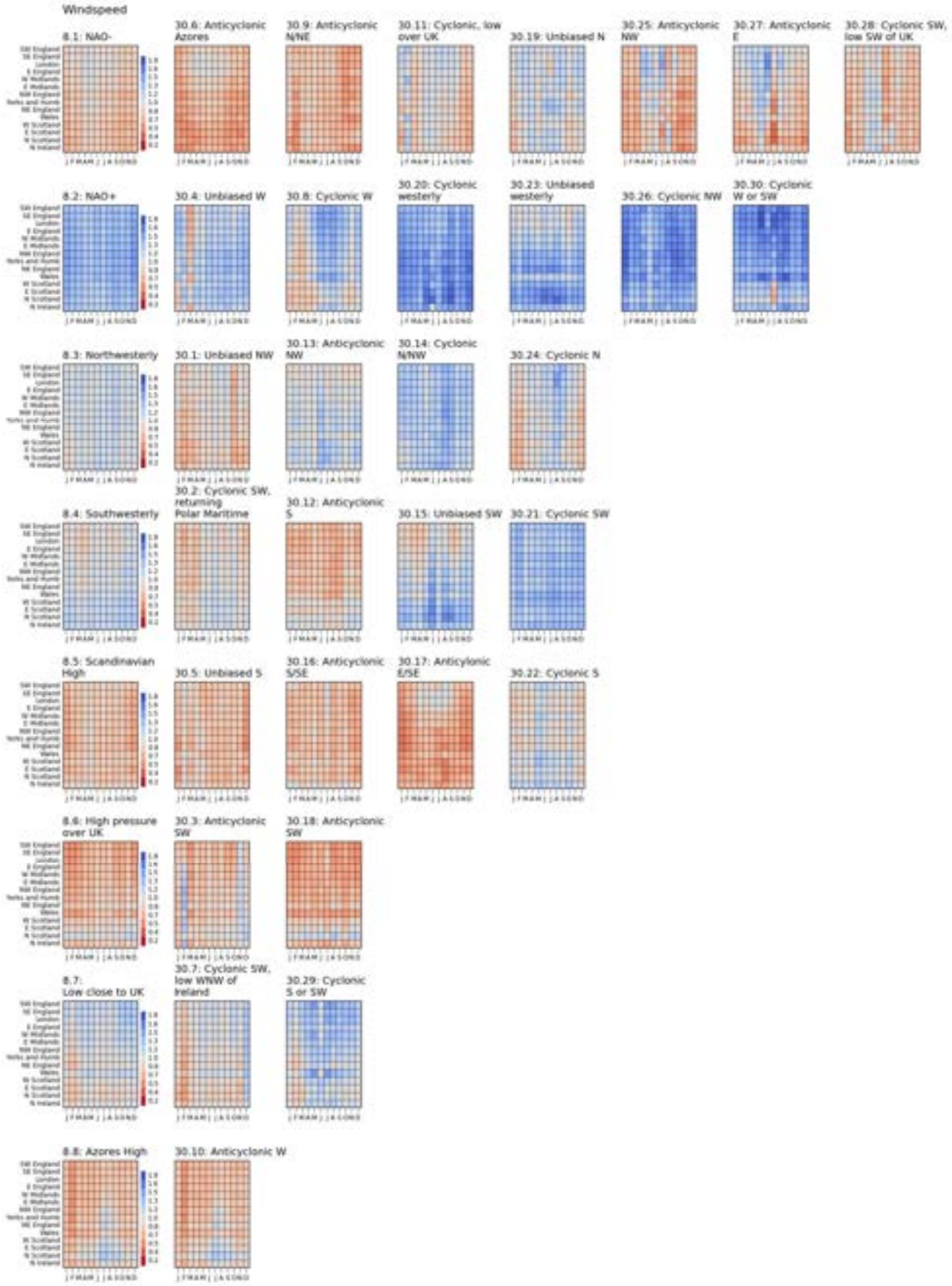

Figure 5.18: Regional average windspeed by weather pattern, as a ratio of the 1981-2010 mean across all patterns. The rows show the patterns in the 8 summary classes and the first graph in each row shows the average across the summary classes.

Figure 5.19: Correlations between monthly climate anomalies and frequency of time in each weather pattern: 1981-2010. Dark blue: strong positive correlation. Dark red: strong negative correlation. Significant correlations (5%, one-tailed) shown with *

The windiest days occur with weather patterns 4, 6 (especially in summer), 14, 20 and 30, with 15 and 23 particularly windy in the north. Perks et al. (2023) also linked pattern 29 to high storm surges in the south west of England, but this does not appear to generate particularly high windspeeds across the UK.

5.5.6 Correlations with drivers

Correlations between variability in (national scale) monthly temperature, rainfall and windspeed and various climate drivers are shown in Figure 5.20. As previously, the national scale hides some regional variability but shows the broad relationships between drivers and temperature, rainfall and windspeed anomaly.

The latitude of the jet stream is generally positively correlated with temperature between winter and summer (a northerly jet means higher temperatures), particularly in northern parts of the UK. Jet latitude is most strongly negatively correlated with rainfall in summer (northerly jet means lower rainfall), particularly in the south. Correlations with windspeed are lower and restricted to some summer months.

The strength of the jet stream is positively correlated with temperature in winter, but negatively correlated in summer. A stronger jet stream is associated with high rainfall and windspeed in winter and summer, but less so in spring or autumn.

A positive NAO is associated with higher temperatures, rainfall and windspeed in winter. In summer, however, the NAO has less effect on temperature but a more positive NAO is associated with lower rainfall and, to a lesser extent, lower windspeeds. The East Atlantic Pattern is most strongly correlated with temperature in spring and autumn and can be more correlated with rainfall and windspeed than the NAO. The Arctic Oscillation is positively correlated with temperature, rainfall and windspeed in winter; in summer a high Arctic Oscillation index is associated with low rainfall. In winter, a negative AO is strongly associated with cold conditions. The relationship between pressure over Scandinavia and UK weather differs between the two indicators of Scandinavian pressure anomalies. In winter, a high EOF-based Scandi index is associated with low temperatures across the UK and, to a lesser extent in January and February, low rainfall and windspeeds. There is a much weaker relationship between the EOF-based Scandi index in summer. The pressure-based index is positively correlated with temperature in winter across northern parts of the UK, and negatively correlated with rainfall in southern regions. In summer, the pressure-based index is very strongly associated with high temperature and low rainfall (except in some summer months in the north).

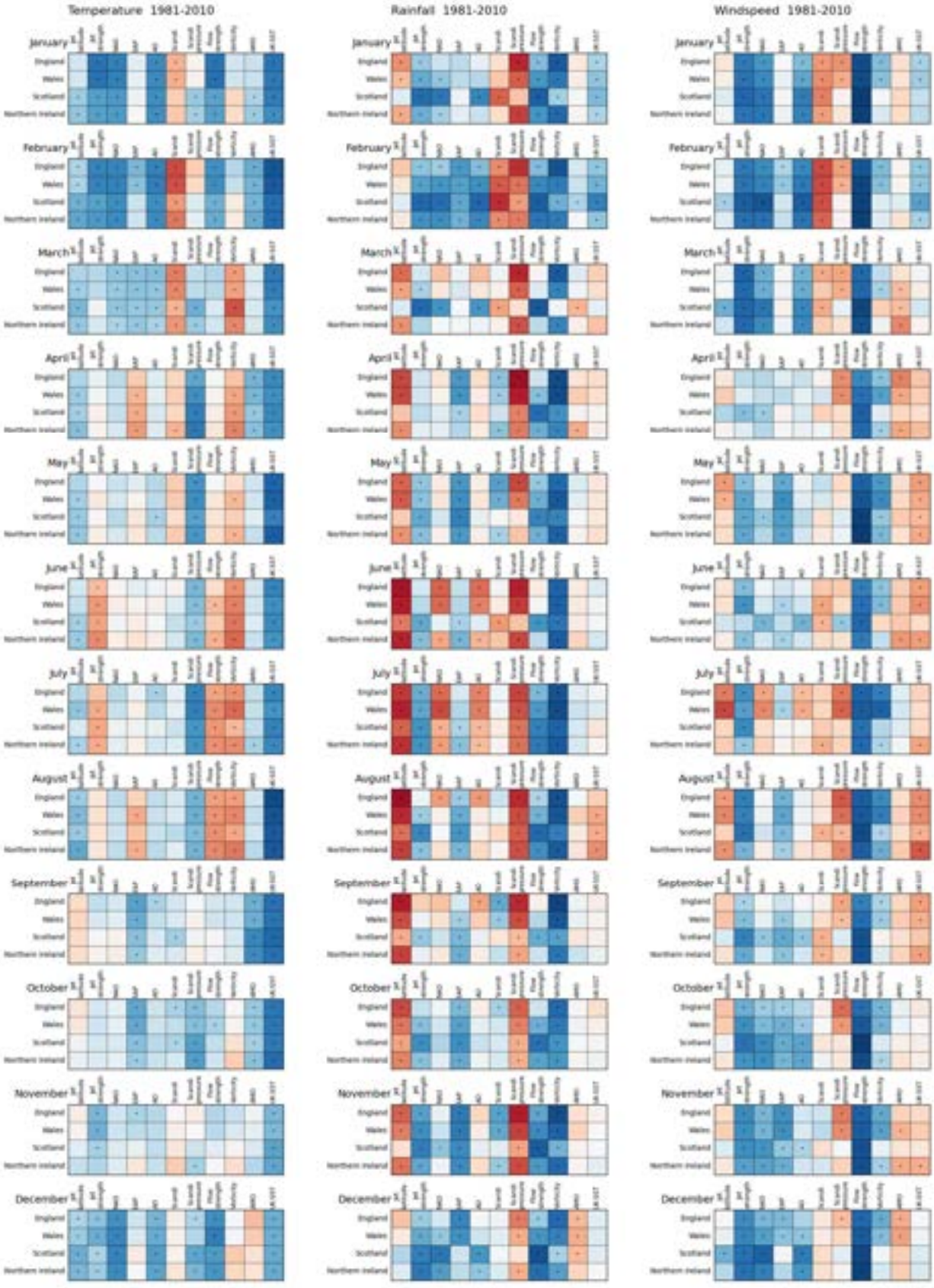

Figure 5.20: Correlations between monthly climate anomalies and climate drivers: 1981-2010. Dark blue: strong positive correlation. Dark red: strong negative correlation. Significant correlations (5%, one-tailed) shown with *

Flow strength is positively correlated with temperature in winter and negatively correlated in summer and is positively correlated with rainfall in most of the year (especially in the north). It is very strongly correlated to windspeeds. Flow vorticity (a measure of the strength of cyclonic behaviour) is positively correlated with rainfall throughout the year but is only negatively correlated with temperature in summer. It is positively correlated in most regions with windspeed.

The Atlantic Meridional Oscillation (AMO) largely represents multi-year variability in ocean temperatures. When the AMO is high (warm temperatures in the North Atlantic) January, February and autumn temperatures in parts of the UK are high but there is little association with year-to-year variability in rainfall.: there is some association with low windspeeds in spring. The relationship between UK sea surface temperature anomalies and air temperature anomalies is more complicated. It is very strong, but not necessarily causal: the same drivers which generate higher sea surface temperatures around the UK also generate high air temperature anomalies. Notwithstanding this, computer simulation experiments show that – other things being held equal – higher sea surface temperatures around the UK lead to higher air temperatures (Petch et al., 2020; Section 5.2).

In almost all cases, empirical relationships between drivers are stronger in winter and summer than in spring and autumn. This is primarily because spring can either be similar to winter (“extended winter”) or summer (“early summer”), and autumn can be either an extended summer or an early winter. The relationships between drivers and temperature in particular differ in winter and summer (Cassou & Cattiaux, 2016; Section 5.2), confounding the relationships in spring and autumn.

The simple correlation plots show that all the potential drivers of UK weather variability can affect weather in some regions and seasons, but some are more strongly correlated than others. The drivers can also themselves be correlated with each other (Figure 5.21), with the strength and direction of correlation varying through the year. It is also potentially the case that the effect of one driver might depend on the class of behaviour of another driver, rather than the magnitude of that driver. The correlations also indicate the general relationship between the drivers and weather anomalies, which may not necessarily also hold in extreme conditions: extreme weather anomalies may be outliers from the general (linear) relationship. Whilst it may be feasible to use correlations and multiple regressions to estimate the generalised effect of varying drivers, it is therefore not feasible to use statistical relationships to seek to quantify the effect of drivers on extreme temperature, rainfall and windspeed.

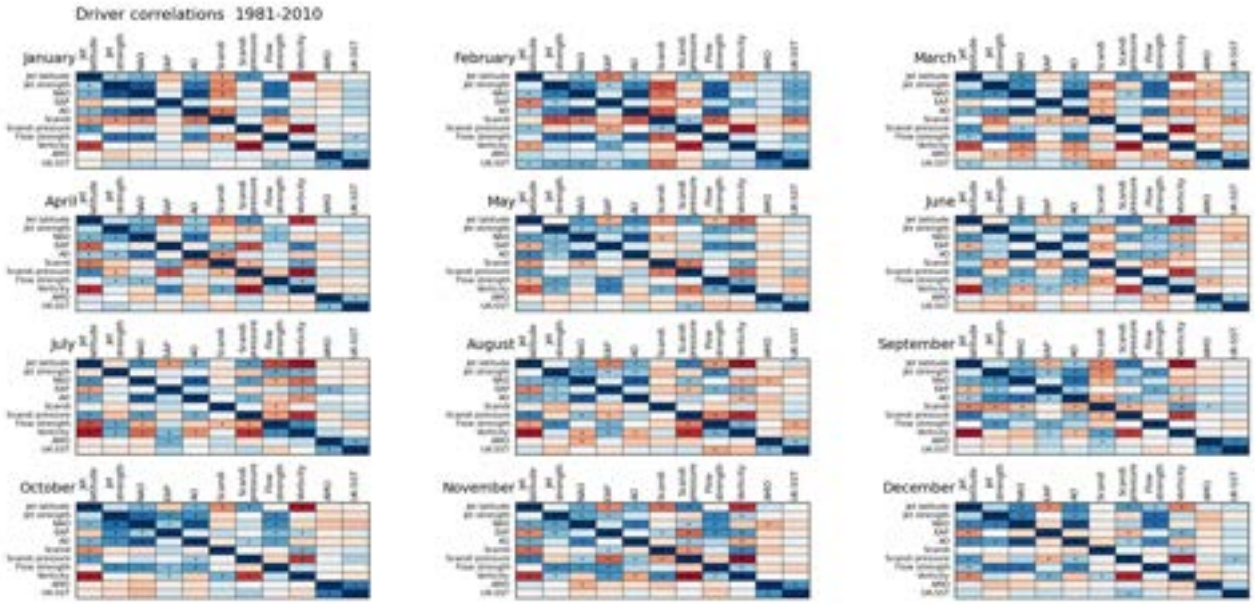

Figure 5.21: Correlations between monthly climate drivers: 1981-2010. Dark blue: strong positive correlation. Dark red: strong negative correlation. Significant correlations (5%, one-tailed) shown with *. Note that the plots are symmetrical around the diagonal

5.5.7 Composites based on climate anomalies

The complexities and subtleties of the relationships between drivers and extreme anomalies in the UK mean that insights into the conditions that generate extremes can best be gained through the analysis of composites: groups of years which share specific defined characteristics. Composites can be based on either the drivers (strongly positive NAO against strongly negative NAO, for example) or on the climate anomalies (very hot against very cold, for example). The focus here is on identifying drivers underlying extremes, so composites are based on the climate anomalies. Specifically, the composites are defined, for each month, to include the most extreme five years (e.g. hottest five) over the period 1970-2015: this period is common to all the data sets. It does not necessarily include the most extreme anomalies on record. The composites are constructed from the raw HadUK-Grid time series. Different subsets of years are selected when detrended temperature data are used, but the overall patterns are the same. The figures here are based on national average temperature, rainfall and windspeed anomalies. There are many similarities across the UK, but also some notable differences which are highlighted below.

The hot and cold temperature composites for England are shown in Figure 5.22: patterns are similar for Scotland, Wales and Northern Ireland. Hot winters are typically associated with a strong jet stream, but jet latitude does not appear to be significant. They are associated with a strongly positive NAO and AO, and usually occur when Atlantic sea surface temperatures are high. There is some indication that hot winters occur when the Scandinavian pattern is negative (low pressure over Scandinavia), but that is not reflected in the Scandinavian pressure index. Hot winters occur when sea surface temperatures are high, but this may be because they are both caused by the same driver. Hot winters have more frequent cyclonic conditions (although vorticity is not particularly high), with Met Office weather patterns 15, 20, 21 and 23 particularly well represented. Air flows preferentially come from the south west or west. Conversely, cold winters are associated with a weak jet, negative NAO and AO, and weak flow strength. Anticyclonic weather patterns (especially 17, 27, 28 and 19) dominate, and air flows are frequently from the north to south east.

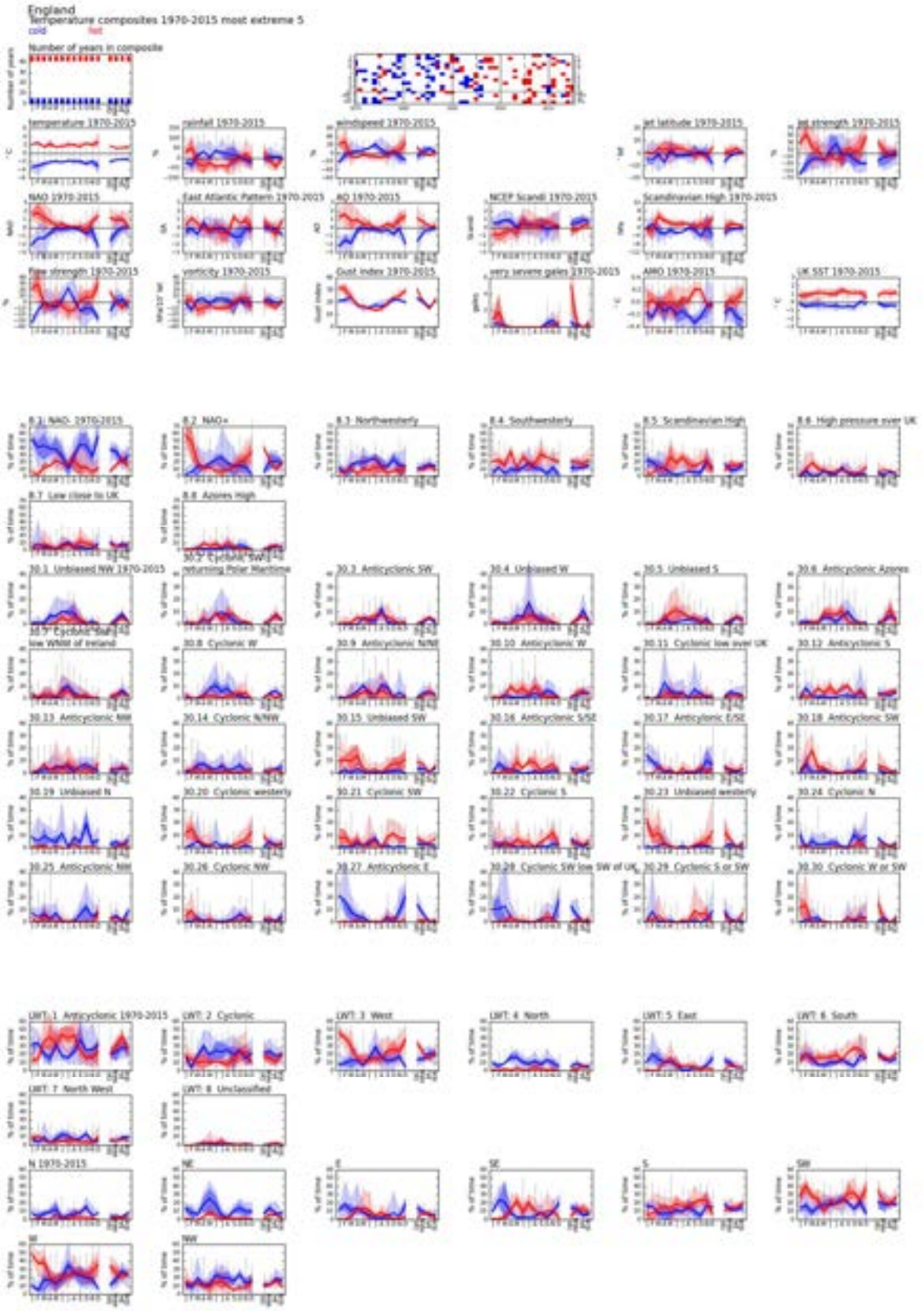

Figure 5.22: Extreme temperature composites: England. Most extreme 5 over the period 1970-2015. The top rows show the average and range in temperature, rainfall and windspeed anomalies (relative to 1981-2010), together with climate drivers. The central rows show the Met Office 8- and 30-class weather patterns, and the bottom rows the Lamb Weather Types and flow direction classes. The vertical bars show the range across all years.

The contribution of different drivers to hot and cool summers is less clear. Hot summers tend to occur when the jet is further north and slightly weaker than usual, but the effects are not as clear as in winter. There is no clear link with NAO, East Atlantic Pattern or AO, but flow strength and vorticity are low in hot summers and pressure over Scandinavia is high. Anticyclonic weather conditions dominate (particularly patterns 16, 5 and 10), and air flow is frequently from the south and east. Cool summers occur when the jet is strong, flow strength is high, vorticity is above average and pressure is low over Scandinavia, but there are no clear associations with NAO, East Atlantic Pattern or AO. Cyclonic weather patterns 4, 8 and 19 are particularly frequent during cool summers, and airflows from the west, north west and north east (to a lesser extent) are more frequent than usual.

Hot springs are less clearly associated with anomalous drivers, although they tend to occur when Scandinavian pressure is high with weather patterns dominated by flows from the west and south west (patterns 15 and 23). Hot autumns are most associated with a positive East Atlantic Pattern, strong flow and high Atlantic sea surface temperatures. Weather patterns 15, 21, 22 and 23 are particularly common. The reverse tends to occur for cold springs and autumns,

Warm winters are typically associated with high rainfall and high windspeeds, and warm summers are typically dry and calm. Cool winters are dry and calm, and cool summers are wet and windy. Warm springs are often dry and calm (and cool springs wet and windy), but the warmest autumns can be either wet and windy (early winter) or dry and calm (late summer).

Wet and dry composites for England and Scotland are shown in Figures 5.23 and 5.24 respectively: there are some differences (Wales is similar to England, and Northern Ireland similar to Scotland). Across England and throughout the year, the wettest months occur when the jet is to the south and, to a lesser extent, when it is strong. Across Scotland, the effect of jet strength is more important than jet latitude. The opposite is the case for dry months. The effects of the NAO and AO in winter are stronger in Scotland than England, with wet winters occurring when the NAO and AO are positive. Summer rainfall is more closely associated with the East Atlantic Pattern in both England and Scotland. Scandinavian high pressure has a greater effect on rainfall anomalies in England than Scotland. Similarly, vorticity has a greater effect in England than Scotland. The source of airflows differs between wet and dry months more in Scotland than further south in England, with south westerly flows particularly frequent during wet months and easterly flows more frequent in dry months. The wettest winters in England have frequent cyclonic weather patterns 20, 21, 26, 29 and 30, but in Scotland 29 is less important and 23 more so. In summer, weather pattern 7 is frequent in both England and Scotland, but 7 and 11 are frequent in England and 2 and 4 in Scotland. Anticyclonic weather patterns are

frequent during dry winters (27 and 28 in both England and Scotland, but different patterns are also important in the different regions) and dry summers (with 6 and 9 important across the UK).

Wet months are typically warm and windy in winter across the UK, and cool but not particularly windy in summer. Dry winter months are cool and calm, and dry summer months are warm.

Extreme windy and calm months (Figures 5.25 and 5.26) show similar patterns to extreme wet and dry months, and similar geographic variability. There is a strong association between wet and windy extremes. However, the relative importance of different weather patterns is different. Most of the patterns generating wet months also generate windy months – but not all. Pattern 29, for example, is not particularly associated with windy months in England, and pattern 21 is not associated with windy months in Scotland.

Compound temperature and rain composites are shown for England in Figure 5.27: to be included in the compound composite, a year has to have both a temperature and a rainfall anomaly in the top 10 over the period 1970-2015. As outlined above there is a strong (but not perfect) overlap between rainfall and wind extremes.

Hot and dry (and calm) compound extreme months (red) are rare in winter but can occur between spring and autumn. They typically have a northerly jet and, in spring, a strong jet. The NAO and AO are positive in spring but are not clearly anomalous in summer, when the East Atlantic Pattern is negative. Flow strength is high in spring and low in summer, and vorticity is low. During spring westerly (non-cyclonic) and anticyclonic weather patterns dominate (15 and 18), and in summer anticyclonic patterns (6 and 10) are frequent. South easterly flows are slightly more prevalent than normal, but there is not clear effect of direction.

Hot and wet (and windy) compound extreme months (orange) are rare in summer but can occur between late autumn and the end of winter. Jet strength is typically high, but there is no clear pattern to jet latitude. The NAO, AO and East Atlantic Pattern are all positive and Scandinavian pressure is low. Flow strength and vorticity are high. Cyclonic weather patterns (particularly 20, 21, 22, 23 and 30) are frequent, and westerly and south westerly air flows are more frequent than normal.

Cold and dry compound extreme months (green) occur in winter. They have a weak jet stream which can be either to the north or the south, a strongly negative NAO and AO and anomalously high Scandinavian pressure. Flow strength and vorticity are low. Anticyclonic patterns 27 and 16 are frequent, but so is the more cyclonic pattern 28. Airflows are predominantly from the east and south east.

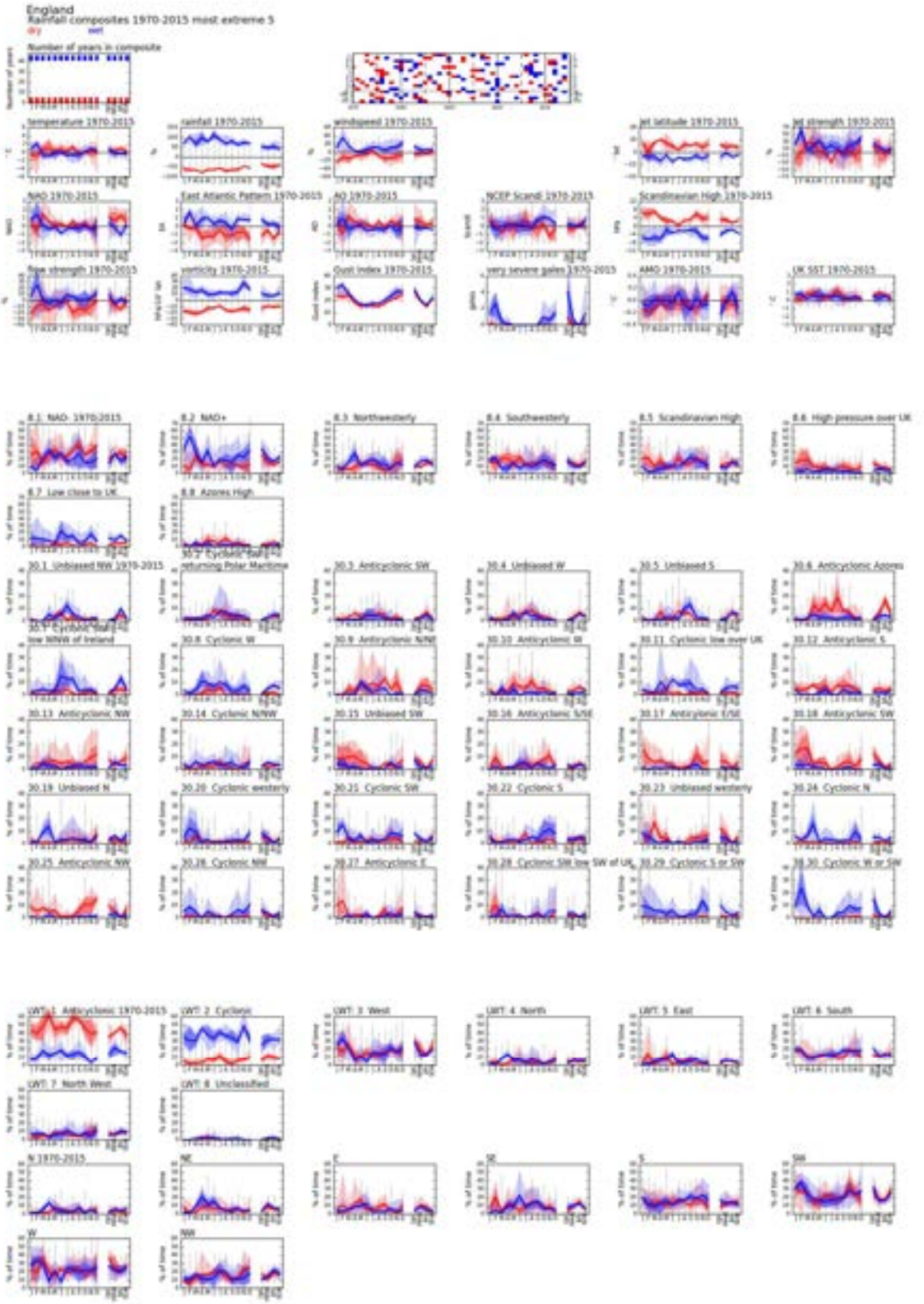

Figure 5.23: Extreme rainfall composites: England. Most extreme 5 over the period 1970-2015. The top rows show the average and range in temperature, rainfall and windspeed anomalies (relative to 1981-2010), together with climate drivers. The central rows show the Met Office 8- and 30-class weather patterns, and the bottom rows the Lamb Weather Types and flow direction classes. The vertical bars show the range across all years.

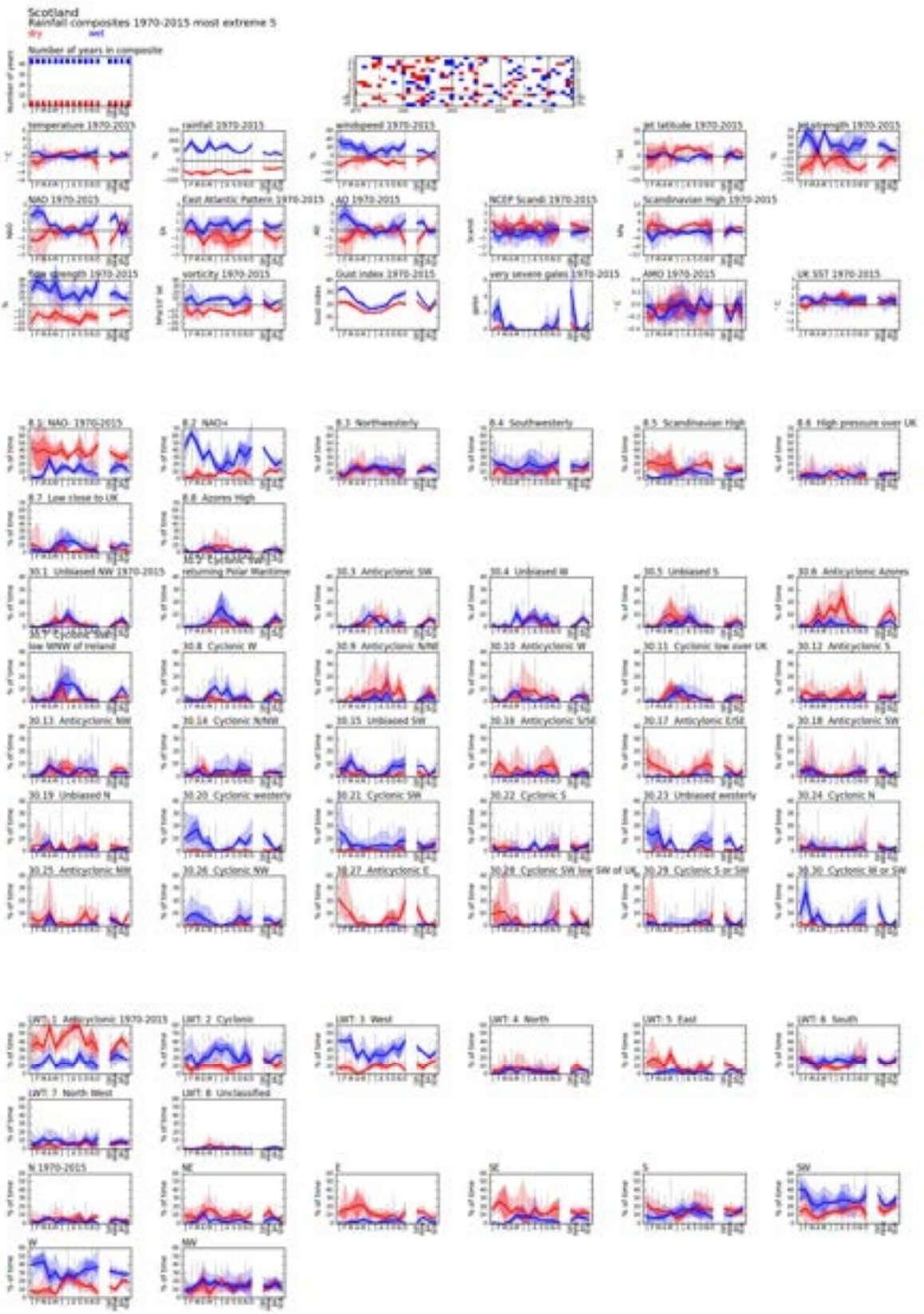

Figure 5.24: Extreme rainfall composites: Scotland. Most extreme 5 over the period 1970-2015. The top rows show the average and range in temperature, rainfall and windspeed anomalies (relative to 1981-2010), together with climate drivers. The central rows show the Met Office 8- and 30-class weather patterns, and the bottom rows the Lamb Weather Types and flow direction classes. The vertical bars show the range across all years.

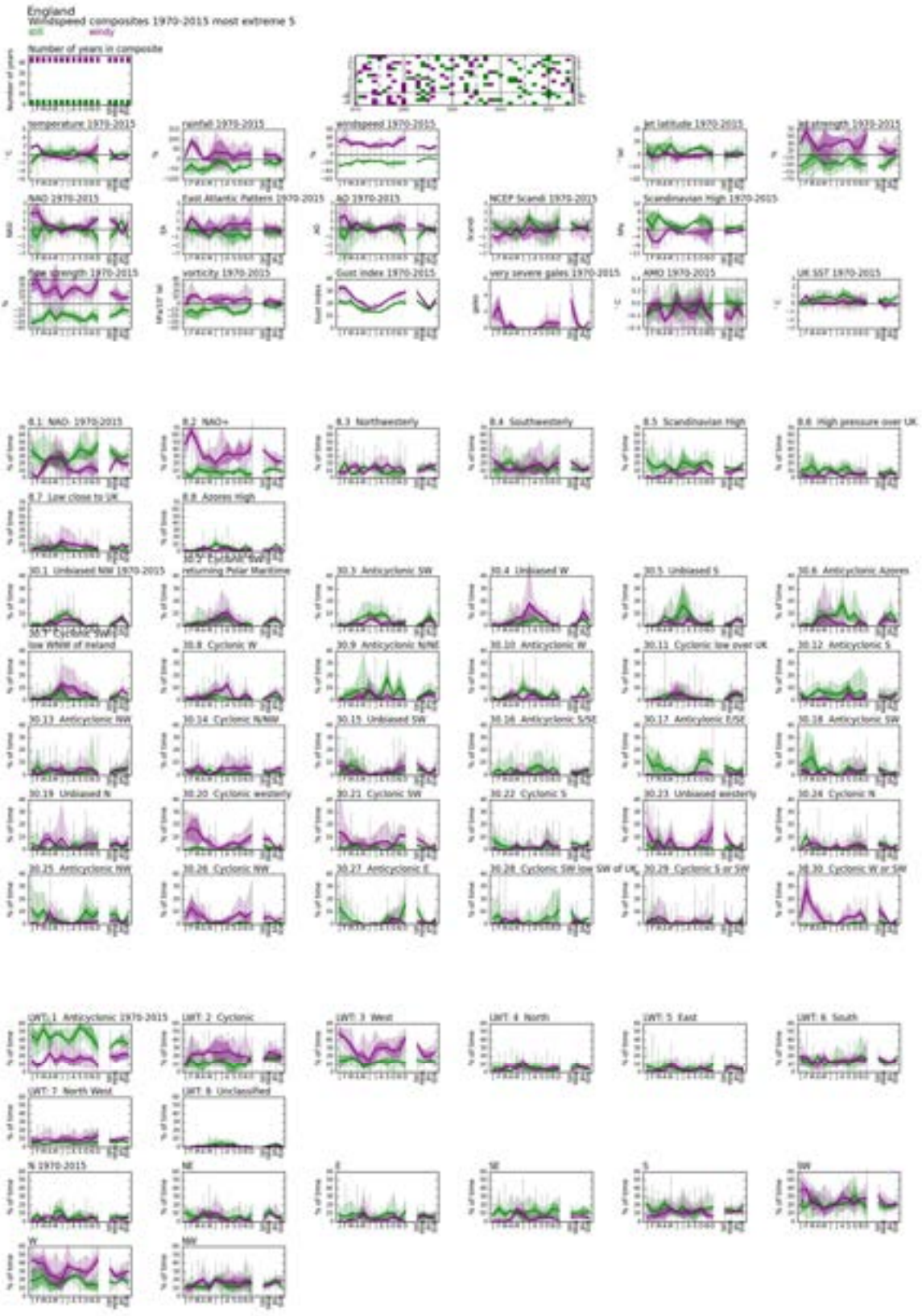

Figure 5.25: Extreme windspeed composites: England. Most extreme 5 over the period 1970-2015. The top rows show the average and range in temperature, rainfall and windspeed anomalies (relative to 1981-2010), together with climate drivers. The central rows show the Met Office 8- and 30-class weather patterns, and the bottom rows the Lamb Weather Types and flow direction classes. The vertical bars show the range across all years.

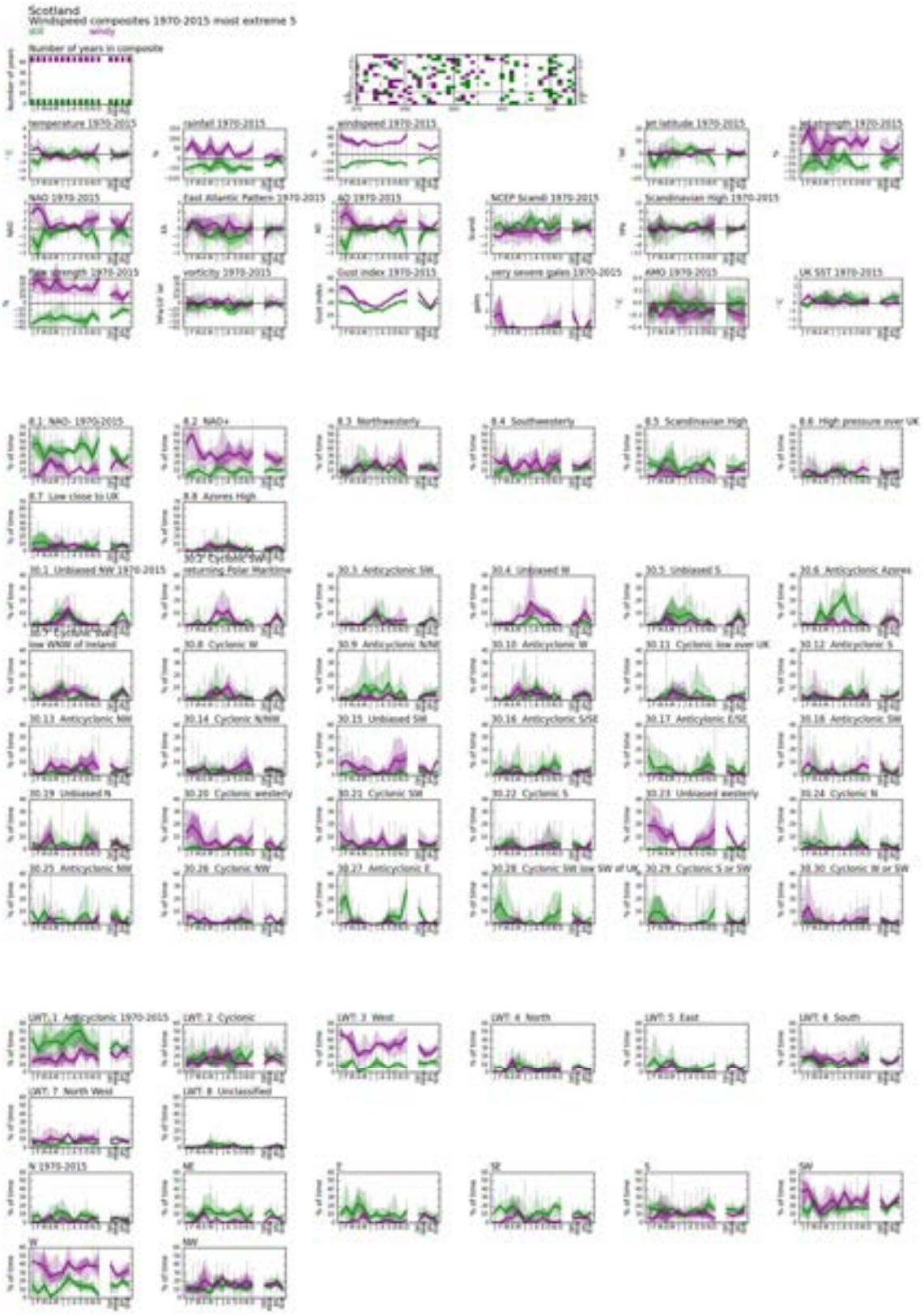

Figure 5.26: Extreme windspeed composites: Scotland. Most extreme 5 over the period 1970-2015. The top rows show the average and range in temperature, rainfall and windspeed anomalies (relative to 1981-2010), together with climate drivers. The central rows show the Met Office 8- and 30-class weather patterns, and the bottom rows the Lamb Weather Types and flow direction classes. The vertical bars show the range across all years.

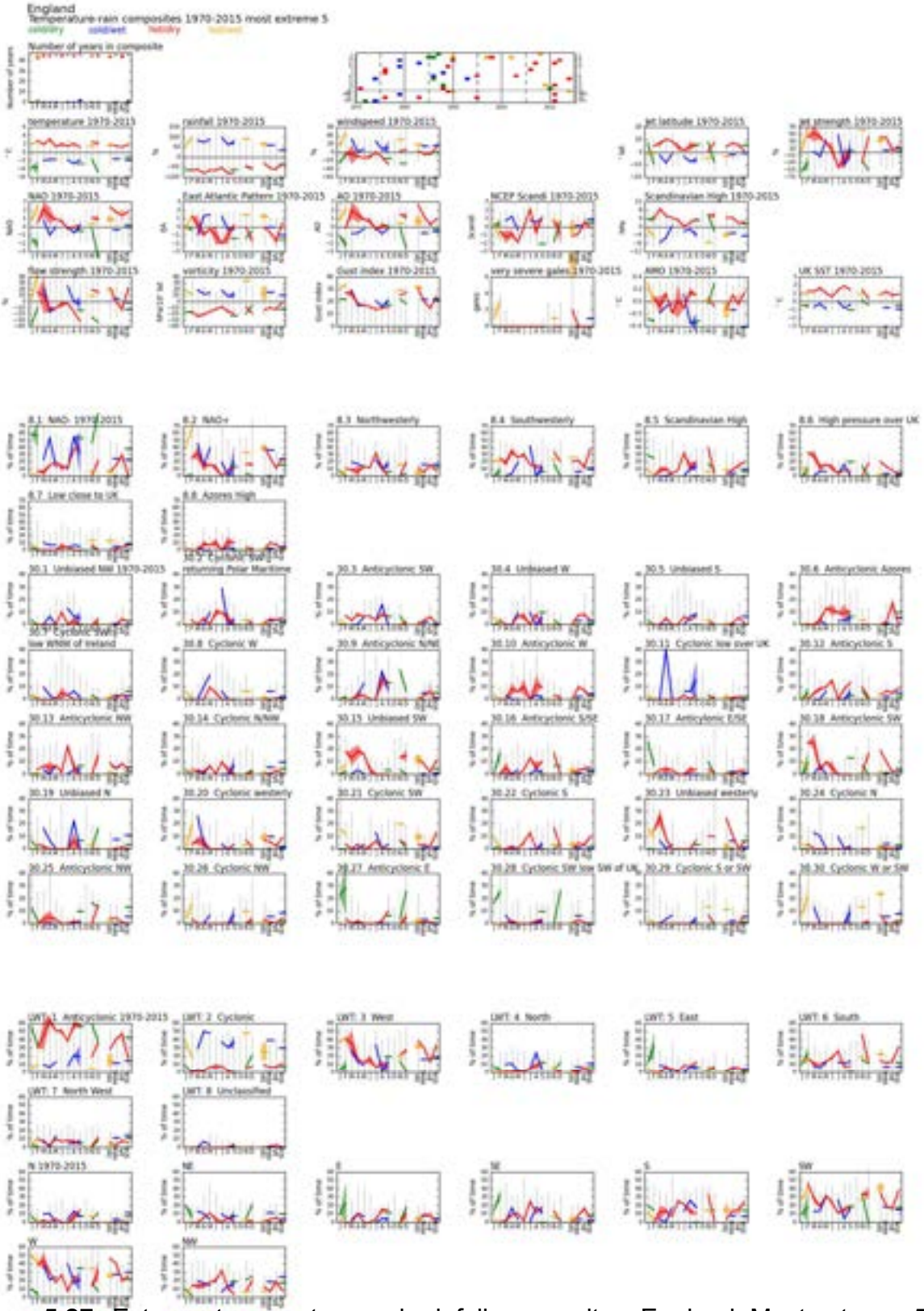

Figure 5.27: Extreme temperature and rainfall composites: England. Most extreme 5 over the period 1970-2015. The top rows show the average and range in temperature, rainfall and windspeed anomalies (relative to 1981-2010), together with climate drivers. The central rows show the Met Office 8- and 30-class weather patterns, and the bottom rows the Lamb Weather Types and flow direction classes. The vertical bars show the range across all years.

Cold and wet compound extreme months (blue) occur between spring and autumn. They have a southerly strong jet and a high East Atlantic Pattern index. Flow strength and vorticity are also high. Cyclonic weather patterns (especially 2 and 11) are common, together with patterns with flow from the north (19).

5.5.8 Summary and implications for the construction of scenarios

Seven key implications for the construction of scenarios can be drawn from the evidence from the published literature coupled with the empirical analysis of observed and model data.

First, the complexity of the relationships between the drivers of extreme months and seasons, and the conditional nature of these relationships, means that it is most effective to define extreme scenarios in terms of temperature, rainfall and windspeed and work 'backwards' to create plausible backstories of the conditions which generate those extremes. This is the opposite direction to that used in most storyline approaches, which start from a driver. Empirical relationships between driver and climate anomaly depend on which drivers are considered, and are most suited to helping understand average, rather than extreme behaviour.

Second, the long historical record of temperature and rainfall (but not windspeed) available in the UK provides a good empirical basis for an assessment of plausible extreme months and seasons. More extreme months and seasons may have occurred before the mid-19th century (based on data from long record sites, the Central England Temperature record and the HadUKP rainfall record), but the available evidence suggests that these were not materially different to extremes over the last 150 years or so. Removing the observed trend in temperature data does not materially affect the estimated historical range in extremes, although the years with those extremes vary. There is more consistency in the variation in historical extreme temperatures from month to month (with a smooth seasonal cycle) than in the variation in historical rainfall extremes, but it is plausible to assume that an extreme that occurred in one month could have occurred in an adjacent month.

Third, the magnitude of the most extreme rainfall anomaly varies considerably with scale: the finer the spatial scale, the more extreme the anomaly. At the 5x5km resolution, the maximum rainfall anomaly can be four times the mean whilst the largest anomaly at the regional scale is just twice the mean. At scales finer than the region, months can have no rainfall. There is less variation in the most extreme temperature anomalies with scale: the difference is up to 1^{o}C at the 5x5km scale.

Fourth, simulated extreme anomalies since 1900 (based on UKCP18 global strand projections and evidence from the literature) are typically larger than the observed

extreme anomalies, although the extent of the difference depends on the bias adjustment approach used. This is because the model simulations reproduce a wider range of plausible climates than was actually experienced. This is to be expected and is the basis for the UNSEEN methodology.

Fifth, most historical extreme anomalies have been focused on part of the UK, but some have been very extreme across the whole of the UK even if not the largest on record everywhere. In winter months, compound extremes are either ‘mild and wet (and windy)’ or ‘cold and dry (and calm)’, and in summer they are either ‘cool and wet (and windy)’ or ‘hot and dry (and calm)’. Extreme compound anomalies in spring and autumn can follow either the winter or the summer pattern (Cotterill et al., 2023). As climate changes, it can be expected that springs and autumns will increasingly follow the summer pattern. The most extreme months and seasons on record do not necessarily also contain the most extreme shorter-duration events, but sometimes have done. Conversely, the most extreme short-duration events do not necessarily generate the most extreme months. There is empirical evidence that anomalous conditions can persist from one month or season to the next, and also evidence that anomalous conditions can flip (‘whiplash’) from one month or season to another.

Sixth, it is plausible to assume that extreme temperature and windspeed anomalies relative to a long-term mean do not change substantially as the long-term mean changes into the future. Winter, spring and autumn rainfall anomalies can also be assumed to remain broadly constant over time. However, model projections show that rainfall anomalies during summer months increase over time when expressed as a percentage anomaly. This is primarily due to a reduction in mean rainfall in summer months due to a reducing proportion of ‘wet’ summers. Anomalies expressed as a number of standard deviations from the mean are more consistent over time but, as noted above, standard deviations are not available from the UKCP18 User Interface.

Seventh, the most extreme months and seasons typically occur when the weather patterns affecting the UK are either strongly cyclonic or strongly anticyclonic. Strongly cyclonic weather patterns are wet and windy throughout the year, but mild in winter and cool in summer. They typically occur when the jet stream is strong, the North Atlantic Oscillation index is strongly positive in winter or negative in summer, and pressure over Scandinavia is lower than average. Spring and autumn extremes can follow the winter or summer patterns. Persistently strong cyclonic conditions would therefore generate higher rainfall and windspeeds throughout the year and milder winters and cooler summers, but at some point in spring and autumn temperatures would be close to average. Strongly anticyclonic weather patterns are dry and calm throughout the year, but cold in winter and hot in summer. They typically occur when the jet stream is weak and strongly meandering, with persistent

blocked conditions. Persistently strong anticyclonic conditions would be dry and calm throughout the year, but cold in winter and hot in summer. Again, at some point in spring and autumn temperatures would be close to average.

5.6 Scenarios for extreme monthly and seasonal anomalies

5.6.1 Introduction

Based on the analysis in Section 5.5, three sets of scenarios describing extreme months and seasons are defined. The first set characterises individual extreme months or seasons. The five basic scenarios in this set describe hot, cold, wet, dry or windy months or seasons. Note that there is a language issue here: 'hot' winters (and springs and autumns) are more typically described as 'mild' winters, whilst 'cold' summers are more typically described as 'cool' summers. 'Hot' and 'Cold' are here used in the summary descriptions of the extreme scenarios, but the text uses mild or cool as appropriate. Each has compound variants describing plausible combinations of temperature, rainfall and windspeed (for example hot, wet and windy), and each has a 'backstory' describing the meteorological conditions associated with the extreme.

The second set of scenarios explicitly assumes that persistent anomalous weather continues for successive months. They are based on two storylines describing the climatic conditions generating anomalous weather (strongly cyclonic or strongly anticyclonic) in two seasons (extended winter, from November to April, and extended summer, from May to October). Each scenario describes compound anomalies – relative to a long-term mean - in monthly temperature, rainfall and windspeed for sequences of months.

The third set of scenarios is based on observed historical extreme monthly events (analogue scenarios). These scenarios are less extreme than the first two sets but incorporate realistic spatial variability and compound anomalies in temperature, rainfall and windspeed.

Sets 1 and 2 are presented as rounded numbers at the national scale, informed by the analysis in Section 5.5. Factors are given to estimate extremes at spatial scales down to approximately 25km^2. The scenarios are not to be interpreted too literally: they are guides to maximum plausible changes. Users have different detailed requirements for information in different seasons, with different interests in sequences and compound scenarios so the scenarios as presented are not too prescriptive. Users can build on the extreme month and season scenarios here by

adding further information (on, for example, numbers of windstorms or coincident sea surface temperature anomalies), informed by the narrative backstories.

5.6.2 Set 1: extreme monthly and seasonal anomalies

This set defines five scenarios, describing hot, cold, wet, dry and windy months and seasons (scenarios for calm months and seasons are not provided as they are relevant only to very specific energy sectors who already have extreme 'wind drought' scenarios).

Each of the five scenarios presents an extreme month or season as an anomaly from a long-term mean, expressed either in ºC (temperature) or factor change from the mean. Each has a 'back-story' describing the climatic conditions generating the extreme season. It can be plausibly assumed that the extreme anomaly covers the whole of the UK simultaneously, and that sequences of extreme months (up to three months) or seasons (up to two seasons) can be constructed by assuming that each month or season is independent of the previous one. For example, a sequence of hot then cold then hot months is plausible.

Each scenario also has associated extreme changes in the other two weather variables, based on the backstory of conditions which generate the extreme. In each case the relationships between variables are different in the winter and summer months, and extreme conditions during spring and autumn can follow either the winter or the summer pattern. As climate changes, it can be expected that springs and autumns will increasingly follow the summer pattern (Cotterill et al., 2023).

5.6.3 Set 2: persistently extreme monthly anomalies

This set of scenarios explicitly assume that the conditions which drive extreme anomalous months persist for several months. It consists of four scenarios.

Persistently cyclonic conditions produce wet and windy extremes throughout the year, but warm winters (above average) and cool summers (below average). At some point in spring and autumn temperatures will be close to average. It is assumed here that this occurs in April and October but could plausibly be assumed to be earlier in spring and later in autumn.

Persistently anticyclonic conditions produce dry and calm extremes throughout the year, but cold winters and hot summers. At some point in spring and autumn temperatures will be close to average. It is assumed here that this occurs in April and October but could plausibly be assumed to be earlier in spring and later in autumn.

Cyclonic conditions in winter and anticyclonic conditions in summer produce hot extremes throughout the year, but wet and windy conditions in winter and dry and calm conditions in summer. It is assumed that conditions shift abruptly in April and September.

Anticyclonic conditions in winter and cyclonic conditions in summer produce cold extremes throughout the year, but dry and calm conditions in winter and wet and windy in summer. It is again assumed that conditions shift abruptly in April and September.

5.6.3 Set 3: historical extremes

These scenarios are based directly on the analysis presented in Sections 5.5.3.1 and 5.5.3.3. The describe the most extreme months and seasons as observed since 1884 (temperature), 1836 (rainfall) and 1969 (windspeed), based on HadUK-Grid regional-scale climate. More extreme months or seasons may have occurred previously and may be captured in some longer historical records and can be used instead of the scenarios presented here. Similarly, more extreme months and seasons may have occurred at a more local scale.

6. Final comments

This report has described the conceptualisation and construction of high-impact low-likelihood (HILL) transient and extreme scenarios. These scenarios are designed to inform adaptation and resilience planning. There are three broad general concluding comments.

First, the scenarios describe high-impact low-likelihood *drivers* of potential impact rather than high-impact low-likelihood *outcomes*. The distinction is important. Whilst the scenarios defined here are ‘low likelihood’ and may have ‘high’ impacts, no attempt has been made to determine whether the impacts resulting from these scenarios will be ‘high’. It is simply assumed that the impacts will be ‘high’ because the changes in climate defined in them are outside the range of changes in climate conventionally assumed. In practice, the difference in impacts in some of the transient scenarios (especially HILL-2 and HILL-4) may be small relative to the range in potential impacts under conventional UKCP18 scenarios, particularly in the first couple of decades. The impact of HILL-3 (volcanic cooling) is likely to be short-lived compared with the effects of greenhouse gas forcing.

Second, there are several different approaches to adaptation and resilience planning which can broadly be grouped into two categories: preparing for the ‘most likely

outcome' or preparing for the 'worst' outcome. The approach that an organisation follows depends on a number of factors, including the organisation's degree of risk aversion, the consequences if actions are insufficient, opportunities to revise actions as more information becomes available, and regulatory requirements. The scenarios provided here are directly relevant when adaptation and resilience planning focuses on 'preparing for the worst' and complement the wider set of UKCP18 projections.

Third, the scenarios are based on current understanding of the potential for high-impact low-likelihood drivers of change. This understanding is evolving as new research is undertaken and published, and new understanding may lead to revisions to the plausible changes described here, both in terms of their quantification and their assessed likelihood. It may also identify further potential high-impact low-likelihood scenarios which may impact directly upon the UK or conclude that some of the scenarios described here are no longer physically plausible. The approach developed in this analysis can be followed to develop further high-impact low-likelihood scenarios.

Acknowledgements

This report was produced for the UK Climate Resilience Programme, with funding from the UK Met Office under project CR20-4. The authors thank the contributions from the Stakeholder and Technical Advisory Groups.

References

Alexander, L.V. & Jones, P.D. (2001) Updated precipitation series for the UK and discussion of recent extremes. *Atmospheric Science Letters* 1, 10.006/asle.2001.0025.

Allen, R. J. (2015), A 21st century northward tropical precipitation shift caused by future anthropogenic aerosol reductions, *J. Geophys. Res. Atmos.*, 120, 9087– 9102.

Allen, R. J., A. T. Evan, and B. B. B. Booth (2015) Interhemispheric aerosol radiative forcing and tropical precipitation shifts during the late Twentieth Century. *J. Climate*, 28, 8219–8246.

Andrews, T. et al. (2019) Forcings, feedbacks and climate sensitivity in HadGEM3-GC3.1 and UKESM1. *J. Adv. Model. Earth Syst*. 11, 4377-4394.

Armstrong McKay, D.I. et al. (2022) Exceeding 1.5ºC global warming could trigger multiple climate tipping points. *Science* 377, eabn7950.

Arnell, N.W. (2006) *Global impacts of abrupt climate change: an initial assessment*. Tyndall Centre for Climate Change Research Working Paper 99.

Arnell, N.W. (2024) *The use and interpretation of 'extreme' and 'worst-case' climate scenarios in the UK*. Department of Meteorology, University of Reading. Prepared for the UK Climate Resilience Programme. Project CR20-4. Available from https://www.metoffice.gov.uk/research/approach/collaboration/spf/spf-uk-climate-resilience/

Baker, L.H., Shaffrey, L.C. & Scaife, A.A. (2018) Improved seasonal prediction of UK regional precipitation using atmospheric circulation. *Int. J. Climatol.* 38, 437-453.

Baker, L., Shaffrey, L. & Hawkins, E. (2021) Has the risk of a 1976 north-west European summer drought and heatwave event increased since the 1970s due to climate change? *Quart. J. Roy. Met. Soc.* 147, 4143-4162.

Bamber, J. L. et al. (2019). Ice sheet contributions to future sea level rise from structured expert judgment. *Proc. Nat. Acad. Sci.*, 116, 11195–11200.

Bank of England (2015) *The Bank of England's approach to stress testing the UK banking system*. October 2015

Barnes, E.A. & Screen, J. A. (2015) The impact of Arctic warming on the midlatitude jet-stream: can it? Has it? Will it? *WIREs Climate Change* 6, 269-286.

Berry, P. and Brown, I. (2021) National environment and assets. In: *The Third UK Climate Change Risk Assessment Technical Report* [Betts, R.A., Haward, A.B. and Pearson, K.V. (eds.)]. Prepared for the Climate Change Committee, London

Bethke, I. et al. (2017) Potential volcanic impacts on future climate variability. *Nature Climate Change*, 7, 799–805.

Bett, P.E., Thornton, H.E. & Clark, R.T. (2017) Using the Twentieth Century Reanalysis to assess climate variability for the European wind industry. *Theoretical and Applied Climatology* 127, 61-80.

Betts, R.A. and Brown, K. (2021) Introduction. In: *The Third UK Climate Change Risk Assessment Technical Report* [Betts, R.A., Haward, A.B. and Pearson, K.V. (eds.)]. Prepared for the Climate Change Committee, London

Bittner, M. et al. (2016) Using a large ensemble of simulations to assess the Northern Hemisphere stratospheric dynamical response to tropical volcanic eruptions and its uncertainty. *Geophysical Research Letters* 43, 9324-9332.

Black, E. et al. (2004) Factors contributing to the summer 2003 European heatwave. *Weather* 59, 217-223.

Blackford, R. & Screen, J.A. (2020) Weakened evidence for mid-latitude impacts of Arctic warming. *Nature Climate Change* 10, 1064-1066.

Booth, R.E. (1968) The severe winter of 1963 compared with other cold winters, particularly that of 1947. *Weather* 23, 477-479.
Braneon, C. et al. (2024) NPCCC4: New York City climate risk information 2022 – observations and projections. *Annals of the New York Academy of Sciences* 1539, 13-48.
Brogli, R. et al. (2023) The pseudo-global-warming (PGW) approach: methodology, software package PGW4ERA5 v1.1, validation, and sensitivity analysis. *Geoscientific Model Development* 16, 907-926.
Burt, S. & Burt, T. (2019) *Oxford Weather and Climate since 1767*, Oxford University Press.
Burt, S. & Burt, T. (2022) *Durham Weather and Climate since 1841*. Oxford University Press.
Canadell, J.G. et al. (2021) Global carbon and other biogeochemical cycles and feedbacks. In *Climate Change 2021: The Physical Science Basis*. *Contribution of Working Group I to the Sixth Assessment Report of the Intergovernmental Panel on Climate Change*. Masson-Delmotte, V. et al. (eds) Cambridge University Press, Cambridge. 673-816.
Cassou, C. & Cattiaux, J. (2016) Disruption of the European climate seasonal clock in a warming world. *Nature Climate Change* 6, 589-594.
Cattiaux, J. et al. (2010) Winter 2010 in Europe: a cold extreme in a warming climate. *Geophysical Research Letters* 37, L20704.
Chan, W.C.H. et al. (2023) Current and future risk of unprecedented hydrological droughts in Great Britain. J. Hydrol. 625, 130074.
Chan, W.C.H. et al. (2024) Added value of seasonal hindcasts to create UK hydrological drought storylines. *Nat. Hazards Earth Syst. Sci*. 24, 1065-1078.
Chen, D. et al. (2021) Framing, context, and methods. In *Climate Change 2021: the Physical Science Basis. Contribution of Working Group I to the Sixth Assessment Report of the Intergovernmental Panel on Climate Change*. Masson-Delmotte, V. et al. (eds) Cambridge University Press, Cambridge. 147-286.
Climate Action Tracker (2023) *The CAT Thermometer* https://climateactiontracker.org/global/cat-thermometer/. Accessed 25/6/2024
Climate Change Committee (2021) *Independent Assessment of UK Climate Risk. Advice to Government for the UK's third Climate Change Risk Assessment (CCRA3).* Climate Change Committee, June 2021
Cohen, J. et al. (2020) Divergent consensus on Arctic amplification influence on midlatitude severe winter weather. *Nature Climate Change* 10, 20-29.
Cohen, J., Angel, L., Barlow, M. & Entekhabi, D. (2023) No detectable trend in mid-latitude cold extremes during the recent period of Arctic amplification. *Communications Earth and Environment* 4, 341.
Cohen, J., Francis, J.A. & Pfeiffer, K. (2024) Anomalous Arctic warming linked with severe winter weather in Northern Hemisphere continents. *Communications Earth and Environment* 5, 557.
Compo, G.P. et al. (2011) The Twentieth Century Reanalysis Project. *Quart. J. Roy. Met. Soc.* 137, 1-28.
Copernicus Climate Change Service (C3S) (2017): *ERA5: Fifth generation of ECMWF atmospheric reanalyses of the global climate*. Copernicus Climate Change Service Climate Data Store (CDS), *30/07/2019*. https://cds.climate.copernicus.eu/cdsapp#!/home
Cornes, R.C. & Jones, P.D. (2024) The seasonal characteristics of English Channel storminess have changed since the 19th century. *Communications Earth and Environment* 5, 160.
Cotterrill, D.F., Pope, J.O. & Stott, P.A. (2023) Future extension of the UK summer and its impact on autumn precipitation. *Climate Dynamics* 60, 1801-1814.

Coumou, D. et al. (2018) The influence of Arctic amplification on mid-latitude summer circulation. *Nature Communications* 9, 2959.
Coupe, J. & Robock, A. (2021) The influence of stratospheric soot and sulfate aerosols on the Northern Hemisphere wintertime atmospheric circulation. *J. Geophys. Res. Atmospheres* 126, e2020JD034513
Crawford, A.J. et al. (2021) Marine ice-cliff instability modelling shows mixed-mode ice-cliff failure and yields calving rate parameterization. *Nature Communications* 12, 2701.
Davies, P.A. et al. (2021) The wet and stormy UK winter of 2019/20. *Weather* 76, 396-402.
Day, J.J. et al. (2019) Increased Arctic influence on the midlatitude flow during Scandinavian Blocking episodes. *Quart. J. Roy. Met. Soc*. 145, 3846-3862.
DeConto, R. M. et al. (2021). The Paris Climate Agreement and future sea level rise from Antarctica. *Nature*, 593, 83–89.
Defra (2024) *Accounting for the effects of climate change*. Supplementary Green Book Guidance, March 2024
Department for Business, Energy and Industrial Strategy (2019) *National Policy Statement for Geological Disposal Infrastructure*. July 2019
Department for Energy Security and Net Zero (2023) *Overarching National Policy Statement for Energy (EN-1)*. November 2023
DMI (2024) *Methods used in Klimaatlas, the Danish Climate Atlas* (v2024b). DMI Report 24-12. https://doi.org/10.5281/zenodo.13753022
Docquier, D. & Koenigk, T. (2021) Observation-based selection of climate models projects Arctic ice-free summers around 2035. *Communications Earth and Environment* 2, 144.
Dong, B. et al. (2025) Key drivers of large scale changes in North Atlantic atmospheric and oceanic circulations and their predictability. *Climate Dynamics* 63, 113.
Douville, H. et al. (2021) Water cycle changes. In *Climate Change 2021: The Physical Science Basis*. *Contribution of Working Group I to the Sixth Assessment Report of the Intergovernmental Panel on Climate Change*. Masson-Delmotte, V. et al. (eds). Cambridge University Press, Cambridge. 1055-1210.
Drouard, M., Kornhuber, K. & Woollings, T. (2019) Disentangling dynamic contributions to summer 2018 anomalous weather over Europe. *Geophysical Research Letters* 46, 12537-12546.
Dunstone, N. et al. (2016) Skilful predictions of the winter North Atlantic Oscillation one year ahead. *Nature Geoscience* 9, 809-814.
Dunstone, N. et al. (2018) Skilful seasonal predictions of summer European rainfall. *Geophysical Research Letters* 45, 3246-3254.
Dunstone, N. et al. (2023) Skilful predictions of the summer North Atlantic Oscillation. *Communications Earth and Environment* 4, 409.
Edwards, T.L. et al. (2021) Projected land ice contributions to twenty-first century sea level rise. *Nature* 593, 74-82.
Endfield, G. H. (2016). Historical narratives of weather extremes in the UK: on behalf of the Weather Extremes team. *Geography* 101, 93–99.
Fereday, D. & Knight, J. (2022) The roles of atmospheric circulation and sea surface temperature in UK surface climate. *Atmospheric Science Letters* 24, e1139.
Ferranti, E.J.S., et al. (2021). *Review of Network Rail's Weather Resilience and Climate Change Adaptation Plans.* A report for the Office of Rail and Road. Climate Sense Ltd and Birmingham Centre for Railway Research & Education (BCRRE), University of Birmingham. March 2021.
Fischer, E.M. et al. (2023) Storylines for unprecedented heatwaves based on ensemble boosting. *Nature Communications* 14, 4643.

Folland, C.K. et al. (2009) The summer North Atlantic Oscillation: past, present and future. *J. Climate* 22, 1082-1103.
Forster, P.M. et al. (2021) The Earth's energy budget, climate feedbacks, and climate sensitivity. In *Climate Change 2021: The Physical Science Basis*. *Contribution of Working Group I to the Sixth Assessment Report of the Intergovernmental Panel on Climate Change*. Masson-Delmotte, V. et al. (eds) Cambridge University Press, Cambridge. 923-1054.
Fox-Kemper, B. et al. (2021) Ocean, Cryosphere and Sea Level Change. In *Climate Change 2021: the Physical Science Basis. Contribution of Working Group I to the Sixth Assessment Report of the Intergovernmental Panel on Climate Change*. Masson-Delmotte, V. et al. (eds) Cambridge University Press, Cambridge. 1211-1362.
Francis, J.A. & Vavrus, S.J. (2012) Evidence linking Arctic amplification to extreme weather in mid-latitudes. *Geophysical Research Letters* 29, L06801.
Francis, J.A. & Vavrus, S.J. (2015) Evidence for a wavier jet stream in response to rapid Arctic warming. *Environmental Research Letters* 10, 014005.
Francis, J.A., Skific, N. & Zobel, Z. (2023) Weather whiplash events in Europe and North America assessed as continental-scale atmospheric regime shifts. *npj Climate and Atmospheric Science* 6, 216.
Friedlingstein, P. et al. (2023) Global Carbon Budget 2023. *Earth System Science Data* 15, 5301-5369.
Garner, G. G. et al. (2021) *IPCC AR6 Sea-Level Rise Projections*. Version 20210809. PO.DAAC, CA, USA. Dataset accessed 2024-06-27
Garrido-Perez, J.M. et al. (2024) Storylines of projected summer warming in Iberia using atmospheric circulation, soil moisture and sea surface temperature as drivers of uncertainty. *Atmospheric Research* 311, 107677.
Gessner, C. et al. (2021) Vary rare heat extremes: quantifying and understanding using ensemble reinitialization. *J. Climate* 34, 6619-6634.
Gessner, C. et al. (2022) Multi-year drought storylines for Europe and North America from an iteratively perturbed global climate model. *Weather and Climate Extremes* 28, 100512.
Gessner, C. et al. (2023) Developing low-likelihood climate storylines for extreme precipitation over central Europe. *Earth's Future* 11, e2023EF003628.
Golledge, N.R. et al. (2019) Global environmental consequences of twenty-first-century ice-sheet melt. *Nature*, 566(7742), 65–72
Goosse, H. et al. (2018) Quantifying climate feedbacks in polar regions. *Nature Communications* 9, 1919.
Grams, C.M. et al. (2017) Balancing Europe's wind-power output through spatial deployment informed by weather regimes. *Nature Climate Change* 7, 557-562.
Greatbatch, R.J. et al. (2014) Tropical origin of the severe European winter of 1962/63. *Quart. J. Royal Met. Soc*. 141, 153-165.
Hall, R.J. & Hanna, E. (2018) North Atlantic circulation indices: links with summer and winter temperature and precipitation and implications for seasonal forecasting. *Int. J. Climatol.* 38, 660-677.
Hanlon, H., Palmer, M. & Betts, R. (2021) *Effect of potential climate tipping points on UK impacts*. Met Office.
Hardiman, S.C. et al. (2020) Predictability of European winter 2019/20: Indian Ocean dipole impacts on the NAO. *Atmospheric Science Letters* 21, e1005.
Harrington, L.J. et al. (2019) Circulation analogues and uncertainty in the time-evolution of extreme event probabilities: evidence from the 1947 Central European heatwave. *Climate Dynamics* 53, 2229-2247.

Harrison, S. et al. (2022) Identifying weather patterns associated with increased volcanic ash risk within British Isles airspace. *Weather and Forecasting* 3, 1157-1168.
Harvey, B. et al. (2020) The response of the northern hemisphere storm tracks and jet streams in the CMIP3, CMIP5 and CMIP6 climate models. *J. Geophys. Res.: Atmospheres* 125(23) p.e2020JD032701
Harvey, B., Hawkins, E. & Sutton, R. (2023) Storylines for future changes of the North Atlantic jet and associated impacts on the UK. *Int. J. Climatol*. 43, 4424-4441.
Hassan, T. et al. (2021) Anthropogenic aerosol forcing of the Atlantic meridional overturning circulation and the associated mechanisms in CMIP6 models, *Atmos. Chem. Phys*., 21, 5821–5846.
Hausfather, Z. (2025) An assessment of current policy scenarios over the 21st century and the reduced plausibility of high-emissions pathways. *Dialogues on Climate Change* 1-7, 10.1177/29768659241304584
Hausfather, Z. & Peters, G.P. (2020) Emissions – the 'business as usual' story is misleading. *Nature* 577, 618-620.
Hawkins, E. et al. (2011) Bistability of the Atlantic overturning circulation in a global climate model and links to ocean freshwater transport. *Geophysical Research Letters* 38, L10605.
Hawkins, E. et al. (2023a) Millions of historical monthly rainfall observations taken in the UK and Ireland rescued by citizen scientists. *Geoscience Data Journal* 10, 246-261.
Hawkins, E., Compo, G.P. & Sardeshmukh, P.D. (2023b) ESD Ideas: Translating historical extreme weather events into a warmer world. *Earth System Dynamics* 14, 1081-1084.
Hazeleger, W. et al. (2015) Tales of future weather. *Nature Climate Change* 5, 107-113.
HM Government (2016) *National Flood Resilience Review*
HM Government (2022a) *UK Climate Change Risk Assessment 2022*. 17 January 2022
HM Government (2022b) Flood risk assessments: climate change allowances. 27 May 2022 https://www.gov.uk/guidance/flood-risk-assessments-climate-change-allowances accessed 30/06/2022
Hollis, D. et al. (2019) HadUK-Grid – a new UK dataset of gridded climate observations. *Geoscience Data Journal* 6, 151-159.
House of Lords (2021) *Preparing for Extreme Risks: Building a Resilient Society*. Select Committee on Risk Assessment and Risk Planning. Report of Session 2021-2022. 3 December 2021 HL Paper 110.
Huang, W.T.K. et al. (2020) Weather regimes and patterns associated with temperature-related excess mortality in the UK: a pathway to sub-seasonal risk forecasting. *Environmental Research Letters* 15, 124052.
Humphrey, K. & Murphy, J. (2016) *UK Climate Change Risk Assessment Evidence Report: Chapter 1, Introduction*. Contributing authors: Harris, G. et al. Report prepared for the Adaptation Sub-Committee of the Committee on Climate Change, London
Hurrell, J. &, Phillips, A. & National Center for Atmospheric Research Staff (Eds) (2018). Last modified 2024-04-18 "The Climate Data Guide: Hurrell North Atlantic Oscillation (NAO) Index (PC-based)." Retrieved from https://climatedataguide.ucar.edu/climate-data/hurrell-north-atlantic-oscillation-nao-index-pc-based on 2024-07-16.
IPCC (2021) Annex VII: Glossary [Matthews, J.B.R. et al. (eds.)]. *In Climate Change 2021: The Physical Science Basis. Contribution of Working Group I to the Sixth Assessment Report of the Intergovernmental Panel on Climate Change* [Masson-Delmotte, V., et al. (eds.)]. Cambridge University Press, Cambridge, United Kingdom and New York, NY, USA, pp. 2215–2256.

IPCC (2023a) *Synthesis Report of the IPCC Sixth Assessment Report (AR6). Summary for Policymakers*. Intergovernmental Panel on Climate Change.
IPCC (2023b) *Synthesis Report of the IPCC Sixth Assessment Report (AR6). Longer Report*. Intergovernmental Panel on Climate Change.
Jackson, L. et al. (2015) Global and European climate impacts of a slowdown of the AMOC in a high resolution GCM. *Climate Dynamics* 45, 3299-3316.
Jackson, L.C. et al. (2022) Understanding AMOC stability: the North Atlantic Hosing Model Intercomparison Project. *Geoscientific Model Development Discussions* 10.5195/gmd-2022-277.
Jaroszweski, D., Wood, R., and Chapman, L. (2021) Infrastructure. In: *The Third UK Climate Change Risk Assessment Technical Report.* [Betts, R.A., Haward, A.B., Pearson, K.V. (eds)] Prepared for the Climate Change Committee, London
Jenkinson, A.F. & Collison, F.P. (1977) *An initial climatology of gales over the North Sea*. Synoptic Climatology Branch Memorandum no. 62, Meteorological Office.
Jones, P.D., Hulme, M. & Briffa, K.R. (1993) A comparison of Lamb circulation types with an objective classification scheme. *Int. J. of Climatol.* 13, 655-663.
Jones, P.D., Jonsson, T. & Wheeler, D. (1997) Extension to the North Atlantic Oscillation using early instrumental pressure observations from Gibraltar and South-West Iceland. *Int. J. Climatol.* 17, 1433-1450.
Jones, P.D. et al. (2010) *UK Climate Projections Science Report: Projections of future daily climate for the UK from the Weather Generator*. University of Newcastle
Jones, P.D., Harpham, C. and Briffa, K.R. (2013) Lamb Weather Types derived from Reanalysis Products. *Int. J. Climatol.* **33**, 1129-1139.
Kandlbauer, J. et al. (2013) Climate and carbon cycle response to the 1815 Tambora volcanic eruption. *J. Geophys. Res. Atmospheres* 118, 12497-12507.
Kay, G. et al. (2020) Current likelihood and dynamics of hot summers in the UK. *Environmental Research Letters* 15, 094099
Kendon, M. (2022) *Unprecedented extreme heatwave, July 2022*. Met Office.
Kendon, M. & McCarthy, M. (2015) The UK's wet and stormy winter of 2013/2014. *Weather* 70, 40-47.
Kendon, M., Sexton, D. & McCarthy, M. (2020) A temperature of 20ºC in the UK winter: a sign of the future? *Weather* 75, 318-324.
Kendon, M. et al. (2023) State of the UK climate 2022. *Int. J. of Climatol.* 43 (Suppl. 1), 1-82.
Kennedy, J.J. et al. (2019) An ensemble data set of sea-surface temperature change from 1850: the Met Office Hadley Centre HadSST.4.0.0.0 data set. *J. Geophys. Res. Atmospheres* 124, 7719-7763.
Kent, C. et al. (2022) Estimating unprecedented extremes in UK summer daily rainfall. *Environmental Research Letters* 17, 014041
Kerr, R.A. (2000) A North Atlantic climate pacemaker for the centuries. *Science* 288, 1984-1986.
Kim, Y.-H. et al. (2023) Observationally-constrained projections of an ice-free Arctic even under a low emission scenario. *Nature Communications* 14, 3139.
Kopp, R.E. et al. (2023) The Framework for Assessing Changes to Sea-level (FACTS) v1.0: a platform for characterizing parametric and structural uncertainty in future global, relative and extreme sea level change. *Geoscientific Model Development* 16, 7461-7489.
Kornhuber, K. et al. (2019) Extreme weather events in early summer 2018 connected by a recurrent hemispheric wave-7 pattern. *Environmental Research Letters* 14, 054002.

Kovats, S. and Brisley, R. (2021) Health, communities and the built environment. In: *The Third UK Climate Change Risk Assessment Technical Report* [Betts, R.A., Haward, A.B., Pearson, K.V. (eds.)]. Prepared for the Climate Change Committee, London

Lavers, D., Prudhomme, C. & Hannah, D.M. (2010) Large-scale climate, precipitation and British river flows: identifying hydrological connections and dynamics. *J. Hydrol.* 395, 242-244.

Leach, N.J. et al. (2022) Generating samples of extreme winters to support climate adaptation. *Weather and Climate Extremes* 36, 100419.

Lee, J.-Y. et al. (2021) Future global climate: scenario-based projections and near-term information. In: *Climate Change 2021: The Physical Science Basis. Contribution of Working Group I to the Sixth Assessment Report of the Intergovernmental Panel on Climate Change* Masson-Delmotte, V., et al. (eds.). Cambridge University Press, Cambridge. 553-672.

Leverman, A. et al. (2005) Dynamic sea level changes following changes in the thermohaline circulation. *Climate Dynamics* 24, 347-354.

Li, C. *et al.* (2017) India Is overtaking China as the world's largest emitter of anthropogenic sulfur dioxide. *Scientific Reports* 7, 14304.

Li, M. et al. (2020) Collaborative impact of the NAO and atmospheric blocking on European heatwaves, with a focus on the hot summer of 2018. *Environmental Research Letters* 15, 114003.

Little, C.M. et al. (2019) The relationship between U.S. East Coast sea level and the Atlantic Meridional Overturning Circulation: a review. J*. Geophys.Res. Oceans* 124, 6435-6458.

Lo, Y.T.E. et al. (2023) Changes in winter temperature extremes from future Arctic sea-ice loss and ocean warming. *Geophysical Research Letters* 50, e2022GL102542.

Lowe, J.A. et al. (2009) *UK Climate Projections science report: Marine and coastal projections*. Met Office Hadley Centre, Exeter, UK

Lowe, J.A. et al. (2018) *UKCP18 Science Overview Repor*t. Met Office Hadley Centre. November 2018 (updated March 2019).

Lund, M. T., Myhre, G., and Samset, B. H. (2019) Anthropogenic aerosol forcing under the Shared Socioeconomic Pathways, *Atmos. Chem. Phys*., 19, 13827–13839.

Luo, F. et al. (2020) Projected near-term changes of temperature extremes in Europe and China under different aerosol emissions. *Environmental Research Letters* 15, 034013.

Madonna, E. et al. (2017) The link between eddy-driven jet variability and weather regimes in the North Atlantic-European Sector. *Quart. J. Roy. Met. Soc.* 143, 2960-2972.

Mann, M.E. et al. (2017) Influence of anthropogenic climate change on planetary wave resonance and extreme weather events. *Scientific Reports* 7, 45242.

Marvel, K., M. Biasutti, C. Bonfils, (2020) Fingerprints of external forcings on Sahel rainfall: aerosols, greenhouse gases, and model-observation discrepancies. *Environmental Research Letters* 15, 084023.

Matthews, T. et al. (2014) Stormiest winter on record for Ireland and UK. *Nature Climate Change* 4, 738-749.

Matthews, T. et al. (2016) Past and future climate change in the context of memorable seasonal extremes. *Climate Risk Management* 11, 37-52.

McCarthy, M., Christidis, N., Dunstone, N. *et al*. (2019) Drivers of the UK summer heatwave of 2018. *Weather* 74, 390–396.

McCormick, M.P., Thomason, L.W. & Trepte, C.R. (1999) Atmospheric effects of the Mt Pinatubo eruption. *Nature* 373, 399-404.

Mecking, J. et al. (2016) Stable AMOC off state in an eddy-permitting coupled climate model. *Climate Dynamics* 47, 2455-2470.
Menary, M. B. et al. (2020). Aerosol-forced AMOC changes in CMIP6 historical simulations. *Geophysical Research Letters*, 47, e2020GL088166.
Met Office et al. (2015) *Developing H++ climate change scenarios for heat waves, droughts, floods, windstorms and cold snaps*. Report for Adaptation Sub-Committee of the Committee on Climate Change, Met Office, CEH and University of Reading.
Milillo, P. et al., (2019) Heterogeneous retreat and ice melt of Thwaites Glacier, West Antarctica. *Science Advances*, 5(1), eaau3433
Ministry of Housing, Communities and Local Government (2021) *National Planning Policy Framework*, July 2021
Myhre, G. et al. (2013) Aerosols and their relation to global climate and climate sensitivity. *Nature Education Knowledge* 4:7
Neal, R. et al. (2016) A flexible approach to defining weather patterns and their application in weather forecasting in Europe. *Meteorological Applications* 23, 389-400.
Neal, R. (2022) Daily historical weather pattern classifications for the UK and surrounding European area (1950 to 2020) *Pangaea* doi.org/10.1594/PANGAEA.942896.
Newhall, C., Self, S. & Robock, A. (2018) Anticipating future Volcanic Explosivity Index (VEI) 7 eruptions and their chilling impacts. *Geosphere* 14, 572-603.
Notz. D. & SIMIP Community (2020) Arctic sea ice in CMIP6. *Geophysical Research Letters* 47, e2019GL086749.
Office for Nuclear Regulation and Environment Agency (2017) *Principles for flood and coastal erosion risk management*. ONR and Environment Agency, July 2017.
Oman, L. et al. (2005) Climatic response to high-latitude volcanic eruptions. *J. Geophys. Res. Atmospheres* 110, D13103
Orihuela-Pinto, B. et al. (2022) Interbasin and interhemispheric impacts of a collapsed Atlantic Overturning Circulation. *Nature Climate Change* 12, 558-565.
Overland, J.E. et al. (2016) Nonlinear response of mid-latitude weather to the changing Arctic. *Nature Climate Change* 6, 992-999.
Overland, J.E. et al. (2021) How do intermittency and simultaneous processes obfuscate the Arctic influence on midlatitude winter extreme weather events? *Environmental Research Letters* 16, 043002.
Palmer, M., et al. (2018a) *UKCP18 Marine Report*. Met Office Hadley Centre.
Palmer, M.D., Harris, G.R. & Gregory, J.M. (2018b) Extending CMIP5 projections of global mean temperature change and sea level rise due to thermal expansion using a physically-based emulator. *Environmental Research Letters* 13, 84003.
Palmer, M.D. et al. (2020) Exploring the drivers of global and local sea-level change over the 21st century and beyond. *Earth's Future* 8:e2019EF001413.
Palmer, M.D. et al. (2024) A framework for physically consistent storylines of UK future mean sea level rise. *Climatic Change* 177:106.
Parker, D.E., Legg, T.P. and Folland, C.K. (1992) A new daily Central England Temperature Series, 1772-1991. *Int. J. Clim*., 12, 317-342.
Parker, T. et al. (2019) Seasonal predictability of the winter North Atlantic Oscillation from a jet stream perspective. *Geophysical Research Letters* 46, 10159-10167.
Pausata, F.S.R. et al. (2015) Impacts of high-latitude volcanic eruptions on ENSO and AMOC. *Proc. Nat. Acad. Sci*. 112, 13784-13788.
Pedersen, J. S. T. et al., 2020: Variability in historical emissions trends suggests a need for a wide range of global scenarios and regional analyses. *Commun. Earth Environ.*, **1**(1), 1–7

Perks, R.J. et al. (2023) The influence of future weather pattern changes and projected sea-level rise on coastal flood impacts around the UK. *Climatic Change* 176, 25.
Persad, G.G., Samset, B.H. & Wilcox, L.J. (2022) Aerosols must be part of climate risk assessments. *Nature* 611, 662-664.
Petch, J.C. et al. (2020) Sensitivity of the 2018 summer heatwave to local sea temperatures and soil moisture. *Atmospheric Science Letters* 21, e948.
Polson, D., M. et al. (2014) Decreased monsoon precipitation in the Northern Hemisphere due to anthropogenic aerosols. *Geophysical Research Letters* 41, 6023–6029.
Previdi, M., Smith, K.L. & Polvani, L.M. (2021) Arctic amplification of climate change: a review of underlying mechanisms. *Environmental Research Letters* 16, 093003.
Raible, C.C. et al. (2016) Tambora 1815 as a test case for high impact volcanic eruptions: earth system effects. *WIREs Climate Change* 7, 569-589.
Ranger, N., Lowe, J. A., & Reeder, T. (2013). Addressing deep uncertainty over long-term climate in major infrastructure projects: Four innovations of the Thames Estuary 2100 Project. *EURO Journal on Decision Processes*, 1, 233–262.
Rantenen, M. et al. (2022) The Arctic has warmed nearly four times faster than the globe since 1979. *Communications Earth and Environment* 3, 168.
Rao, S., et al. (2017) Future air pollution in the Shared Socio-economic Pathways. *Glob. Environ. Change*. 42, 346–358.
Riahi, K. et al. (2022) Mitigation pathways compatible with long-term goals. In *Climate Change 2022: Mitigation of Climate Change*. *Contribution of Working Group III to the Sixth Assessment Report of the Intergovernmental Panel on Climate Change*. Shukla, P.R. et al. (eds). Cambridge University Press, Cambridge 295-408.
Richardson, D. et al. (2018) A new precipitation and drought climatology based on weather patterns. *Int. J. of Climatol.* 38, 630-648.
Richardson, D. et al. (2019) Weekly to multi-month persistence in sets of daily weather patterns over Europe and the North Atlantic Ocean. *Int. J. of Climatol.* 39, 2041-2056.
Richardson, D. et al. (2020) Linking weather patterns to regional extreme precipitation for highlighting potential flood events in medium- to long-term forecasts. *Meteorological Applications* 27, e1931.
Ritchie, P.D.L. et al. (2020) Shifts in national land use and food production in Great Britain after a climate tipping point. *Nature Food* 1, 76-83.
Robock, A. (2000) Volcanic eruptions and climate. *Reviews of Geophysics* 98, 191-219.
Robson, J. et al. (2022) The role of anthropogenic aerosol forcing in the 1850–1985 Sstrengthening of the AMOC in CMIP6 historical simulations. *J. Climate*, 35, 3243–3263
Rousi, E. et al. (2022) Accelerated western European heatwave trends linked to more persistent double jets over Eurasia. *Nature Communications* 13, 3851.
Samset, B. H., et al. (2018). Climate impacts from a removal of anthropogenic aerosol emissions. *Geophysical Research Letters*, 45, 1020– 1029.
Sanchez-Benitez, A. et al. (2022) The July 2019 European heat wave in a warmer climate: storyline scenarios with a coupled model using spectral nudging. *J. Climate* 35, 2373-2390.
Scaife, A.A. et al. (2014) Skilful long-range prediction of European and North American winters. *Geophysical Research Letters* 41, 2514-2519.
Scaife, A.A. et al. (2016) Tropical rainfall, Rossby waves and regional winter climate predictions. *Quart. J. Roy. Met. Soc.* 143, 1-11.
Scannell, C. et al. (2019) The influence of remote aerosol forcing from industrialized economies on the future evolution of East and West African rainfall. *J. Climate*, 32, 8335–8354.

Schär, C., Frei, C., Lüthi, D., and Davies, H. C. (1996) Surrogate climate change scenarios for regional climate models, *Geophysical Research Letters*, 23, 669–672.
Schmale, J., P. Zieger, A. M. L. Ekman (2021) Aerosols in current and future Arctic climate. *Nature Climate Change* 11, 95–105.
Schneider, D.P. et al. (2013) Climate data guide spurs discovery and understanding. *Eos Trans. AGU* 94, 121-122.
Schwalm, C.R., Glendon, S. & Duffy, P.B. (2020) RCP8.5 tracks cumulative CO_2 emissions. *Proc Nat Acad. Sci* 117, 19656-19657.
Sexton, D.M.H. et al. (2021) A perturbed parameter ensemble of HadGEM3-GC3.05 coupled model projections: part 1: selecting the parameter combinations. *Climate Dynamics* 56, 3395-3436.
Sgubin, G. et al. (2017) Abrupt cooling over the North Atlantic in modern climate models. *Nature Communications* 8, 14375.
Sgubin, G. et al. (2019) The impact of possible decadal-scale cold waves on viticulture over Europe in the context of global warming. *Agronomy* 9. 397.
Shepherd, T.G. (2019) Storyline approach to the construction of regional climate change information. *Proceedings of the Royal Society A: Mathematical, Physical and Engineering Sciences*, 475(2225), 20190013
Shepherd, T.G. et al. (2018) Storylines: an alternative approach to representing uncertainty in physical aspects of climate change. *Climatic Change* 151, 555-571.
Shu, Q. et al. (2022) Arctic Ocean Amplification in a warming climate in CMIP6 models. *Science Advances* 8, eabn9755.
Simpson, I. et al. (2024) North Atlantic atmospheric circulation indices: links with summer and winter temperature and precipitation in north-west Europe, including persistence and variability. *Int. J. of Climatol.* 44, 1-21.
Slingo, J. (2021) Latest scientific evidence for observed and projected climate change. In: *The third UK Climate Change Risk Assessment Technical Report* [Betts, R.A., Haward, A.B. and Pearson, K.V. (eds.)] Prepared for the Climate Change Committee, London
Smith, D.M. et al. (2019) The Polar Amplification Model Intercomparison Project (PAMIP) contribution to CMIP6: investigating the causes and consequences of polar amplification. *Geosci. Model Dev*. 12, 1139-1164.
Smith, D.M. et al. (2022) Robust but weak winter atmospheric circulation response to future Arctic sea ice loss. *Nature Communications* 13, 727.
Spaeth, J. & Birner, T. (2022) Stratospheric modulation of Arctic Oscillation extremes as represented by extended-range ensemble forecasts. *Weather and Climate Dynamics* 3, 883-903.
Stoffel, M. et al. (2015) Estimates of volcanic-induced cooling in the Northern Hemisphere over the past 1500 years. *Nature Geoscience* 8, 784-788.
Sutton, R. (2018) ESD ideas: a simple proposal to improve the contribution of IPCC WG1 to the assessment and communication of climate change risks. *Earth System Dynamics* 9, 1155-1158.
Sutton, R. (2019) Climate science needs to take risk assessment much more seriously. *Bull. Am. Met. Soc.*, 100, 1637-1642.
Sutton, R. & Dong, B. (2012) Atlantic Ocean influence on a shift in European climate in the 1990s. *Nature Geoscience* 5, 788-792.
Swingedouw, D. et al. (2021) On the risk of abrupt changes in the North Atlantic subpolar gyre in CMIP6 models. *Ann. New York Acad. Sci.* 1504, 187-201.
Szopa, S. et al. (2021) Short-Lived Climate Forcers. In *Climate Change 2021: The Physical Science Basis*. *Contribution of Working Group I to the Sixth Assessment Report of*

the Intergovernmental Panel on Climate Change. Masson-Delmotte, V. et al. (eds). Chapter 8. Cambridge University Press, Cambridge. 817-922.
Tejedor, E. et al. (2021) Global hydroclimatic response to tropical volcanic eruptions over the last millennium. *Proc. Nat. Acad. Sci*. 118, e2019145118.
Thompson, D.W.J., Baldwin, M.P. & Wallace, J.M. (2002) Stratospheric connections to northern hemisphere wintertime weather: implications for prediction. *J. Climate* 15, 1421-1428.
Thompson, V. et al. (2017) High risk of unprecedented UK rainfall in the current climate. *Nature Communications* 8, 107.
Thornton, H.E., Smith, D.M., Scaife, A.A. & Dunstone, N.J. (2023) Seasonal predictability of the East Atlantic Pattern in late autumn and early winter. *Geophysical Research Letters* 50, e2022GL100712.
Trenberth, K.E. & Shea, D.J. (2006) Atlantic hurricanes and natural variability in 2005. *Geophysical Research Letters* 33, L12704
Trenberth, K. et al. (2023). Last modified 2023-09-01 *The Climate Data Guide: Atlantic Multi-decadal Oscillation (AMO) and Atlantic Multidecadal Variability (AMV)*. Retrieved from https://climatedataguide.ucar.edu/climate-data/atlantic-multi-decadal-oscillation-amo on 2024-07-16.
Turner, S. et al. (2021) The 2018/2019 drought in the UK: a hydrological appraisal. *Weather* 76, 248-253.
Vallis, G.K. & Gerber, E.P. (2008) Local and hemispheric dynamics of the North Atlantic Oscillation, annular patterns and the zonal index. *Dynamics of Atmospheres and Oceans* 44, 184-212.
van de Wal, R. S. W. et al. (2022). A high-end estimate of sea level rise for practitioners. *Earth's Future*, 10, e2022EF002751.
van Dorland, R. et al. (2024) *KNMI National Climate Scenarios 2023 for the Netherlands*. KNMI de Bilt, Scientific Report WR-23-02, March 8 2024
van Garderen, L., Feser, F. & Shepherd, T.G. (2021) A methodology for attributing the role of climate change in extreme events: a global spectrally-nudged storyline. *Nat. Hazards Earth Syst. Sci*. 21, 171-186.
van Westen, R.M., Kliphuis, M. & Dijkstra, H.A. (2024) Physics-based early warning signal shows that AMOC is on tipping course. *Science Advances* 10, 10.1126/sciadv.adk1189.
Vellinga, M. & Wood, R. (2008) Impacts of thermohaline circulation shutdown in the twenty-first century. *Climatic Change* 91, 43-63.
Wang, L. & Ting, M. (2022) Stratosphere-troposphere coupling leading to extended seasonal predictability of summer North Atlantic Oscillation and boreal climate. *Geophysical Research Letters* 49, e2021GL096362.
Watkiss, P. and Betts, R.A. (2021) Method. In: *The Third UK Climate Change Risk Assessment Technical Report* Betts, R.A., Haward, A.B. and Pearson, K.V. (eds.). Prepared for the Climate Change Committee, London
Weeks, J.H. et al. (2023) The evolution of UK sea-level projections. *Environmental Research Communications* 5, 032001.
Weijer, W. et al. (2020) CMIP6 models predict significant 21st century decline of the Atlantic Meridional Overturning Circulation. *Geophysical Research Letters* 47, e2019GL086075
West, H., Quinn, N. & Horswell, M. (2022) The influence of the North Atlantic Oscillation and East Atlantic Pattern on drought in British catchments. *Frontiers in Environmental Science* 10, 754597.

Wilcox, L. J., E. J. Highwood, N. J. Dunstone (2013) The influence of anthropogenic aerosol on multi-decadal variations of historical global climate. *Environmental Research Letters* 8, 024033.
Wilcox, L. J. et al. (2019) Mechanisms for a remote response to Asian anthropogenic aerosol in boreal winter, *Atmos. Chem. Phys*., 19, 9081–9095.
Wilcox, L. J. et al. (2020) Accelerated increases in global and Asian summer monsoon precipitation from future aerosol reductions, *Atmos. Chem. Phys*., 20, 11955–11977.
Wolf, G. et al. (2017) Quasi-stationary waves and their impact on European weather and extreme events. *Quart. J. Roy. Met. Soc.* 144, 2431-2448.
Wood, R.A. et al. (2023) A climate science toolkit for high impact-low likelihood climate risks. *Earth's Future* 10.1029/2022EF003369
Woollings, T., Hannachi, A. & Hoskins, B. (2010) Variability of the North Atlantic eddy-driven jet stream. *Quart. J. Roy. Met. Soc*. 136, 856-868.
Woollings, T., Czuchnicki, C. & Franzke, C. (2014) Twentieth century North Atlantic jet variability. *Quart. J. Roy. Met. Soc*.140, 783-791.
Woollings, T. et al. (2015) Contrasting interannual and multidecadal NAO variability. *Climate Dynamics* 45, 539-556.
Woollings, T. et al. (2018) Daily to decadal modulation of jet variability. *J. Climate* 31, 1297-1314.
Yamazaki, K. et al. (2021) A perturbed parameter ensemble of HadGEM3-GC3.05 coupled model projections: part 2: global performance and future changes. *Climate Dynamics* 56, 3437-3471.
Yule, E.L. et al. (2024) Using analogues to predict changes in future UK heatwaves. *Environmental Research Climate* 10.1088/2752-5295/ad57e3
Zanchettin, D. et al. (2022) Effects of forcing differences and initial conditions on inter-model agreement in the VolMIP volc-pinatubo-full experiment. *Geosci. Model Dev*. 15, 2265-2292.
Zappa, G. & Shepherd, T.G. (2017) Storylines of atmospheric circulation change for European regional climate impact assessment. *J. Climate* 30, 6561-6577.
Zhang, M. et al. (2022) Heat wave tracker: a multi-method multi-source heat wave measurement toolkit based on Google Earth Engine. *Environmental Modelling and Software* 147, 105255.
Zhao, J. et al. (2022) Constraining CMIP6 projections of an ice-free Arctic using a weighting scheme. *Earth's Future* 10, e2022EF002708.
Zhou, Z. et al. (2021) Climate impact of volcanic eruptions: the sensitivity to eruption season and latitude in MPI-ESM ensemble experiments. *Atmos. Chem. Phys*. 21, 13425-13442.